

AD-A034 076

DUMONT ELECTRON TUBES CLIFTON N J
STUDY AND IMPROVEMENT OF THE S-1 PHOTOEMISSIVE SURFACE (U)
JUL 69 H TIMAN
ETC-116-69-A

F/G 17/5

DA-44-009-AMC-1811(E)
NL

UNCLASSIFIED

1 OF 2
AD
A034076

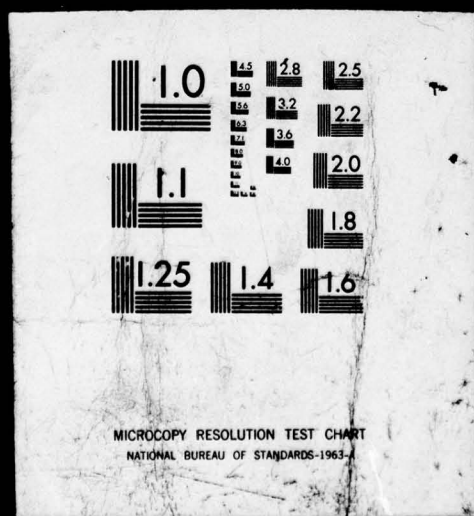


FILED

1 OF 2

AD

A034076



ADA034076

14
ETC-116-69-A

UNCLASSIFIED

~~CONFIDENTIAL~~

COPY 15 OF 25

9
FINAL REPORT
RE: DD-254 4/14/70
Jul 66 - Jun 69

FOR

2

6
STUDY AND IMPROVEMENT OF THE S-1 PHOTOEMISSIVE SURFACE.

THIS REPORT COVERS PERIOD JULY, 1966 TO JUNE, 1969

10 Hans Timan

COPY AVAILABLE TO DDC DOES NOT
PERMIT FULLY LEGIBLE PRODUCTION

DU MONT ELECTRON TUBES, A DIVISION OF FAIRCHILD
CAMERA AND INSTRUMENT CORPORATION
750-760 BLOOMFIELD AVENUE
GLIFTON, NEW JERSEY 07015

UNITED STATES ARMY ENGINEER
RESEARCH AND DEVELOPMENT LABORATORIES
FORT BELVOIR, VIRGINIA

DDC
RECEIVED
DEC 8 1976
A

15
DA-44-009-AMC-1811(E)

Copy available to DDC does not
permit fully legible reproduction

11
18 Jul 1969

12/30

DISTRIBUTION STATEMENT A
Approved for public release;
Distribution Unlimited

This document contains information
affecting the National Defense of
the United States within the meaning
of the Espionage Laws, Title 18,
U.S.C., Sections 793 and 794. Its
transmission or the revelation of its
contents in any manner to an un-
authorized person is prohibited by law.

UNCLASSIFIED
DOWNGRADED AT 3 YEAR INTER-
VALS; DECLASSIFIED AFTER
12 YEARS
DDI DIR 5200.10

118460
~~CONFIDENTIAL~~

383812

I. INTRODUCTION

(U) This final report summarizes the research effort from July 1966 to June 1969 under Contract No. DA-44-009-AMC-1811(E), which was a continuation of a previous effort from May 1963 to June 1966 under Contract No. DA-44-009-AMC-136(T).

(U) As in the above mentioned previous contract, the primary interest in this investigation was directed toward practical goals. In the first two-thirds of the effort, this meant improvement of the luminous and infrared sensitivity of the semitransparent S-1 and suppression of its thermionic emission.

(U) In the last third of the contractual period, the effort was shifted to a practical study of formation and performance of the space reflective S-1.

(U) As a secondary goal, the derivation of a model of the S-1 and a theoretical explanation of its main features was desired.

(U) In all specified areas considerable progress has been achieved. Several new processing methods have been developed for good infrared response of semitransparent cathodes. Although

(U) repeatability is still a major problem, there has been a reasonable yield of high cathodes with the best of the developed methods. As already previously observed, it was re-affirmed that geometrical configuration and substrate conditions require selection and adjustment of a particularly suited processing method. Towards the end of this contract, a specific method was arrived at which appears to lessen this dependence considerably.

(U) Optical enhancement possibilities were studied in the last eighteen months of this work. Although the optical properties of the S-1 do not allow for improvements similar to those found in the S-20, methods for processing a space reflective S-1 were found, and a reliable schedule for processing such cathodes has been developed.

(U) Finally, the computation of the optical constants of the S-1 has resulted in plausible values which fit reasonably well over the range of measurement. By virtue of these optical constants, an intensity-based model of the S-1 was sketched out.

~~CONFIDENTIAL~~

RE: DD-254 4/14/70

(U) This model appears to be able to explain some of the features of the spectral response.

(U) Since this report is partly based upon findings detailed in the previous final report under AMC-136(T), cross-references to that document will be made throughout this report. The numbers of individual reports are given as reference to specific points for more detailed discussion. For performance data of selected surfaces extending over the entire period of both contracts, see also Tables and Figures in this report.

II. PROGRESS IN PROCESSING SEMITRANSSPARENT CATHODES

(U) The previous contract, AMC-136(T), had resulted in several methods which gave high luminous sensitivities with a moderate IR sensitivity percentage. For a review of sensitivities achieved, we refer to Table I of the Final Report, AMC-136(T), dated 12 May 1967.

^u
(S) The highest IR sensitivities reported there were:

~~CONFIDENTIAL~~

~~CONFIDENTIAL~~

RE: DD-254 4/14/70

^u
(S) Tube #126 - Luminous Sensitivity, 80 $\mu\text{a/l}$; 2540, 9.2 $\mu\text{a/l}$.

Tube #606 - Luminous Sensitivity, 60 $\mu\text{a/l}$; 2540, 9.1 $\mu\text{a/l}$.

The percentage of IR response ran, usually, between 8 and 12%.

^u
(S) The doping methods which were investigated thoroughly for thermionic emission suppression did not help the IR sensitivity either. Potassium as well as rubidium doping resulted in a lowering of the IR sensitivity percentage.

(U) All dopants resulted in a change of the spectral response shape, as compared to the normal cathode, processed with Cs only. This change usually showed up as a "chopping off" of the long wavelength response with increased sensitivity in the 8000 \AA to 9500 \AA region. These changes concurred, at that time, with the expressed interest of the contracting agency for high sensitivity to 9500 \AA radiation.

(U) At the beginning of this new contract, however, emphasis was shifted, in that high sensitivity to the 10600 \AA laser line was desired.

~~CONFIDENTIAL~~

~~CONFIDENTIAL~~

RE: DD-254 4/14/70

(U) A great deal of the effort in the first eighteen months was therefore directed toward the development of a high IR processing method ("Hip"). Such a method was developed during the first year.

(U) For a detailed description of the evaluation of "Hip" see Rpts. No. 3 through No. 9.

^u
(a) A typical "Hip" schedule is as follows:

1. Prewet glass surface with Cs to a predetermined value.

2. Evaporate Ag to a 40-65% coverage.

Evaporation is monitored with an IR monochromatic line, because the onset of "bad layers" (i.e., conductive layers) is distinguished by abnormally high IR absorption. (Ref. Rpt. No. 3.)

3. Drift Cs at 30-50°C until the transmission change is completed.

4. Bake surface until no further increase in photosensitivity is being observed.

~~CONFIDENTIAL~~

CONFIDENTIAL

~~(S)~~ 5. Peak with O₂.

RE DD-254 4/14/70 *JS*

6. If "bake off" (loss of sensitivity) had occurred during step No. 4, step No. 5 is followed by additional steps 3, 4, 5.

~~(S)~~ This method was an outgrowth of a brief investigation of the classical cathode which had been conducted during the first quarter. (Ref. Rpt. No. 1-3.) The investigation of the "classical" method itself gave the expected result: Average cathodes, below 40 μ a/l with 8-12% IR sensitivity. It should be noted that, in sharp contrast with the classical method, no after-silvering is employed.

~~(S)~~ This "Hip" method was used as a base for further improvements of IR sensitivity during the remainder of the contract. Selective O₂ peaking with a monochromatic filter at 10600 \AA then resulted in very high IR sensitivities. (Ref. Rpt. No. 8,9.) The highest sensitivity was achieved in Tube No. 202: W.L., 69 μ a/l; 2540, 13.5 μ a/l. For representative electrical performance data, see Table I of this report.

CONFIDENTIAL

~~CONFIDENTIAL~~

RE: DD-254 4/14/70

^u
(S) It was, however, found that "Hip" could not be doped

for lower thermionic emission. Efforts to suppress thermionic emission also resulted in a suppression of the very high IR sensitivity and gave surfaces comparable to those previously achieved. (Ref. Rpt. No. 9.) A possible exception was only prewetting with Potassium instead of Cs which in a few instances retained high IR sensitivity with somewhat lower thermionic emission. (Ref. Rpt. No. 16.)

^u
(S) The highest IR sensitivities, however, undoubtedly resulted from the application of Cs only with selective O₂ peaking. For typical spectral response curves, see Fig. 1-3.

^u
(S) On the whole, the high cathodes processed with "Hip" retained their sensitivity well. Slump was observed primarily on those cathodes which showed "bake-off" during processing. (Ref. Rpt. No. 11.)

(U) Several environmental factors during Ag evaporation were investigated. One series of experiments explored the

~~CONFIDENTIAL~~

(U) influence of the substrate temperature on cathode formation. It was found that if the substrate was held at temperatures above 90°C, a different behavior of the Ag base was observed. The Ag layer looked more metallic and was highly reflecting. Also, the "uptake" of Cs during the following activation was much larger than usual. These effects became stronger with increased substrate temperature. (Ref. Rpt. No. 5-7.)

(U) Lowering of the substrate temperature to the range of -10 to -15°C resulted in somewhat colorless Ag bases. Neither extreme resulted in high cathodes. (Ref. Rpt. No. 6,7.)

(U) We feel, therefore, that the range of 25 to 40°C, which was used in the large majority of our experiments, is the optimum temperature for the laydown of the Ag base.

Vacuum during Ag evaporation was typically in the range of $2-8 \times 10^{-8}$ mm.

(U) Several experiments were undertaken to study the

(U) effect of a high field between evaporator and cathode area. With +2500V or +5000V applied to the cathode area, deflection of the Ag beam apparently takes place. Heavier deposits were observed in the center of the cathode area while the deposit close to the aluminized ring was much thinner. An application of high negative voltage to the cathode area did not result in any observable effects. This, of course, supports the contention that at least some of the Ag atoms are positively charged. (Ref. Rpt. No. 6.)

(U) Similar ionic currents were also observed later on during Ag evaporation, as a rule. The interesting observation was made that such currents were quite strong in the beginning of the Ag evaporation, declined and remained at a steady level during continued Ag evaporation, and began to increase again as measurable conductivity of the Ag layer began to appear. (Ref. Rpt. No. 24.)

CONFIDENTIAL

(U) Changes of the voltage applied for the ^{RE DD-254 4/14/70} glow

discharge after Ag evaporation did not result in any observable changes of performance. (Ref. Rpt. No. 20.)

^u
~~(S)~~ It was observed in the related "PIP" contract that a short evaporator-to-substrate distance resulted in poor cathodes. An increase of this distance from the usual 1-1/2" in the bulb structure to 2-3/4", however, did not produce any noticeable change. (Ref. Rpt. No. 17,18.) We can conclude that a distance of 1-1/2" is sufficiently large for good cathode formation.

^u
~~(S)~~ In two tubes (No. 0-256, 0-285), a thin film of bismuth was evaporated deliberately to about 2-3% coverage, followed by the usual overnight bake. Cathodes formed reasonably well. (Ref. Rpt. No. 13, 15.) However, the expected suppression of the thermionic emission was not observed. These two experiments were made to amplify the possible existing condition of a thin Bi film formed on the

CONFIDENTIAL

CONFIDENTIAL

RE: DD-254 4/14/70

^u
(S) cathode area during the extended high temperature bake.

While it was thus proven that good cathodes can be formed on such thin Bi films, a positive identification of a thermionic emission suppression could not be shown. This is in contrast to the proven suppression effect of the Bi aftertreatment after completed cathode formation (See Final Rpt., pg. 24-25).

(U) Two optical improvement thoughts were tried on the semitransparent cathode.

(U) One semitransparent cathode was formed on a "grooved glass plate" which was supplied by Ft. Belvoir. The exact geometry of the grooves was not known. An optical enhancement was observed at the blue end of the spectrum. It had been shown in the previous contract, AMC-136(T), Rpt. No. 37-39, that optical enhancement effects would be expected in the region of high transmission of the semitransparent cathode which is in the blue and green.

(U) The expected change of response with angle of incidence was observed on the grooved plate. The pertinent Table in Rpt.

CONFIDENTIAL

(U) No. 21 is reproduced under Table II of this report. It should be noted that the enhancement, compared with the sensitivity of a normal semitransparent cathode, is about 6-10X for the 3900Å and 4535Å line, about 3-5X for the 5050Å line with factors getting much lower with increasing wavelengths.

(U) Another idea was investigated in connection with the preparation of space reflective cathodes. The use of a dielectric spacer of a coupling refractive index between the glass and the cathode should result in a lowering of the reflection from the high refractive index cathode into the low refractive index glass. Although the reflection of the S-1 is not very high in the IR region, it is still in the range of 12-25%. (the reasons for the fact that the S-1, also a very high refractive index medium, has a low reflection into the glass, are explained in Chapter IV of this report). We have formed several cathodes on TiO₂ films which were deposited on glass. (The refractive index of TiO₂ is around 2.6 for the IR.) Front reflection suppression was actually

(U) observed. However, only average cathodes were achieved on the TiO_2 , in the few trials performed and did not allow evaluation of the idea. On these few surfaces it was also observed that the thermionic emission was unusually high for the IR sensitivity range. No explanation for this can be given. For a detailed description of the optical and electrical behavior of such cathodes and the observations of generally increased absorption with a slower drop-off in the IR, see Rpt. No. 12, pg. 5-7, and Table II; also, Rpt. No. 21, pg. 5. Figures 4-7 are reproduced here and show optical and electrical performance of two such surfaces. (For sensitivity data see also Table I of this report.)

(U) It should be stressed that the method which eventually resulted in the best cathodes on the dielectric spacer in the SpRC (layer method) was not tried out in this connection. Any further attempt to improve the semitransparent S-1 should also evaluate the "layer cathode" processed on high refractive index, transparent, dielectric substrates.

(U) Performance data for surfaces of interest are given

~~CONFIDENTIAL~~

RE DD-254 4/14/70

(U) in Table I. These data cover, where available, the entire period of 1963-1969 for both S-1 research contracts.

III. THE LAYER METHOD

(U) The observation that "Hip" seemed to represent the best achievable method, based on the original Du Mont method, led to the exploration of other, radically different, preparation techniques.

^u
~~40~~ It had been found earlier that a thin layer of Ag (3-8% coverage) was able to accommodate Cs, expressed as a fairly large change of transmission readings and that cycling of Ag and Cs could be continued until a cathode with the usual thickness was built up. Final exposure to oxygen then resulted in a reasonable sensitivity. (See, e.g., Tube No. 0-215, 0-216, Ref. Rpt. No. 10, pg. 4.)

(U) The interpretation of the optical data of the S-1 then suggested the investigation of Cs₂O layers. (See also Chapter IV of this report.)

~~CONFIDENTIAL~~

~~CONFIDENTIAL~~

RE: DD-254 4/14/70

^u
~~(S)~~ The experiments showed that, although Cs-O layers

cannot be built up on glass alone - apparently because of a poor accommodation coefficient - such heavy layers can be built up through alternating cycles of cesium and oxygen in a form similar to the one described before with Ag-Cs. Figures 8 and 9 show the development of such a heavy Cs-O layer.

^u
~~(S)~~ Because of the similar activation schedule, we had reason to assume that the cesium oxide formed, in this case, was the same type of oxide which was formed in the S-1. The color of this film was usually a light rose-violet, which upon additional evaporation of Ag changed toward the more blue-violet color of the normal S-1. Optical aspects are discussed in Chapter IV of this report; for data see Table III here.

^u
~~(S)~~ This film, consisting primarily of cesium oxide, had reasonable sensitivity with some IR, but processing was rather touchy, i.e., if cycling of Cs-O was continued above a certain optimum point, sensitivity usually disappeared permanently.

For detailed reference, see Rpt. No. 24, pg. 6-9.

~~CONFIDENTIAL~~

CONFIDENTIAL

RE: DD-254 4/14/70

^u
(S) We then tried to use this phenomenon for the development of a new processing schedule. It was found that additional evaporation of Ag onto such a heavy Cs-0 film usually resulted in good sensitivity. (Ref. Rpt. No. 27, pg. 3-5.)

^u
(S) A typical processing method resulting from this aspect of the investigation is as follows:

- 1) A thin layer of Ag (2-8% coverage) is evaporated onto the glass (no prewetting).
- 2) A number of cycles Cs-0 is then applied onto this thin base until stability of sensitivity is achieved.
- 3) Peaking of response is then achieved by additional Ag evaporation.
- 4) If the sensitivity does not rise satisfactorily upon additional Ag, the evaporation of Ag is stopped and additional Cs-0 cycles are again applied, and so on.

^u
(S) The transmission measurements of the layer cathode show a reversal of percentages of Ag versus Cs-0:

CONFIDENTIAL

~~CONFIDENTIAL~~

RE: DD-254 4/14/70

u
(6)

<u>Tube No.</u>	<u>% Ag, Total</u>	<u>% Cs-O, Total</u>
5235	26.5	40.5
5238	30.5	37.5
5642	35.5	28.5
5644	32.0	38.0

(6) In comparison with the normal semitransparent cathode (initial Ag coverage: 45-55%), the percentages are considerably changed. It appears, however, that the "missing thickness" of Ag is made up by increased thickness of cesium oxide until a certain optimum thickness, necessary for good response is achieved. Thus it appears that optimum performance, which is in the case of the S-1. synonymous with good IR response, requires a certain thickness, but that the individual constituents can vary in wide ranges. Similar "compensation" effects have also been observed in the spectral response. (See Final Rpt., AMC-136(T), pg. 35.)

(U) This peculiar behavior becomes understandable in connection with the optical constants of the S-1 (See Chapter IV, this report), which requires this surface to have a thickness of n^d/λ close to .5 if processed to optimized performance.

~~CONFIDENTIAL~~

~~CONFIDENTIAL~~

RE DD-254 4/14/70 *ff*

(U) It appears, by the way, from our optical measurements and determinations of the thickness d , refractive index n , absorption coefficient k , that similar compensation effects occur in other photocathodes also.

^u
(S) The main advantage of the layer method seems to be that it apparently obviates the acute dependence of the cathode quality on the initial condition of the Ag base. (For a detailed discussion of this influence, see Final Rpt., AMC-136(T), dated May 12, 1967, pgs. 8-15.)

^u
(S) Thus it was possible to form good cathodes in the unfavorable image converter geometry with this method. Also, the investigations of cathode processing in the SpRC (Chapter V of this report), have eventually led to the layer method as the best possible formation schedule.

^u
(S) Spectral response of the better layer cathodes also show a more shallow slope towards the threshold which is a desirable effect. (See Fig. 10, 11, this report.)

~~CONFIDENTIAL~~

~~CONFIDENTIAL~~

RE: DD-254 4/14/70 *B*

(c) The observation that cesium oxide layers could be built

up on very thin Ag films to fairly heavy deposits (40-50% transmission) led to the speculation that similar Cs-O deposits can be built up on other thin metal films resulting in different types of cathodes. Only one such attempt was made on a thin Bi film. However, no "build-up" of cesium oxide deposits was possible. The entire change of transmission took place upon the first cesium interaction, with subsequent O₂ exposure having very little effect. In optical performance and appearance, this cathode more closely resembled a cesium antimony type. Because of the shift of interest to the SpRC, no other investigations on other metals was made.

(c) A continued effort in this direction, however, seems warranted with metals more resembling Ag than Bi does. It is possible that other IR-sensitive cathodes could be found in this manner. This assumption is based on the fact that the structure of any very thin film of metal will resemble the island structure of an Ag film. This is in contrast to heavier films where the structure of the Ag film is rather unique.

~~CONFIDENTIAL~~

IV. OPTICAL DATA AND CONSTANTS OF THE S-1 AND RELATED

(U) In the last two quarters of the previous effort, (AMC-136(T) attempts were made to determine the optical constants n (refractive index) and k (absorption coefficient).

(U) During this previous effort, the three optical data:

Reflection into the substrate (glass) R_p

Reflection into vacuum R_v

Transmission through substrate and photocathode T

were measured on several model surfaces.

(U) All three quantities were measured as percentages: The reflectances against the reflection $1 - \epsilon_\lambda$ of an opaque Ag mirror, (where ϵ_λ is a wavelength dependent factor ranging from .06 for 3900\AA to .01 in the infrared), the transmission against an uncoated bulb under analogous geometrical conditions.

(U) In theory these three data should be sufficient to determine n , k , and the physical thickness d . In practice, however, the computational problems are formidable. The three quantities can be solved only with the help of a computer program and then only in fair approximation.

(U) The equations, which give these three quantities in involuted form, were developed in Rpt. No. 12 and these derivations are reproduced here in Addendum I; see also Fig. 12 this report.

(U) Simplified equations of the type I, II, III, (See Addendum I) were used in Rpts. 37-39 of the previous effort, AMC-136(T) to compute n and k for one model surface, tube No. 113A. The values arrived at, at that time, are in error because no consideration has been given to the presence of the second glass-air boundary.

(U) It is quite obvious that these corrections for the air-glass boundary will decrease the already rather small front reflection of the S-1. It is because of this reason that the values derived previously are not considered representative for the true optical data of the surface. The corrected optical data for our model surfaces are shown in Fig. 13-19 of this report.

(U) Equations VII - IX of Addendum I are now the corrected quantities R_{PC} , R_{VC} , T_c which constitute the triplet sought in the computer program.

(U) The at first available program gave these quantities for:

$$\begin{array}{llll} 0 < k < 7.0 & \text{Stepsize } \Delta k & = & .20 \\ 1.0 < n < 5.0 & " & \Delta n & = .25 \\ 0 < d/\lambda < .20 & " & \Delta d/\lambda & = .005 \end{array}$$

Graphs were made to determine the general behavior and are shown in Fig. 20-34. (See also discussion in Rpt. No. 18, pg. 3-5.)

(U) The practical procedure is that one tries to match one triplet of corrected data as accurately as possible to a triplet of computer data. Actual computation requires interpolation between the values of the computer program.

(U) It soon became obvious that the evaluation of this program for the optical data of the S-1 was unusually cumbersome. The low front reflection together with the large vacuum reflection and the fairly high transmission could only occur in the region around $n^d/\lambda = 1/2$. As the enclosed graphs show, the maxima and minima are very steep there and very small changes in one or the other parameter caused large changes of the optical performance. Furthermore, values to the left and right of the minima are fairly equal. It was for this reason that a search for solutions took an inordinate amount of computational effort.

~~CONFIDENTIAL~~

RE: DD-254 4/14/70 *JS*

(U) A similar situation is even more pronounced in the case of the Ag-layer alone. (Tube No. 168, 559; see Fig. 13, 14.) These layers have very small R_F combined with high R_V . This again results in a much larger thickness than expected and also in high refractive indices.

~~(S)~~ A possible explanation for these results may lie in the fact that, as we definitely know, the Ag layer is not a homogeneous slab of material but consists of clearly separated micro-crystals. This structure is also retained in the completed S-1, as our photomicrographs have shown.

~~(S)~~ It is quite possible that a layer of such structure displays a rather abnormal optical behavior in the direction of its base versus the direction of its top surface. The properties of the Ag layer, i.e., the large difference between front and vacuum reflection seem, to a large extent, retained in the S-1.

~~(S)~~ To my knowledge, there are no combined measurements of vacuum reflection and front reflection for thin Ag films or S-1 cathodes known in the literature and this problem, therefore, has not been considered at all.

~~CONFIDENTIAL~~

~~CONFIDENTIAL~~

RE DD-254 4/14/70

(S) Similar difficulties do not seem to exist for the alkali

antimonides. In their case, the evaluation of the three measured data (T , R_p , R_v) have resulted tentatively in a certain thickness which fits reasonably over the entire spectrum. The thickness thus derived at is in reasonable agreement with previous estimates.

(S) Of course, the formula for R_p , R_v , and T are derived with the assumption of a homogeneous, isotropic material. It seems that such a condition is reasonably well fulfilled in the case of the group of the alkali antimonides while this may not be the case at all for the S-1. The S-10, whose optical data seem to point to a connecting link between these two groups, also seems closer to the alkali antimonides.

(S) While it appears that under such circumstances the determination of the optical constants may not result in an agreement between "optical thickness" and actual physical dimensions, I do think that values which will represent the behavior of the admittedly inhomogeneous S-1 can be used to determine and predict its behavior. It is also clear that values of the optical constants

~~CONFIDENTIAL~~

~~CONFIDENTIAL~~

RE: DD-254 4/14/70

~~147~~ which fit the optical data of the S-1 can also be used with a better chance for success in any model of this complicated surface. Of course, the knowledge of the optical constants is of special importance in the space reflective mode.

(U) With the computer program available only up to $n=5$, it was found that a certain thickness d/λ which fitted to the data of the S-1 model surface in the IR did not fit with the shorter wavelengths below 5000\AA . The values computed for n also did not fit a smooth curve.

(U) Calculations, at that stage, were made for four surfaces:

R5 - which is a Rubidium Cs-processed surface.

340, 113A - which are good Cs-processed cathodes.

332 - appearance-wise a somewhat thinner, low IR, cathode.

For R5, a thickness $d\ 1170\text{\AA}$ - gave an excellent fit at 6000\AA & 11150\AA .

For 340, $d\ 1150\text{\AA}$ - gave a very good fit at 11500\AA and 6570\AA .

For 113A, $d\ 1080\text{\AA}$ - gave a good fit at 11500\AA and 5600\AA .

For 332, the seemingly thinner cathode, a thickness $d\ 1300\text{\AA}$, was arrived at with good fit at 10500\AA and 6500\AA .

(U) The data computed are reproduced in Addendum II.

~~CONFIDENTIAL~~

(U) Between these points, a fit with refractive indices $n < 5.0$ was not possible. It appeared thus that the curve for n would have to show a jump to higher values and back again. Although the fit computed for the lines given above was quite good, the large thickness and the behavior of n did not seem satisfactory.

(U) At that time, an investigation of the optical properties of cesium oxide - hopefully the one which is present in the S-1 - was begun. Processing techniques have been described in Chapter III. For the optical and electrical characteristics of one such heavy Cs oxide layer (final coverage 40% white light) on a thin Ag base (5% coverage), see the enclosed Table III.

(U) This investigation was undertaken, primarily, to try for another explanation of the optical data of the S-1, because the results quoted above did not allow satisfactory interpretation with one thickness for the entire spectral range, and was based on the island structure of the Ag-layer and finished cathode, which was revealed in numerous microphotographs under AMC-136(T).

(U) The assumption was that it may be possible to explain these data through an addition of the optical properties of the Ag base, covering X% of the cathode area and the optical properties of a Cs oxide layer covering the previously empty portion (1-X%) of the cathode area. To this purpose, we attempted to use previous measurements on one surface, where optical data were measured throughout the development of the surface: Tube #597, Rpt. No. 29, AMC-136(T); see also Fig. 35, 36, 37, this report. The following uncorrected optical data were measured there:

<u>in n</u>		<u>.39</u>	<u>.45</u>	<u>.505</u>	<u>.60</u>	<u>.80</u>	<u>.90</u>
R _F	I	5.0	8.0	8.0	8.0	7.0	--
R _F	II	6.8	11.0	15.0	17.0	13.5	--
R _F	III	7.0	11.5	15.0	18.0	15.0	14.0
T	I	68.0	59.0	52.0	52.0	60.5	66.5
T	II	73.0	60.5	48.0	34.5	37.0	44.5
T	III	74.0	60.5	48.0	33.5	35.0	43.5

(U) Here State I refers to the very lightly oxidized Ag base; State II refers to this base after cesiation; State III refers to State II + O₂ peaking. R_F stands for Front Reflection, T for Transmission.

(U) In this sample we see quite clearly the peculiar effect of the increase in blue transmission of the finished cathode vs. the Ag base, while IR transmission greatly decreased. Vacuum reflection had not been measured on this sample.

(U) The following relations would have to apply:

$$R_I = X \cdot R_{Ag} + (1-X)R_{GL} = X \cdot R_{Ag} + (1-X) \cdot .08 \quad (GL = \text{Glass})$$

$$R_{III} = X \cdot R_{Ag} + (1-X)R_{CsO_2}$$

$$T_I = X \cdot T_{Ag} + (1-X) \cdot .92$$

$$T_{III} = X \cdot T_{Ag} + (1-X)T_{CsO_2}$$

$$R_{III} - R_I = (1-X) \cdot (R_{CsO_2} - .08)$$

$$T_{III} - T_I = (1-X) \cdot (T_{CsO_2} - .92)$$

(U) A simple cross-check with the values given in Table III for Tube No. O-429, which can be considered representative of the optimum Cs oxide thickness which still gives photosensitivity (see Chapter III of this report), shows that these relations are not at all fulfilled. The absorption properties of the Cs oxide layer, per se, in the IR are not sufficient to explain the large changes in this region, while the decrease of absorption in the blue is not at all understandable

(U) neither because of the relatively heavy absorption of the Cs oxide layer in the blue. This proves conclusively that the Ag base is changed and a homogenization of the entire cathode film takes place. We therefore decided to continue explanation efforts under the assumption of a homogeneous film as before.

(U) We tried to get a continuation of the computer program for higher values of " n ". Such a continuation was received for $5 < n < 7.5$, through private channels and only in the last months of the contract. Again, the evaluation of these data took a considerable amount of time because of the same reasons as mentioned above. It was therefore only possible to compute one model surface, No. 113A. The measured and interpolated values of the optical quantities of this surface which have been used are given in Table IV of this report. The best results for several wavelengths are reproduced in Table V.

(U) The best results are obviously achieved for the range $d = 570-590\text{\AA}$. Values above 9000\AA could no longer be computed because the refractive index increases above 7.5. We see that $n \cdot d/\lambda$ is always close to .5 with an apparent minimum around 5000\AA and a slight increase

(U) towards the blue and IR. It appears that the strong increase of n towards the IR is necessary to maintain the condition nd/λ close to .5. As the previous computations show, the numerical values of n will get smaller for larger thicknesses but the previous values do not fit a smooth curve as the best solution here, around $d = 570\text{\AA}$, does

(U) A graphical representation of n and k against λ in \AA and eV is given in Fig. 38,39, this report. As can be seen, a certain range of thickness results in nearly parallel curves for n , with n inversely related to d in order to maintain the condition $nd = \lambda/2$. A family of parallel curves which fit for several triplets covers a range of d ; probably within only $\pm 10\%$ around the best value of 572\AA . It was not possible to determine the exact width of this range within the time available, however. Values above 610\AA and below 550\AA have not resulted in acceptable fits over larger spectral regions. From the previous computations (see Addendum II), it is expected that the other S-1 surfaces will show a similar behavior.

(U) The shape of the curve for k is rather insensitive to small changes of d (actual numerical values of k become, of course, slightly smaller with larger d). The curve seems to indicate a minimum around

(U) 3500\AA , which is to be expected and would be followed further by a steep increase due to the Ag absorption edge, in the UV.

(U) Another independent estimate of the thickness of the S-1 can be gained from surface O-244T; see Fig. 4 this report (for reference see also Rpt. No. 31, Fig. 1 and pg. 5). This surface was formed on a dielectric spacer of TiO_2 whose thickness was computed to be 200\AA . This surface displays a clear interference minimum in reflection around 5100\AA . If we take the usual phase condition for a reflection minimum which will apply to a good approximation regardless of the absorbing properties of the S-1, we have:

$$2\pi/\lambda (n_1 d_1 + n_2 d_2) = \pi \quad n_1 = n_{\text{TiO}_2} \approx 2.6$$

$$(2.6 \times 200 + n_2 d_2) = 2550$$

$$n_2 d_2 = 2030\text{\AA}$$

(U) If we take the refractive index of 113A at that point, as an approximation, $n_{5100\text{\AA}} = 3.8$, we get $d_2 = 535\text{\AA}$. This close correlation is certainly gratifying especially if we consider that the initial Ag coverage in 113A was 55%, while it was only 50% in O-244T, which would even explain the somewhat lower value of d arrived at.

(U) Although outside of the scope of this contract, several optical constants of other photocathodes were computed. The following data are given:

S-10 Tube No. 835

3900Å : $n = 2.32$ $k = 1.0$
 $d/\lambda = .11$ Thickness $d = 430\text{Å}$

S-20 Tube No. SS-20

5050Å : $n = 2.875$ $k = .43$
 $d/\lambda = .095$ Thickness $d = 480\text{Å}$

S-20 Tube No. 086

4535Å : $n = 3.58$ $k = .56$
 $d/\lambda = .105$ Thickness $d = 475\text{Å}$

9450Å : $n = 2.26$ $k = .10$
 $d/\lambda = .05$ Thickness $d = 470\text{Å}$

S-9 Tube No. 103

4535Å : $n = 4.62$ $k = .82$
 $d/\lambda = .10$ Thickness $d = 455\text{Å}$

S-11 Tube No. BX3

3900Å : $n = 4.75$ $k = 1.22$
 $d/\lambda = .095$ Thickness $d = 370\text{Å}$

6000Å : $n = 3.25$ $k = .055$
 $d/\lambda = .065$ Thickness $d = 390\text{Å}$

K-Cs Surface Tube No. B-1

3900Å : $n = 4.50$ $k = 1.07$
 $d/\lambda = .095$ Thickness $d = 370\text{Å}$

(U) The interpretation of the optical data is not unduly difficult for all other photocathodes, except the S-1, and a thickness arrived at usually fits well over the whole spectrum. This is due to the fact that none of the other photocathodes, like the S-1 does, comes close to the region $n^d/\lambda \sim 0.5$ where the interpretation becomes very difficult. The computed values agree generally well with other published data, if any.

(U) It is planned to present more complete data in a publication.

IV. SPACE REFLECTIVE CATHODE

(U) After the first three quarters of this contract, an ever increasing part of the effort was devoted to the formation of a space reflective S-1.

(U) This was done because of the expressed interest of the contracting agency, although we had made it clear that strong enhancement effects in the IR region were not to be expected because of the already known optical behavior of the S-1. Specifically, any effect

(U) comparable to the S-20 - which is nearly optically transparent around 8000-8500Å - was not to be expected.

(U) The study was, in the beginning, hampered through the choice of TiO_2 as the dielectric spacer which turned out to be unsatisfactory. TiO_2 was selected because of its high refractive index of 2.6 in the IR. It was thought, at that time, that we could add a side line and also improve the performance of the semitransparent S-1 because of front reflection suppression due to this high refractive index.

(U) We assumed that formation of the S-1 on a dielectric substrate monitored for vacuum incidence response would not be very different from the processing of the S-1 on the same substrate backed by a metallic mirror. But we observed that growth of response and processing behavior was quite different if vacuum incidence response was monitored. The very different reflection for the two sides of the cathode makes that understandable.

(U) Aluminum was selected initially for the metallic backing because it was assumed that possibly an interaction between the Ag film and the cathode processing would take place. We found, however,

(U) that it was impossible to convert Ti into the wanted dielectric TiO_2 on aluminum without severe "break up" effects.

(U) We were not able to develop any satisfactory method of forming TiO_2 layers on aluminum. We then switched to silver as the backing mirror. Results were somewhat better and we were able to form several low, space reflective cathodes. For a description of the best method developed for conversion of metallic Ti into TiO_2 , see Rpt. No. 19, pg. 3 and Table I there.

(U) On the whole, the combination of Ag + TiO_2 gave an unsatisfactory yield of usable reflectors. In most cases, the Ag mirror showed a tendency to cloud upon the TiO_2 conversion. All our efforts to correct this remained unsuccessful. We therefore decided to switch to SiO as the dielectric spacer. A satisfactory method of evaporation was eventually developed by evaporating from a generator type SiO source which is fitted with a small opening. This source resembles a point source and good uniformity of the deposit on the spherical bulb type was usually achieved. (This uniformity was verified through the uniform color of the finished cathode over the entire deposition

(U) area). Through the uniform heating of the evaporant through the Ta generator envelope, sputtering was virtually eliminated.

(U) However, even with SiO the Ag mirror still showed clouding tendencies upon exposure to cleaning solvents or baking. Only after we switched back to Al a satisfactory yield of good films was observed. As a matter of routine, the glass substrate was heated to 150-200°C during SiO evaporation. On the aluminum mirror SiO films of any desired thickness could be deposited, cleaned, and baked without "break up".

(U) It should be mentioned here that TiO as well as SiO films of any thickness could be deposited to glass proper, adhered well and showed no "break up" effects.

(U) A schedule of the preparation of the reflector is as follows:

- a. After the usual hard glass cleaning, the Ag strip cathode connection is painted onto the glass and baked at 120°C for about 1 hr.
- b. Aluminum is evaporated in a 10^{-6} vacuum to opacity.

This evaporation is completed in 7-10 seconds. A mask of approximately one-half inch in diameter shields a portion of the later cathode area which can be used for front transmission measurements.

(U) c. The aluminum mirror is baked at 250°C in air for 2 hours.

d. SiO is evaporated from a generator-like source to the desired optical characteristics in a 10^{-6} vacuum.

e. After deposition, the SiO deposit is washed with deionized water, isopropyl and acetone and then blown dry.

(U) During evaporation, the transmission through the glass plus SiO deposit is measured through the open hole in the mirror. At the same time, the reflection from the aluminum backing plus growing SiO deposit is measured. Both of these measurements are done with suitable monochromatic (or color) filters. The evaporation of the SiO is performed stepwise and these two optical characteristics are measured after each step.

(U) As the optical data of opaque Al and SiO are known in the IR (at least in good approximation) the thickness of the SiO deposit can be computed from reflection and transmission measurements.

(U) These computations have been performed and their results and discussion are presented in Addendum III.

(U) The optical behavior of the sandwich Ag-SiO-Ag (essentially an interference filter) was studied in stepwise evaporation of the Ag layer onto the space reflector. Figure No. 40, this report, shows the behavior of two samples, observing the expected minimum and turn-around to higher values in reflection. For a detailed discussion see Rpt. No. 27, pg. 7.

(U) Only when the problem of the space reflector was solved satisfactorily - after an undue amount of time and effort - could we proceed to the problem of cathode formation. All previous attempts to form cathodes on substrates with any degree of "breakup" had resulted in poor cathodes.

(U) During cathode formation, two optical measurements were made: Transmission through an area covered with the SiO layer only and vacuum reflection of a monochromatic line (usually 9500Å). This allows us to compare performance and "thickness" of the cathode formed on the space reflector with the semitransparent cathode. At the same time, reflection of a monochromatic line (here 9500Å), is measured from the space reflective cathode simultaneously with the sensitivity at this line.

~~CONFIDENTIAL~~

RE DD-254 4/14/70

²²
(c) Thus we gain some insight in the formation mechanism. In the initial stages, Ag evaporation and cesium interaction lower the reflection drastically while oxygen interaction increases reflection (as well as transmission). The very strong sensitivity of the vacuum reflection with increasing thickness becomes less and less pronounced as the cathode becomes heavier. This is, of course, explainable from the fact that we are getting closer to a minimum in the turnover point of the reflection. We have indeed observed that additional Ag evaporation would lead to an increase of the reflection. This behavior would also be shown from the two examples in Figure 40. Figure 41 shows a graphical representation of the formation. This surface #5243 is an example of the layer cathode.

²²
(c) The layer method (see Chapter III) has given the best yield of good cathodes from among all the processing methods investigated. The layer method, of course, permits, by its nature, to observe the effect of small dosages of the cathode constituents and their effect upon absorption properties of the SpRC. This method which builds the thickness of the cathode up, layer by layer, has also demonstrated

~~CONFIDENTIAL~~

(S) nicely the fact that IR sensitivity appears only after a certain thickness of the cathode has been reached. It was found that, although monochromatic absorption (as a minimum of reflection) could be peaked quite clearly, this did not always result in a peak of photoresponse. The 9500Å response usually peaked around or slightly before the 9500Å absorption and additional attempts to increase absorption (usually through small additions of Ag) had, in the majority of cases, no beneficial effects.

(U) While the evaporation of the SiO film on the Al mirror causes only slight interference phenomena, the formation of the cathode produces sharp interference effects in reflection. These effects are, of course, strongly dependent on the uniformity of the spacer and the thickness of the cathode. Although visually the cathodes appear uniform, rather large variations have been observed. As a comparison of different spots shows, a certain correlation between increased absorption and photoresponse seems to exist in the visible range. For data taken on some early surfaces, see Rpt. No. 24, Table II.

(U) As the layer method was established as the best way to process SpRC's, it was unfortunate that optical constants for this type of cathode had not been computed. There was, however, good reason to expect that the layer S-1 would have a similar curve shape for n as the semitransparent S-1.

(U) The equations for the reflection of $Al+SiO_2$, shown in Addendum III were used to determine the thickness d of our different fractional spacers (percentage of the full possible change of the reflection).

(U) Expressed as percent of initial reading ($100\% = 86.5\%$ true reflection) we get:

1/1 spacer	(100 to 72.2%)	=	880Å
2/3 "	(100 to 81.5%)	=	660Å
1/3 "	(100 to 89.5%)	=	440Å
1/6 "	(100 to 95.0%)	=	300Å
1/9 "	(100 to 96.5%)	=	220Å

(U) Experiments with spacer thicknesses well below 200Å and with thicknesses above 800Å were unsuccessful. The best yield was achieved with the formation of layer cathodes on 1/6 spacers.

(U) In appearance, cathodes on very thin spacers exhibit a silvery color (similar to an opaque cathode), the $1/12$ spacer cathodes are medium dark green, the $1/6$ spacer ones are dark green, the $1/3$ spacer ones are dark blue green, the $2/3$ spacer ones are dark blue-violet, and the heavier spacer cathodes are bright blue.

(U) Electrical properties of the surfaces of interest are shown in Table VI, this report.

(U) In the following, a cursory determination of the thickness of the S-1 SpRC is given in consideration of the results of Chapter IV. To this purpose, we list the measurements of reflection taken on three good SpRC's, No. 52107, 52110, and 52121 (all layer cathodes); see also Fig. 42, this report:

	in μ	<u>.39</u>	<u>.45</u>	<u>.505</u>	<u>.60</u>	<u>.80</u>	<u>.95</u>	<u>1.15</u>
52107	:	28.0	3.0	10.5	20.5	12.0	9.5	16.0
52110	:	14.0	9.5	24.0	28.0	15.5	12.0	14.0
52121	:	30.5	8.5	19.0	25.5	15.0	11.5	47.5?

(U) All of these surfaces were processed with observation of vacuum reflection at 10600\AA . All three show a clear minimum of reflection near 4535\AA and another minimum near 9500\AA . The exact locations

(U) of the minima were not established because of the few discreet points measured. We will, in the following assume a reflection minimum at 9500\AA .

(U) Processing was performed essentially to a minimum of reflection with the initial reflection of the Al+SiO given as starting point.

(U) For the minimum reflection the condition $nd = \lambda/4$ should be observed.

(U) If we insert the refractive indices of our model surface in this equation for the extremes of the curves in Fig. 42 we get

$$4500\text{\AA} : 3.65 \times d = 1125\text{\AA} \quad d = 308\text{\AA}$$

$$9500\text{\AA} : 8.0 \times d = 2375\text{\AA} \quad d = 297\text{\AA}$$

(U) Although the assumption that the S-1 on the space reflector will have the same refractive indices is not assured, the good agreement for d shows conclusively that they will show a proportionality (i.e., lie on a curve parallel to the ones shown for 113A). The numerical values for the extremes of course depend on the actual numerical values of n and k and cannot be computed without them.

(U) The rather shallow second minimum of reflection indicates that no pronounced "hump" in the spectral response curves can be expected and a more shallow slope of the IR response is actually what has been observed (See Fig. 43, 44, this report).

(U) Apparently the condition of optimized absorption in the SpRC and optimized response of the cathode ($n d/\lambda$ close to $1/2$) are quite far apart and this may well explain the inefficiency of the absorption as the intensity distribution will, of course, not be the one outlined for the semitransparent S-1 in Chapter VI.

(U) Future efforts in space reflective mode will have to be directed towards correction of this inequality.

VI. THOUGHTS ABOUT A MODEL OF THE S-1

(U) From all the work performed, the question arises whether it is possible to develop an explanation for the peculiarities of the S-1 photosurface.

(U) The simple sketching of a band model would explain very little because the values would have to be rather random without any theoretical foundation. Such attempts have been made repeatedly in

(U) the literature and have not been able to give a satisfactory theory. This is in contrast to the family of alkali antimonides which can be approached through the usual solid state methods.

(U) In order to understand the difficulties, we will first enumerate the differences between the S-1 and the alkali antimonides: The S-1 is the only photocathode of importance which shows optical absorption into the IR. In some of our measurements, absorption has been shown to exist as far out as 1.6 microns. Numerical values of this absorption may change from surface to surface according to thickness and processing. The fact that optical absorption takes place in the IR, of course, is the factor which permits some photoelectric conversion to take place in this region. (In this connection, some sources in the literature claim that very weak photoelectric emission in the S-1 has been observed as far out as 1.7 microns.) This is in sharp contrast to the alkali antimonides whose absorption goes to zero around .85 - .9 microns.

(U). The optical absorption in the IR appears to be preordained in the Ag base. As our investigations have shown, the Ag base layer

(U) itself has absorption in the IR (in most cases proven out to about 1.2 microns, see Fig. 13, 14) in the thickness commonly used in cathode preparation. Numerical values of this absorption again vary with preparation technique and thickness.

(U) In the Sb thicknesses used for cathode preparation, to the best of our knowledge, IR absorption above .9 microns is rather small.

(U) In cathode processing, the IR absorption increases strongly in the case of the S-1. Numerous examples have been given under the previous effort, AMC-136(T), see also this report, Fig. 35-37. In the processing of alkali antimonides, on the other hand, no IR absorption develops.

(U) It was, however, observed that IR absorption as well as sensitivity were dependent on attaining a certain thickness of the cathode film. The remarkable fact was uncovered that it made no difference in which manner this thickness was attained; that means the constituents of the cathode could be varied to a large extent. The observation of layer cathodes made it possible to observe this quite clearly. Thus, it was possible to obtain IR absorption and sensitivity by depositing

(U) heavy Cs-O layers on very thin Ag bases or depositing Ag-Cs layers with minute amounts of O₂; or, depositing heavy Ag layers with relative small additional changes through cesiation.

(U) Another fact is the quite large difference in the reflection and transmission of the S-1 versus the alkali antimonides. While in the alkali antimonides the reflection into the glass substrate is in the range of 35-45% in the region of high absorption, with values declining towards the IR, and the corresponding vacuum reflection is in a regular fashion higher in dependence on the absorption coefficient; the S-1 shows the previously discussed behavior of very low reflection into the glass (5% - 18%) with very much higher reflection into the vacuum.

(U) These remarkable properties tend to support the theory that the IR response of the S-1 is very much dependent on the achievement of a certain optical condition. This has led us to concentrate a great deal of effort on the determination of the optical data and constants of this surface. In the course of this investigation, we were also able to investigate the other photosurfaces and to draw comparisons. Reliable optical measurements of the S-1 in the IR are, as best we could determine, not available in the literature.

(U) The optical effort resulted in the determination of numerical values of the optical constants for a model surface which can be considered typical for the S-1.

(U) The interesting fact was established that throughout the computed range ($.4\mu$ to $.95\mu$), the values of $n \frac{d}{\lambda}$ had to be very close to .5 in order to explain the optical performance of the S-1. This resulted in very high refractive indices for the IR in order to maintain this condition with decreasing d/λ , see Fig. 38,39.

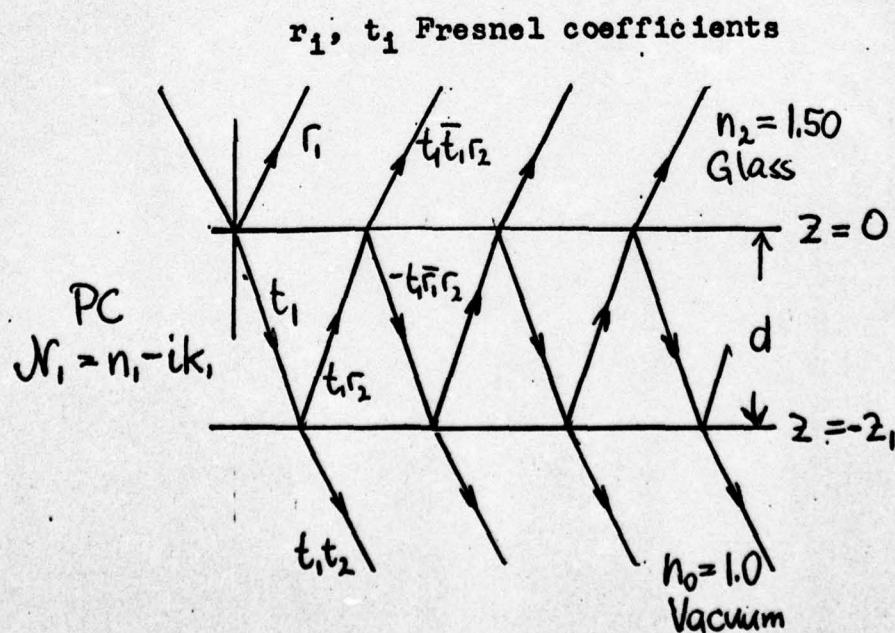
(U) This condition results in an intensity distribution in the cathode which will be shown later, and which is quite different from the one encountered in the alkali antimonides where $n \frac{d}{\lambda}$ is much smaller than .5, especially in the IR. This intensity distribution has also accounted fully for the differences of vacuum - and front absorption as well as the ratio of vacuum-to-front incidence response. Some of the thoughts which enter into this model have already been set forth in the Final Rpt., AMC-136(T), pg. 36-43.

(U) We quote from there: "The IR levels which are created through O_2 doping seem to be very close to the vacuum interface of the

(U) surface, while the states responding to the shorter wavelengths are probably distributed through greater thicknesses of the film. This hypothesis is supported primarily through observation of a slump and aftertreatments.....

(U) The IR response seems to emerge from layers of the film which are close to the vacuum interface. It seems that the further towards the IR we go the thinner the actual photoemissive thickness becomes¹¹.

(U) The following mathematical derivations are based on these thoughts which require the existence of a suitable probability function which governs the efficiency of emission due to the intensity distribution in the film:



(U) We consider a wave of unity amplitude ($E_0 = 1.0$) in normal incidence from $n_2 = 1.5$ (FI) upon the boundary $Z = 0$. Because of normal incidence, which simplifies the computation and shows all significant characteristics of the solution, the difference between the polarized components of E_p and E_s disappears. Very similar derivations apply to the case of vacuum incidence (VI).

(U) The summation of the waves travelling in the negative z direction results in $E^-(z) = t_1 [1 - r_1 r_2 + r_1^2 r_2^2 \mp \dots]$

in the positive z direction in

$$E^+(z) = t_1 r_2 [1 - r_2 r_1 + r_2^2 r_1^2 \mp \dots]$$

The appropriate phase change for moving from $z = 0$ to z inside the film

is $e^{-i\delta_1 z}$. $e^{-i\delta_1 z} = e^{-\delta_k z} (\cos \delta_n z - i \sin \delta_n z)$

$$\delta_1 = \delta_k + i\delta_n = 2\pi d/\lambda (n_1 + ik_1)$$

Adding the appropriate phase changes, and summing the terms shown above results in

$$t_1 e^{-i\delta_1 z} + \sum t_1 r_2 e^{i\delta_1 z} [1 - r_1 r_2 \sum + (r_1 r_2 \sum)^2 \mp \dots]$$

where

$$\sum = e^{-i2\delta_1 z}$$

(U) This leads after summation of the geometrical series to the complex electric field vector

$$\text{VI 1)} \quad E_1(z) = \frac{t_1 e^{-i\delta_1 z} + t_1 r_2 e^{-i\delta_1 (2z_1 - z)}}{1 + r_1 r_2 e^{-i\delta_1 2z_1}}$$

which gives the field in any point z in the film. It can be shown that this solution fulfills Maxwell's boundary conditions at both boundaries $z = 0$ and $z = z_1$. All more explicit calculations and proofs will have to be given in the publication of these findings.

(U) The intensity inside the layer n_1, k_1 is given by

$$I(z) = \frac{\sqrt{n_1^2 + k_1^2}}{n_2} (E_1(z) E_1^*(z))$$

After cumbersome computations we arrive finally at the intensity distribution

$$\text{VI 2)} \quad I(\bar{z}) = \frac{[(1+a_1)^2 + b_1^2] \{ e^{u(1-\bar{z})} + (a_2^2 + b_2^2) e^{-v(1-\bar{z})} + 2[a_2 \cos(u(1-\bar{z})) + b_2 \sin(u(1-\bar{z}))] \}}{e^v + e^{-v} (a_1^2 + b_1^2)(a_2^2 + b_2^2) + 2[(a_1 b_2 - b_1 a_2) \cos u + (a_1 b_2 + a_2 b_1) \sin u]}$$

in the cathode film. Here $\bar{z} = z/z_1 = z/d$

$$u = 2\delta_n d/\lambda$$

$$v = 2\delta_k d/\lambda$$

The denominator M is a constant, given by the thickness and the refractive indices.

(U) $a_1, b_1, a_2, b_2, A, B, C, D$ are the wellknown coefficients which determine the optical behavior of the film. They have been defined in Rpt. No. 12, pg. 8,9. There we find also the expressions which define the reflection and transmission of the cathode film.

For incidence from the vacuum we find the appropriate coefficients

$$\bar{a}_1, \bar{a}_2, \bar{b}_1, \bar{b}_2: \quad \bar{a}_1 = -a_1 \quad \bar{b}_1 = -b_1$$

$$\bar{a}_2 = -a_2 \quad \bar{b}_2 = -b_2$$

Note that a wave of unity amplitude coming from the medium $n_2 = 1.5$ has the energy : $E_2 = n_2 \times (A_2)^2 = 1.5 -$, - while a wave of unity amplitude coming from $n_0 = 1.0$ has the energy $E_0 = 1.0 \times (1.0)^2 = 1.0$

Of course, we obtain the numerical value of the transmission from the solution $I(z = z_1)$ to

$$T_0 = \frac{\sqrt{n_1^2 + K_1^2}}{n_2} E(z_1) E^*(z_1) \equiv I(1)$$

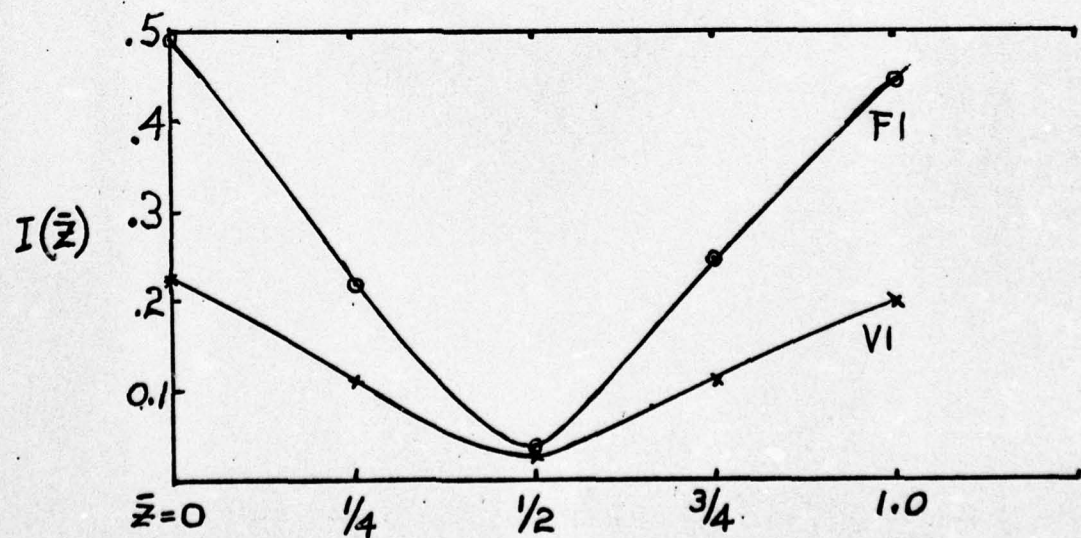
A similar expression then applies for vacuum incidence.

(U) The solution consists of three "waves", one going in the negative z direction ($e^{v(1-\bar{z})}$), one going in the positive z direction ($e^{-v(1-\bar{z})}$) and the third term which is the interference term.

(U) This intensity distribution has now been evaluated for the known n , k of the S-1^(113A) at several wavelengths. The case of 8000Å is shown as an example. Because of the large computational effort involved, approximate values ($n = 6.75$, $k = .60$) available from the computer program have been used. The intensity distribution for glass incidence is as follows: (All numerical values refer to the model surface 113A)

$\bar{z} = 0$	$I(0) = .495$	Glass - Film Boundary
$\bar{z} = 1/4$	$I(1/4) = .219$	
$\bar{z} = 1/2$	$I(1/2) = .037$	
$\bar{z} = 3/4$	$I(3/4) = .248$	
$\bar{z} = 1.0$	$I(1.0) = .436$	Vacuum - Film Boundary

$$\text{Transmission } T = \frac{n_2}{n_1} \times .436 = .29$$



(U) A similar distribution is found for the vacuum incidence:

$$I(0) = .215 \quad \text{Vacuum - Film Boundary}$$

$$I(1/4) = .108$$

$$I(1/2) = .026$$

$$I(3/4) = .110$$

$$I(1.0) = .196 \quad \text{Glass - Film Boundary}$$

$$\text{Transmission } T = \frac{h_1}{h_0} \times .196 = .29$$

The values at $I(1)$ result of course in the same value because the transmittance in both directions is the same.

(U) We can see the important fact that, regardless of the absorbing properties of the film, the intensity has again a maximum at the boundary $z = z_1$. The absorption can be computed from the numerical values of the three wave amplitudes in the brackets of eq. VI 2).

$$\text{Negative } z \text{ wave: } A(0) = e^v = e^{.53} = 1.70 ; \quad A(1) = 1.0$$

$$\text{Positive } z \text{ wave: } A(0) = e^{-v}(a_1^2 + b_1^2) = .33 ; \quad A(1) = .55$$

$$\text{Interference from: } A(0) \approx 2a_2 \cos u + \dots = 1.41 ; \quad A(1) = 1.48$$

This third term results in energy retained in the interference pattern which has to be subtracted.

(U) The absorption in % of unity incident energy is now given by

$$\frac{(1+a_1)^2 + b_1^2}{N} \cdot \frac{6.75}{1.50} \left(|1.70 - 1.0| + |.55 - .33| - |1.48 - 1.41| \right) =$$

$$= .146 \times 4.5 \times .85 = .56$$

The accurate value for 8000Å, computed with the accurate n, k, results in .59, which is a fair agreement.

The analogous calculation for the vacuum incidence results in

$$\frac{(1 + \bar{a}_1)^2 + \bar{b}_1^2}{N} \cdot \frac{1.5}{1.0} \frac{6.75}{1.0} \left(|1.70 - 1.0| + |.40 - .24| - |1.27 - 1.01| \right) =$$

$$= .072 \times 10.1 \times .60 = .43$$

Again a fair agreement is reached as the accurate figure is .415.

We can see thus, that this model is capable of explaining the large differences in vacuum - versus glass incidence absorption.

(U) Because of the condition $n \frac{d}{\lambda} \approx .5$, similar intensity distributions are observed for all wavelengths and similar agreements have been found (the specific example of $\lambda = 4600\text{Å}$ has been computed).

(U) The photoelectron production $i_{ph}(\bar{z})$ at any point \bar{z} is given by

$$i_{ph}(\bar{z}) = \eta I(\bar{z}) p(\bar{z})$$

η Conversion factor independent of λ
 $p(z)$ = Probability of emission

(U) Because of the difference of vacuum - and glass incidence, the two probability functions will be different. Assuming that $p(z) = 1/2$ at the vacuum boundary we get

$$\text{VI 3) Vacuum : } p(\bar{z}) = 1/2 e^{-\bar{z} F(\lambda, k)}$$

$$\text{VI 4) Glass : } p(\bar{z}) = 1/2 e^{-(1-\bar{z}) F(\lambda, k)}$$

if we select, as usual an exponential dependence.

(U) The following table gives some numerical values for escape probabilities for VI and FI.

		F=1.0	F=2.0	F=4.0	
$\bar{z} = 0$	VI	1/2	1/2	1/2	Vacuum-Film Boundary
	FI	.184	.067	.009	Glass-Film Boundary
$\bar{z} = 1/4$	VI	.39	.30	.184	
	FI	.236	.11	.025	
$\bar{z} = 1/2$	VI	.30	.184	.067	
	FI	.30	.184	.067	
$\bar{z} = 3/4$	VI	.236	.11	.025	
	FI	.39	.30	.184	
$\bar{z} = 1.0$	VI	.184	.067	.009	Glass-Film Boundary
	FI	1/2	1/2	1/2	Vacuum-Film Boundary

of course the thickness of the "effective active" layer decreases rapidly with increasing F.

(U) The total photoelectron production in the film is now given by

$$i_{ph} = \eta \int_{\bar{z}=0}^{\bar{z}=1} I(\bar{z}) p(\bar{z}) d\bar{z}$$

Because of the two different probability functions, the results of the integration are different for VI and FI.

VI 5)

$$i_{ph FI} = M \left\{ \frac{e^{v-F} - 1}{v-F} + (a_1^2 + b_1^2) \frac{1 - e^{-(v+F)}}{v+F} + \frac{2}{u^2 + F^2} \left(e^{-F} \left[-F(a_2 \cos u + b_2 \sin u) + u(a_2 \sin u - b_2 \cos u) \right] + a_2 F + b_2 u \right) \right\}$$

VI 6)

$$i_{ph VI} = \bar{M} \left\{ \frac{e^v - e^{-F}}{v+F} + (\bar{a}_1^2 + \bar{b}_1^2) \frac{e^{-v} - e^{-F}}{F-v} + \frac{2}{u^2 + F^2} \left(e^{-F} (u \bar{b}_2 - F \bar{a}_2) + \left\{ F(\bar{a}_2 \cos u + \bar{b}_2 \sin u) + u(\bar{a}_2 \sin u - \bar{b}_2 \cos u) \right\} \right) \right\}$$

Here M, M are the multiplying factors.

As the photonelectron conversion is an elementary process, the intensity

should be expressed in photons: $E_{ph}(\lambda \text{ \AA}) = \frac{19.86}{\lambda \text{ \AA}} \times 10^{-16} \text{ Wat}$

$$N_e = 1 / E_{ph}(\lambda)$$

Number of photons N_e

(U) Then we get

$$M = \frac{(1+a_1)^2 + b_1^2}{2N} \sqrt{n_1^2 + k_1^2} \cdot N_e \cdot C_o$$

$$\bar{M} = \frac{(1+\bar{a}_1)^2 + \bar{b}_1^2}{2N} \cdot 1.5 \cdot \sqrt{n_1^2 + k_1^2} \cdot N_e \cdot C_o$$

(U) Numerous calculations have been made to determine the value of i_{ph} at several wavelengths for the model surface 113A. The absolute sensitivity and the ratio FI/VI had been determined on this surface with a fair degree of accuracy. The following values are listed:

in μ	<u>.39</u>	<u>.45</u>	<u>.505</u>	<u>.60</u>	<u>.80</u>	<u>.90</u>	<u>.95</u>	<u>1.06</u>
FI (mA/W) :	2.35	2.30	3.30	4.20	5.20	3.50	2.15	.70
FI/VI :	1.36	1.31	1.35	1.44	1.44	1.44	1.42	1.45

(U) Any worthwhile model must be able to explain these two data.

(U) Besides the peak sensitivity at 8000Å, we selected two pairs with equal sensitivity for the computation:

4600Å :	2.4 mA/W	5350Å :	3.5 mA/W
9400Å :		9000Å :	

(U) For $F(\lambda, k) = 0$, the following values were computed in relative units:

(U)	8000R	$i_{phFI} = 3.20$	$FI/VI = 1.42$
		$i_{phVI} = 2.25$	
	9000R	$i_{phFI} = 4.50$	$FI/VI = 1.50$
		$i_{phVI} = 3.00$	
	4600R	$i_{phFI} = 1.94$	$FI/VI = 1.37$
		$i_{phVI} = 1.42$	

(U) While the ratio FI/VI has the right magnitude, the photosensitivity does not show the spectral response shape at all. This is of course to be expected from the known fact that the absorption and the photoresponse are not related in a straightforward manner.

(U) We are thus forced to introduce our assumption that in the S-1 different layer thicknesses contribute to the electron production. This concept of course is introduced through a suitable selection of the factor $F(\lambda, k)$ in the probability function.

(U) It is obvious that this probability function will be a rather complicated function because it has to explain the drop of sensitivity towards the high energy photon end of the spectrum as well as towards the low energy photon, infrared.

(U) Much computational effort has been applied in order to determine the governing function and a partial success was achieved.

(U) The function $F(\lambda, k)$ must be of the form

$$F(\lambda, k) = C \left[\frac{1}{(E - E_0)^N} + \frac{1}{k^M} \right]$$

where E_0 is the threshold energy conveniently expressed in eV. This satisfies automatically the condition with vanishing i_{ph} at E_0 and for $k = 0$. For the model 113A, the threshold $E_0 \cong 1.0$ eV. In the determination of the threshold we have of course, as usual, a certain amount of ambiguity. After several tedious trials, we arrived at a function $F(\lambda, k)$ which explains the slope of the infrared and blue response and the peak at 8000\AA :

$$F(\lambda, k) = C \left[\frac{1}{(E - E_0)^3} + \frac{1}{k^{3/2}} \right]$$

$$F(4600\text{\AA}) = 11.4$$

$$F(5350\text{\AA}) = 5.50$$

$$F(8000\text{\AA}) = 7.70$$

$$F(9000\text{\AA}) = 22.1$$

(U) The constant was normalized for $F = 1.50$ at 8000\AA . The choice of this constant is one of the factors which can be used to improve the fit to the spectral response. We then get:

$$4600\text{\AA} \quad F = 2.25$$

$$i_{phFI} = .85$$

$$i_{phVI} = .625$$

$$\text{Ratio FI/VI} = 1.36$$

$$5350\text{\AA} \quad F = 1.05$$

$$i_{phFI} = 1.165$$

$$i_{phVI} = .840$$

$$\text{Ratio FI/VI} = 1.385$$

(U)	8000Å	F = 1.50	$i_{phFI} = 1.805$	Ratio FI/VI = 1.42
			$i_{phVI} = 1.270$	
	9000Å	F = 4.30	$i_{phFI} = 1.285$	Ratio FI/VI = 1.395
			$i_{phVI} = .92$	

With a conversion factor of $\eta = 2.9 \text{ mA/W}$ we get:

4600Å	:	.85	x 2.9	=	2.47 mA/W
5350Å	:	1.165	x 2.9	=	3.38 "
8000Å	:	1.805	x 2.9	=	5.23 "
9000Å	:	1.285	x 2.9	=	3.72 "

(U) Although the fit is not ideal, it shows clearly the general shape of the response curve with the peak at 8000Å and the skirt values in the right order of magnitude. The function F will also account for the valley at 4000Å - 4500Å, which is followed in the UV by the known strong increase of photoresponse, because F will become quite small if k increases again to higher values in the near UV. The other parameter FI/VI also shows the right magnitude.

(U) Improvements could be expected with more accurately defined probability functions but it seems that the general character of these functions is sufficiently well described by our definition, since the numerical value of F will also change from surface to surface.

(U) It seems thus assured that the optical characteristics of the S-1 are a determining factor in its response. The fact that the field intensity always has a peak at the vacuum-cathode boundary apparently makes IR response possible. The probability of escape from any useful thickness, which decreases rapidly with increasing wavelengths, determines the shape and magnitude of the IR response.

(U) In this connection, it is interesting that the S-25 with infrared response comes about with a thickening of the S-20 and may thus also come closer to a condition $n \frac{d}{\lambda}$ for .5.

(U) Of course it would be of great interest to extend the idea of an intensity-based model, determined by the optical constants of the surface onto the other photocathodes. It appears likely that the spectral response of the other cathodes could be explained in a manner similar to the one outlined for the S-1.

(U) These laboratories have measured optical constants of all types of photocathodes of interest, as well as, in most cases, the ratio FI/VI and would welcome the opportunity to pursue such work in the future

TABLE I

PERFORMANCE DATA OF REPRESENTATIVE SEMITRANSSPARENT SURFACES - 1963-1969

Page 1 of 6

~~CONFIDENTIAL~~

Tube No.	Date of Meas.	Luminous Sensitivity in $\mu\text{A/L}$		Absolute Sensitivity in mA/W				Thermionic Emission A/cm ² x10 ¹²	Resistance in Ω/\square	Processing Constituents	Remarks
		WL 2540	4535A	6000A	9000A	9500A	11500A				
66	9/63	45	6.4	-	-	-	-	-	-	-	-
	12/65	46	6.6	-	3.0	4.2	.17	50.0	-	(-) -60%Ag-Cs	High temperature processing
	12/68	53	9.5	-	-	-	-	-	-	-	-
83	10/63	44	3.5	-	-	-	-	-	6.0x10 ⁹	(Cs)-K	"
	12/65	34	3.2	-	4.4	1.4	-	-	-	-	-
	12/68	36	3.9	-	-	-	-	4.4	1.0x10 ¹¹	-	-
93	11/63	40	6.4	-	-	-	-	120.0	3.5x10 ⁵	(Cs)-Cs	"
	12/68	43	6.4	-	3.1	2.0	.35	140.0	1.2x10 ⁸	-	-
113	12/63	73	6.4	3.3	-	-	-	.80	4.5x10 ⁶	(B1,Cs)-Cs	"
	7/66	38	.50	4.1	7.0	-	-	<10 ⁻¹⁴	-	-	-
	10/66	Reprocessing with Cs.									
	2/68	60	3.8	-	-	-	-	-	-	-	-
	12/68	55	2.6	-	-	-	-	.24	8.0x10 ⁷	-	-

RE DD-254 4/14/70

~~CONFIDENTIAL~~

TABLE I (CONT'D)

Page 2 of 6

PERFORMANCE DATA OF REPRESENTATIVE SEMITRANSSPARENT SURFACES - 1963-1969

~~CONFIDENTIAL~~

Tube No.	Date of Mess.	Luminous Sensitivity in $\mu\text{A}/\text{L}$		Absolute Sensitivity in mA/W					Thermionic Emission $\frac{A}{\text{cm}^2 \times 10^{-12}}$	Resistance in Ω/\square	Processing Constituents	Remarks
		WL	2540	4535	6000	9000	9500	11500				
116	12/63	62	6.6	-	-	-	-	-	.90	8.0×10^6	(Bi,Cs)-Cs	High Temperature processing.
	11/65	62	6.2	-	4.8	3.9	-	.08	.50	4.0×10^{10}	-	
	12/68	61	5.7	-	-	-	-	-	.30	1.0×10^{13}	-	
156	5/64	53	4.1	-	-	-	-	-	.35	3.0×10^8	(Bi,K)-Cs	"
	12/68	50	4.5	-	-	-	-	-	1.40	$> 10^{14}$		
182	9/64	45	3.9	-	-	-	-	-	-		(Bi,Cs)-Cs	"Fast Cs" method.
	10/64	Repeated B1 aftertreatments.										
	9/66	45	4.6	-	-	-	-	-	4.0	5.0×10^{10}	-	
	12/68	48	6.0	-	-	-	-	-	5.5	9.0×10^{14}	-	
308	1/65	39	3.2	-	-	-	-	-	16.0	1.5×10^6	(Bi,Cs)-Cs	-
	2/65	B1 aftertreatment.										
	11/65	42	4.6	-	-	-	-	-	-	-	-	
	12/68	43	6.5	-	-	-	-	-	4.0	5.0×10^8	-	

RE: DD-254 4/14/70

~~CONFIDENTIAL~~

TABLE I (CONT'D)

Page 3 of 6

PERFORMANCE DATA OF REPRESENTATIVE SEMITRANSSPARENT SURFACES - 1963-1969

~~CONFIDENTIAL~~

Tube No.	Date of Meas.	Luminous Sensitivity in $\mu\text{A}/\text{L}$			Absolute Sensitivity in mA/W			Thermionic Emission A/cm ² x10 ¹²	Resistance in Ω/\square	Processing Constituents	Remarks
		2540	4535	6000	9000	9500	11500				
340	1/65	51	5.9	1.4	4.3	-	-	.65	1.0x10 ⁵	(Bi,Cs)-Cs	Slow Ag evaporation
	11/65	59	7.2	-	4.2	3.8	.15	2.5	2.0x10 ¹⁰	-	
	7/66	60	7.1	-	-	-	-	6.0	-	-	
365	5/65	43	4.1	-	-	-	-	140.0	2.0x10 ⁵	(Bi,Cs)-Cs	"Fast Cs" method
Repeated Bi after treatments.											
	8/65	41	3.2	1.1	3.3	-	-	33.0	4.0x10 ⁵	-	
	12/68	50	7.1	-	-	-	-	10.0?	3.0x10 ⁸	-	
437	4/65	45	5.2	1.9	3.7	-	-	8.0	>10 ¹³	Ag-Cs-(O ₂)	Multilayer cathode
	12/66	53	7.6	-	-	-	-	-	-	-	
	12/68	53	8.0	-	-	-	-	10.0	>10 ¹⁴	-	
519	6/65	58	5.1	2.5	4.7	-	-	0.9	5.0x10 ⁹	(Bi,Cs)-Cs	"Fast Cs" method
	12/68	71	7.8	-	-	-	-	2.0	8.0x10 ¹⁴	-	
520	6/65	60	6.6	1.7	4.1	-	-	11.0	2.0x10 ⁶	(Bi,Cs)-Cs	-
	12/68	69	11.0	-	-	-	-	8.0	7.0x10 ¹⁴	-	

RE: DD-254 4/14/70

~~CONFIDENTIAL~~

TABLE I (CONT'D)

PERFORMANCE DATA OF REPRESENTATIVE SEMITRANSSPARENT SURFACES - 1963-1969

CONFIDENTIAL

Tube No.	Date of Meas.	Luminous Sensitivity in $\mu\text{A/L}$		Absolute Sensitivity in mA/W				Thermionic Emission $\text{A/cm}^2 \times 10^{12}$	Resistance in Ω/\square	Processing Constituents	Remarks
		2540	2540	4535Å	6000Å	9000Å	9500Å				
528	6/65	40	1.4	1.3	3.8	-	-	2.0	1.0×10^7	(Bi,Cs)-Cs	-
	9/65	54	3.0	1.8	4.8	-	-	-	-	-	-
	12/68	68	7.5	-	-	-	-	2.2	1.0×10^{11}	-	-
606	9/65	60	6.4	2.2	4.9	3.7	-	3.2	1.0×10^7	(Bi,Cs)-Cs	Low temperature Cs interaction
	12/68	75	10.0	-	-	-	-	2.3	2.0×10^{13}	-	-
774	2/66	49	3.6	-	4.0	2.7	-	5.5	6.0×10^8	(Bi,Cs)-K,Rb,Cs	Multialkali cathode
	12/68	46	5.0	-	-	-	-	-	-	-	-
828	5/66	55	5.9	-	4.2	3.4	-	.26	9.0×10^{10}	(Bi,Cs)-Cs	No O ₂ glow discharge
	7/66	Slump and restoration through Cs after treatment.									
	12/68	68	8.0	-	-	-	-	-	-	-	-
0-46	10/66	46	7.5	2.5	3.3	3.3	-	32.0	3.0×10^7	(Bi,Cs)-Cs	High infra-red method
	12/68	60	10.0	-	-	-	-	-	1.0×10^8	-	-
0142	3/67	64	12.0	2.0	3.2	-	2.4	22.0	3.0×10^6	(Bi,Cs)-Cs	" "
	12/68	64	11.5	-	-	-	-	28.0	7.0×10^{11}	RE DB-254	4/14/70

CONFIDENTIAL

TABLE I (CONT'D)

Page 5 of 6

PERFORMANCE DATA OF REPRESENTATIVE SEMITRANSSPARENT SURFACES - 1963-1969

Tube No.	Date of Meas.	Luminous Sensitivity in $\mu\text{A/L}$			Absolute Sensitivity in mA/W			Thermionic Emission $\text{A/cm}^2 \times 10^{12}$	Resistance in Ω/\square	Processing Constituents	Remarks
		WL	2540	4535	4535	6000	9000				
0206	4/67	46	6.2	-	-	-	-	-	-	(Bi,Cs)-Cs	High Infra-red method
	5/67	Cesium after treatment.									
	6/67	57	7.1	1.6	2.9	-	2.0	.06	4.2	1.5×10^6	-
	9/67	63	9.1	-	-	-	-	-	-	-	-
	12/68	71	11.8	-	-	-	-	-	140.0	2.0×10^{10}	-
0216	5/67	46	5.0	2.6	4.0	-	1.9	.18	47.0	1.0×10^9	(Bi,Cs)-Cs Example of an Ag-Cs layer cath.
	9/67	53	6.8	-	-	-	-	-	-	-	-
	11/68	53	7.5	-	-	-	-	-	50.0	3.0×10^{11}	-
0224T	6/67	30	3.4	2.3	2.5	-	1.2	.08	14.0	3.0×10^5	TiO ₂ -Ag-Cs Semitransparent cath.
	1/68	37	3.7	1.5	2.8	-	1.1	.08	10.0	2.0×10^5	- formed on TiO ₂ substrate.
	12/68	38	4.1	-	-	-	-	-	-	2.0×10^5	-
0412T	1/68	44	5.9	1.7	2.4	-	1.2	.10	10.0	1.0×10^5	TiO ₂ -Ag-Cs "
	11/68	43	5.4	-	-	-	-	-	-	-	-

RE: DD-254 4/14/70

TABLE I (CONT'D)

PERFORMANCE DATA OF REPRESENTATIVE SEMITRANSSPARENT SURFACES - 1963-1969

Tube No.	Date of Meas.	Luminous Sensitivity		Absolute Sensitivity in mA/W					Thermionic Emission A/cm ² x10 ¹²	Resistance in Ω /sq	Processing Constituents	Remarks
		WL	2540	4535A	6000A	9000A	9500A	11500A				
5609	5/68	72	12.3	2.0	3.1	-	2.2	.36	360.0	3.0x10 ⁵	(Bi,Cs)-Cs	High infra-red method
	1/69	70	12.8	-	-	-	-	-	52.0	9.0x10 ¹¹	-	
5642	10/68	46	5.2	3.3	3.6	-	1.2	.16	10.0	9.0x10 ⁷	-	Layer method
	5/69	44	5.3	-	-	-	-	-	-	1.0x10 ⁸	-	

Comments to Table I:

This table gives a sampling of the more important methods and their results developed under these contracts. A large number of tubes with similar properties is available in each category. The following data shows that:

- 1) "Good" surfaces have a tendency to increase in sensitivity over long periods of time.
- 2) Bi-aftertreatments (and presumably also Cs aftertreatments, where a lack of Cs is indicated) enhance this slow growth.
- 3) The surface resistance of the surfaces continues to increase greatly with time.

RE: DD-254 4/14/70

TABLE II

COMPARISON OF "GROOVED PLATE" (PL) AND 7056 GLASS (GL)

~~CONFIDENTIAL~~

	Luminous Sensitivity in $\mu\text{A/L}$		Absolute Sensitivity in mA/W for Different Incidences					Resistivity in Ω/\square	
	PL	GL	0° Inc.	20° Inc.	40° Inc.	0° Inc.	20° Inc.	PL	GL
White Light	44	40						3.0×10^7	2.5×10^5
2540 Filter	32	32							
3900Å			7.3	6.4	5.9	2.25	2.25		
4535Å			7.0	6.6	7.0	1.65	1.65		
5050Å			5.9	5.6	4.5	1.85	1.85		
6015Å			4.6	4.5	3.0	2.0	2.0		
7980Å			1.7	1.6	1.1	1.7	1.7		
9500Å			.65	.52	.36	.70	.70		
11500Å			.024	.025	0	.07	.07		

RE: DD-254 4/14/70

~~CONFIDENTIAL~~

#25

TABLE III

OPTICAL AND ELECTRICAL PROPERTIES OF TUBE NO. EX-0429 (HEAVY Cs-O LAYER ON THIN Ag BASE)

~~CONFIDENTIAL~~

Tube No.	Wavelength in μ	Front Reflection R_F %	Vacuum Reflection R_V %	Transmission T %	Ratio of Front Absorption to Vacuum Absorption A_F/A_V		Ratio of Front to Vacuum Incidence Photoresponse $r = FI/VI$	

EX-0429

3900	0.5	11.0	68.5	1.51	1.27
4535	1.0	13.5	60.0	1.47	1.37
5050	3.0	17.0	48.0	1.40	1.42
6015	5.5	18.5	49.5	1.41	1.39
7980	4.5	12.5	70.0	1.46	1.44
9500	5.0	11.5	72.5	1.42	1.46
11500	-	8.0	--	--	--

 I_{th} 22°C : 3.0×10^{-10} A/cm²Resistance: 5.0×10^{10} Ω/\square

RE DD-254 4/14/70

~~CONFIDENTIAL~~

TABLE IV

CORRECTED VALUES OF THE FRONT REFLECTION R_F , VACUUM REFLECTION R_V ,
AND
TRANSMISSION T FOR THE MODEL SURFACE 113A

<u>λ in Å</u>	<u>R_F %</u>	<u>R_V %</u>	<u>T %</u>
3900	6.0	13.0	70.5
4000	6.4	13.8	69.0
4200	7.3	15.4	65.9
4400	8.3	17.3	62.5
4600	9.5	19.3	59.0
4800	10.9	21.3	54.8
5000	12.1	23.3	50.3
5200	13.2	25.4	45.8
5400	14.0	27.2	41.8
5600	14.7	28.7	38.4
5800	15.2	30.1	35.9
6000	15.5	31.2	34.1
6500	15.5	31.6	32.4
7000	14.8	31.3	29.8
7500	13.7	30.7	28.6
8000	12.5	30.0	28.5
8500	11.6	29.3	29.7
9000	10.9	28.7	31.6
9500	10.4	28.0	33.3
10000	10.0	27.1	34.8
10500	9.6	26.1	36.3
11000	9.1	25.3	37.7
11500	8.5	24.4	39.1
12000	8.0	23.4	40.3

TABLE V

COMPUTED OPTICAL CONSTANTS OF THE MODEL SURFACE, 113A

λ in μ	Wanted Triplet $\frac{R}{V}$	Computed Best Triplet Fit	Refractive Index n	Absorption Coefficient k	d/λ	d, μ	$n d/\lambda$	$k d/\lambda$
3950	(.062/.134/.698)	(.063/.125/.690)	3.18	.13	.145	572	.461	.019
4000	(.064/.138/.690)	(.065/.140/.680)	4.31	.14	.11	440	.474	.0155
4575	(.094/.190/.594)	(.093/.187/.591)	3.625	.18	.125	572	.453	.0225
4950	(.118/.228/.515)	(.116/.230/.515)	5.35	.19	.10	495	.535	.019
5200	(.132/.253/.458)	(.133/.251/.453)	4.05	.31	.11	572	.446	.034
5630	(.148/.289/.380)	(.148/.289/.381)	4.15	.40	.105	591	.436	.042
5720	(.150/.295/.368)	(.150/.291/.368)	4.45	.42	.10	572	.445	.042
5800	(.152/.301/.359)	(.153/.301/.358)	5.375	.45	.085	495	.457	.038
6730	(.152/.315/.315)	(.152/.312/.314)	5.40	.54	.085	572	.459	.046
6825	(.151/.314/.310)	(.153/.313/.314)	5.39	.54	.085	580	.458	.046
7625	(.134/.306/.285)	(.134/.308/.290)	6.30	.60	.075	572	.473	.045
7750	(.131/.304/.283)	(.131/.306/.283)	6.31	.62	.075	580	.473	.0465
7880	(.128/.302/.284)	(.126/.303/.286)	6.35	.61	.075	590	.476	.046
8290	(.119/.296/.291)	(.119/.298/.290)	6.89	.60	.07	580	.482	.042
8800	(.112/.290/.308)	(.110/.290/.307)	7.45	.58	.065	572	.484	.038
9075	(.108/.286/.319)	(.109/.286/.319)	7.44	.56	.065	590	.484	.0365

TABLE VI

ELECTRICAL PROPERTIES OF THE SPRC OF INTEREST

Page 1 of 1

Tube No.	Processing Date	Luminous Sensitivity			Absolute Sensitivity in mA/W			I_{th} in 10-12 A/cm ² @ 24°C	Spacer Thickness	Remarks
		WL	2540	in μ A/L	4535	6000	9500			
5273	2/21/69	--	--	--	3.30	2.5	1.25	.18	1/3	
5287	3/18/69	37	3.7	3.7	2.50	2.5	1.25	.06	1/3	
5289	3/20/69	68	8.1	8.1	3.10	4.0	1.90	.06	1/6	
5291	3/21/69	45	5.8	5.8	3.3	3.1	1.35	.12	1/3	
5296	3/26/69	43	2.0	2.0	4.6	4.3	1.45	.005	1/3	Slump
52102	4/04/69	59	4.0	4.0	5.0	4.4	2.55	.025	1/6	
52104	4/09/69	43	5.9	5.9	4.0	2.1	1.70	.08	1/6	
52107	4/10/69	56	7.3	7.3	4.8	4.0	1.80	.16	1/6	280.0!
52109	4/15/69	38	3.0	3.0	4.8	3.6	1.35	.05	1/6	
52110	4/16/69	59	7.0	7.0	5.5	3.0	1.65	.10	1/6	

TABLE VI

ELECTRICAL PROPERTIES OF THE SPRC OF INTEREST

Page 2 of 2

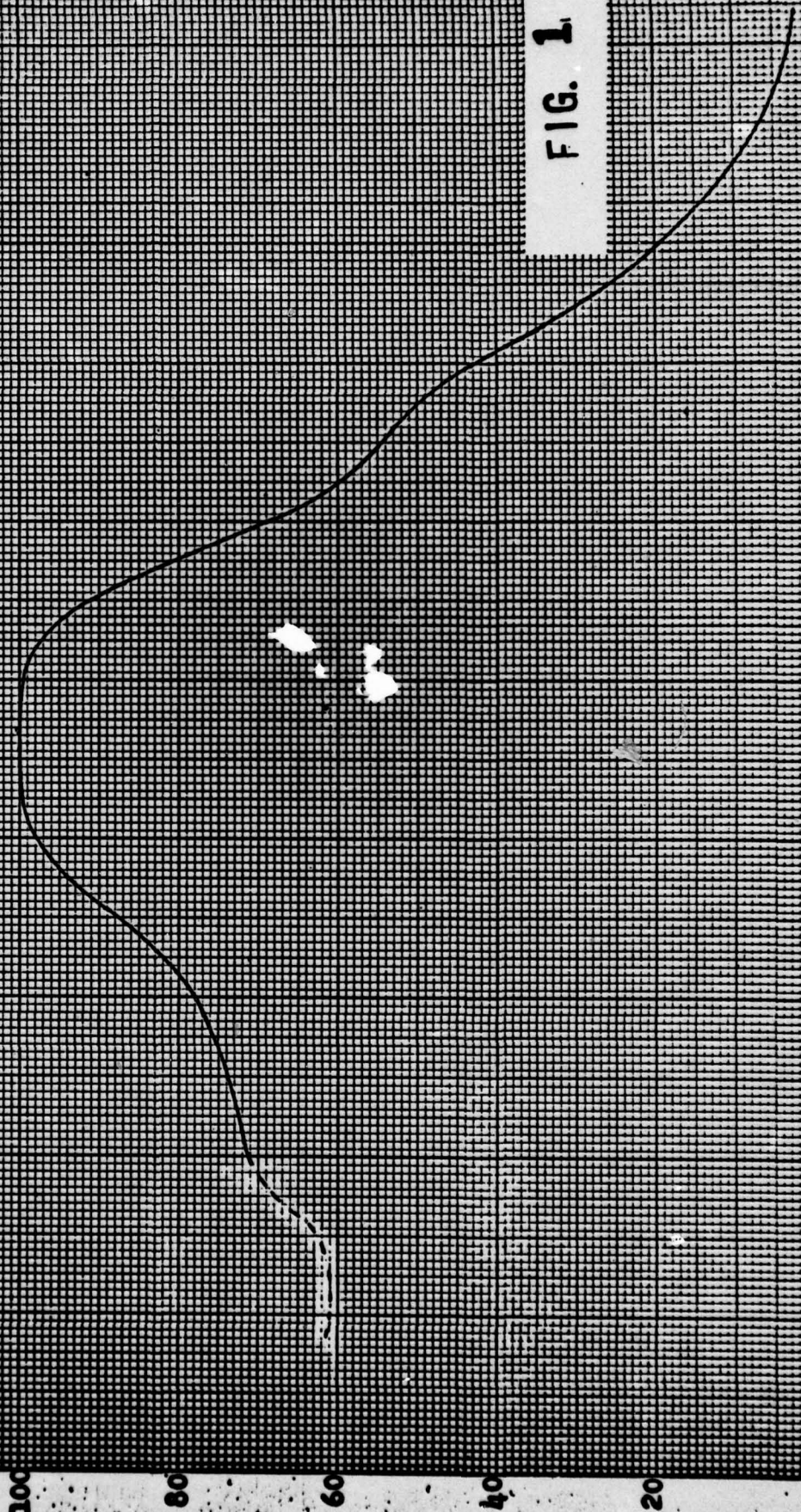
Tube No.	Processing Date	Luminous Sensitivity		Absolute Sensitivity in mA/W			I _{th} in 10-12 A/cm ² @ 24°C	Spacer Thickness	Remarks
		WL	in μ A/L	4535Å	6000Å	9500Å			
52111	4/17/69	57	6.2	4.0	3.0	1.85	.04-.10	3.6	1/6
52115	4/24/69	51	4.3	8.8	5.6	1.50	.03	7.6	1/6
52118	4/29/69	54	6.4	-	-	-	-	1.0	1/6
5660	-	46	6.2	-	-	-	-	2.8	1/6
52119	-	43	5.1	-	-	-	-	-	1/6
52120	-	38	3.5	-	-	-	-	-	1/6
52121	-	57	6.2	-	-	-	-	2.9	1/6
52123	-	57	6.2	-	-	-	-	0.7	1/6
52124	-	43	4.3	-	-	-	-	-	1/6

EUGENE DIETZGEN CO.
MADE IN U. S. A.

NO. 34DR-20 DIETZGEN GRAPH PAPER
30 X 30 PER INCH

SPECTRAL RESPONSE CURVE
FOR TUBE NO. EX 0-209
RUN NO. 1195
DATE: 5-23-67

FIG. 1

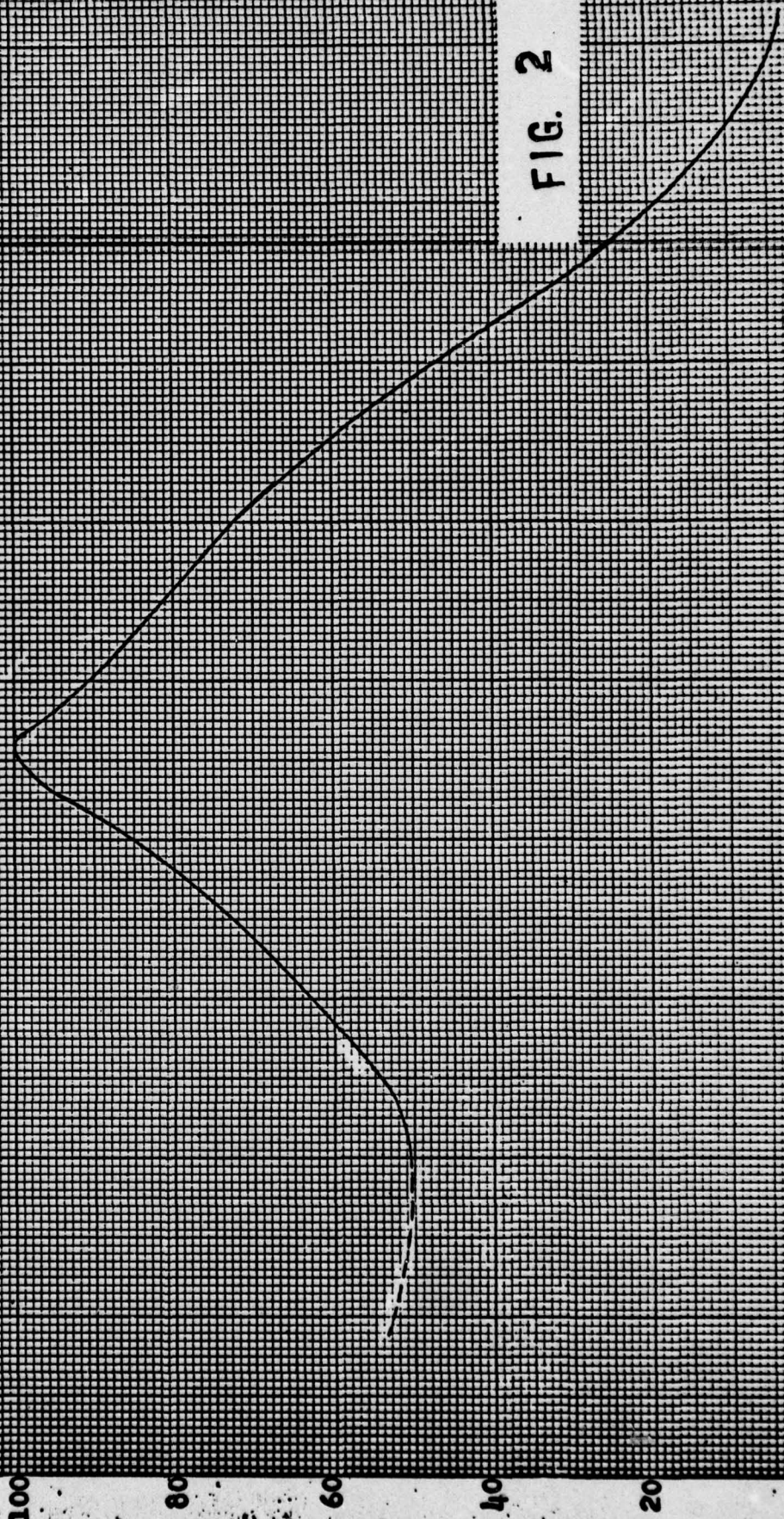


EUGENE DIETZGEN CO.
MADE IN U. S. A.

NO. 340R-20 DIETZGEN GRAPH PAPER
20 X 20 PER INCH

SPECTRAL RESPONSE CURVE
FOR TUBE NO. EX 0-221
RUN NO. 1192
DATE: 5-23-67

FIG. 2



EUGENE DIETZGEN CO.
MADE IN U. S. A.

NO. 340N-20 DIETZGEN GRAPH PAPER
30 X 20 PER INCH

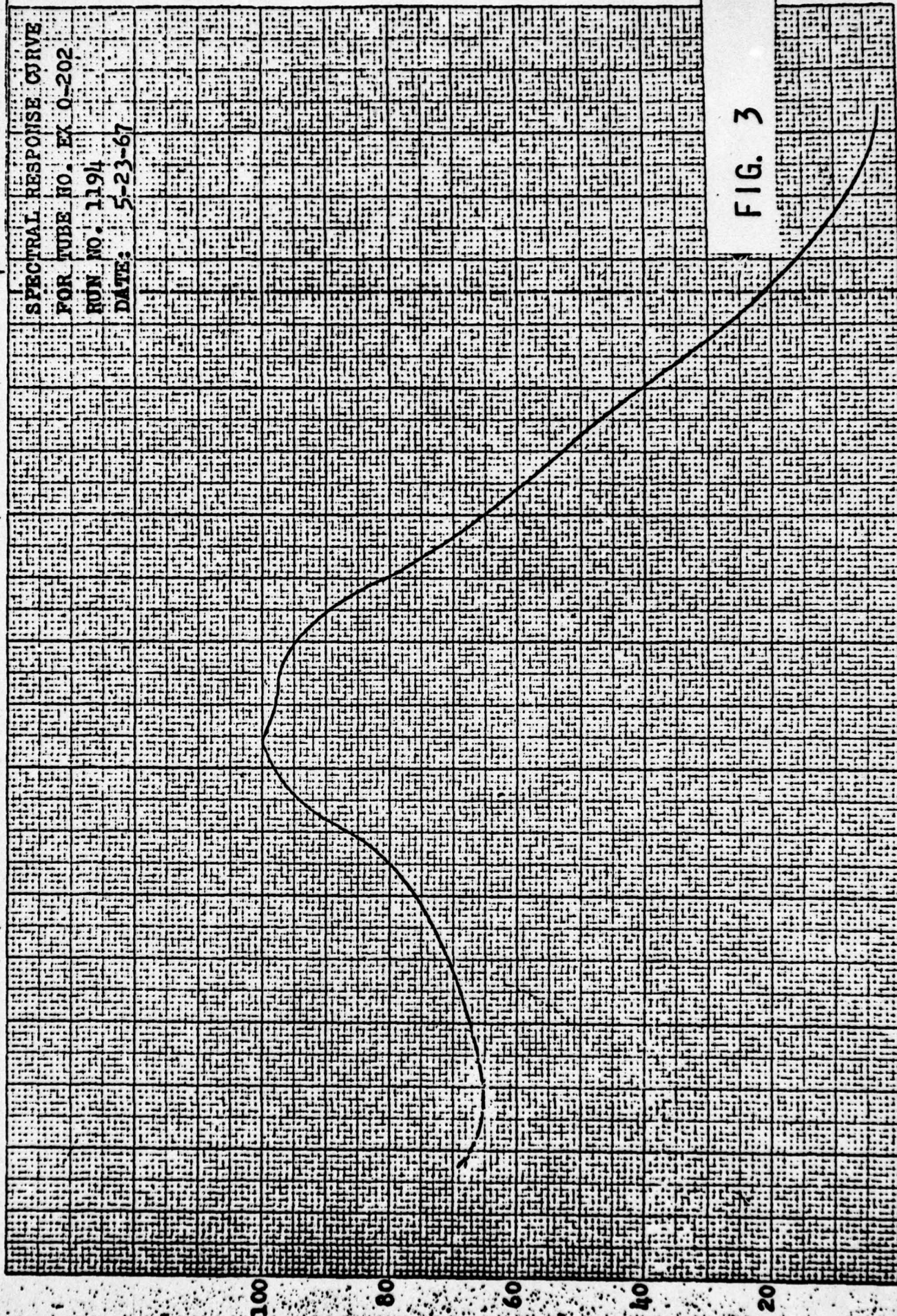
SPECTRAL RESPONSE CURVE

FOR TUBE NO. EX 0-202

RUN NO. 1194

DATE: 5-23-67

FIG. 3



K-E 10 X 10 TO THE CENTIMETER 46 1513
10 X 25 CM.
REUFFEL & ESSER CO.
MADE IN U.S.A.

FRONT REFLECTION R_F
VACUUM REFLECTION R_V

TRANSMISSION

40%
30%
20%
10%
0%
100%
80%
60%
40%
20%

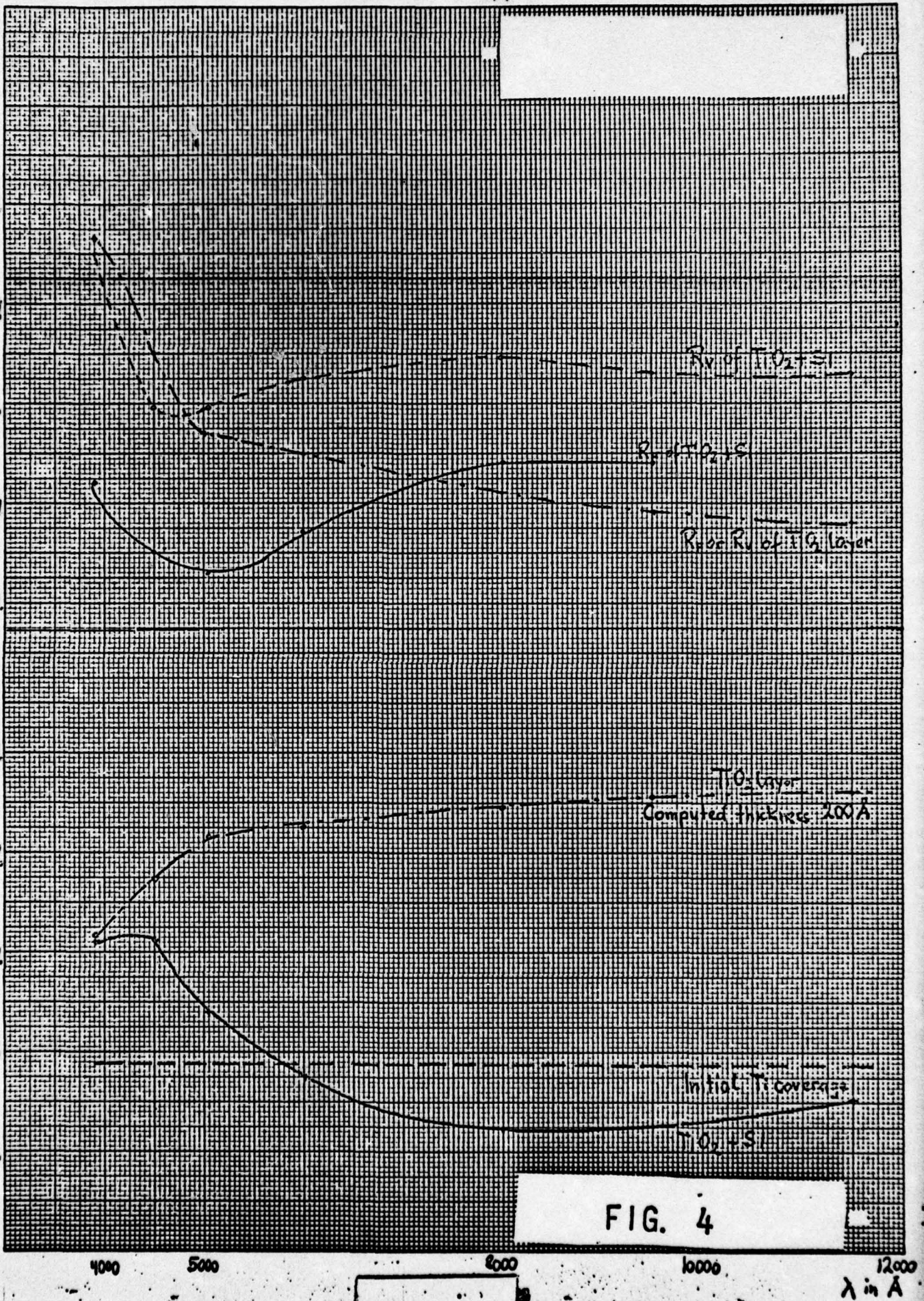


FIG. 4

λ in Å

x 7.55

TUBE NO. 0-244T

RATIOS OF ABSORPTION AND PHOTOESPONSE

K-E 10 X 10 TO THE CENTIMETER 46 1513
10 X 25 CM. KENNEL & ESSER CO.
MADE IN U.S.A.

FRONT ABSORPTION A_F
VACUUM ABSORPTION A_V

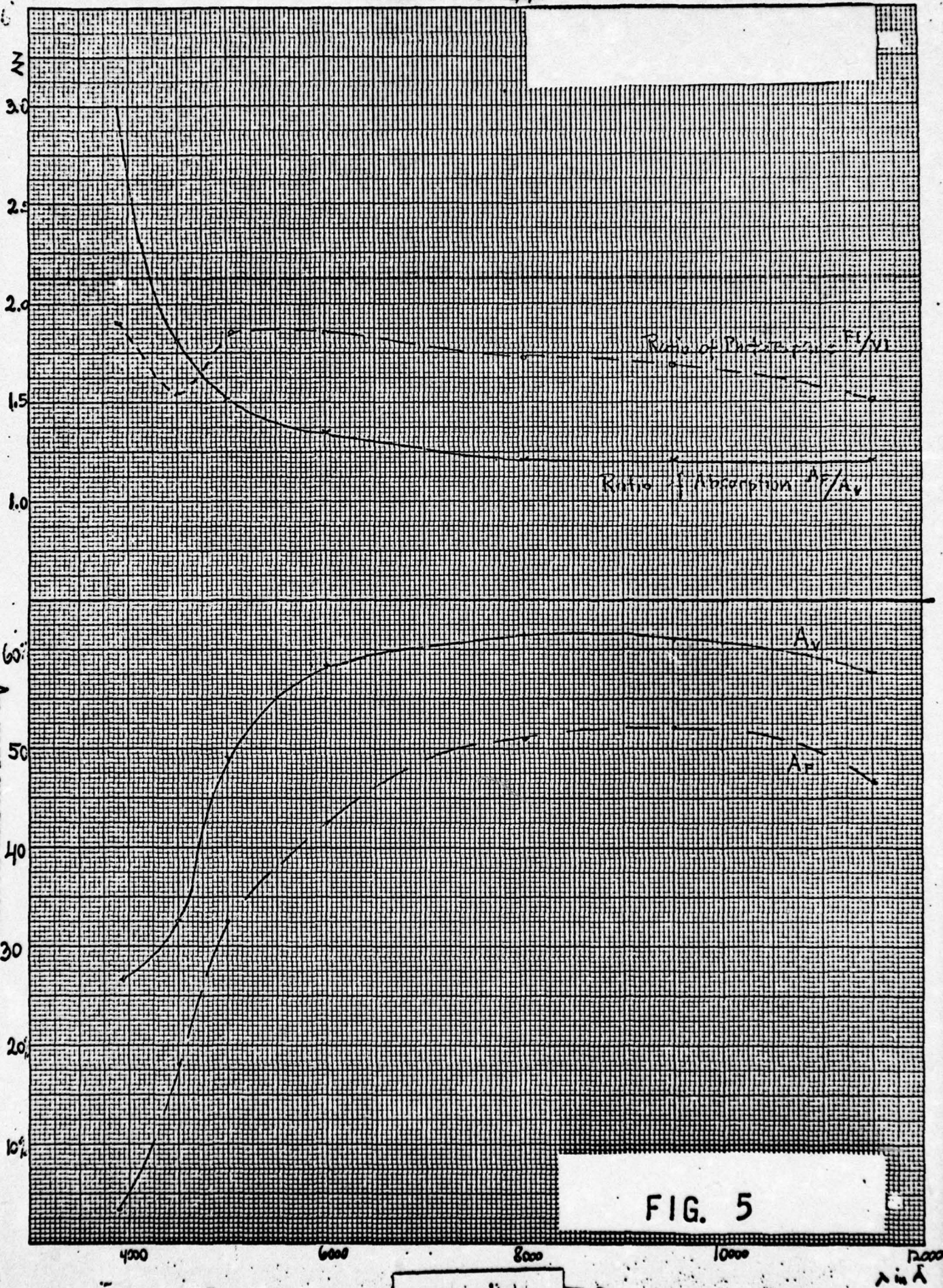


FIG. 5

K·E 10 X 10 TO THE CENTIMETER 46 1513
10 X 25 CM.
KRUUFEL & ESSER CO.
MADE IN U.S.A.

TRANSMISSION

FRONT REFLECTION R_F
VACUUM REFLECTION R_V

40%
30%
20%
10%
0%

100%
80%
60%
40%
20%

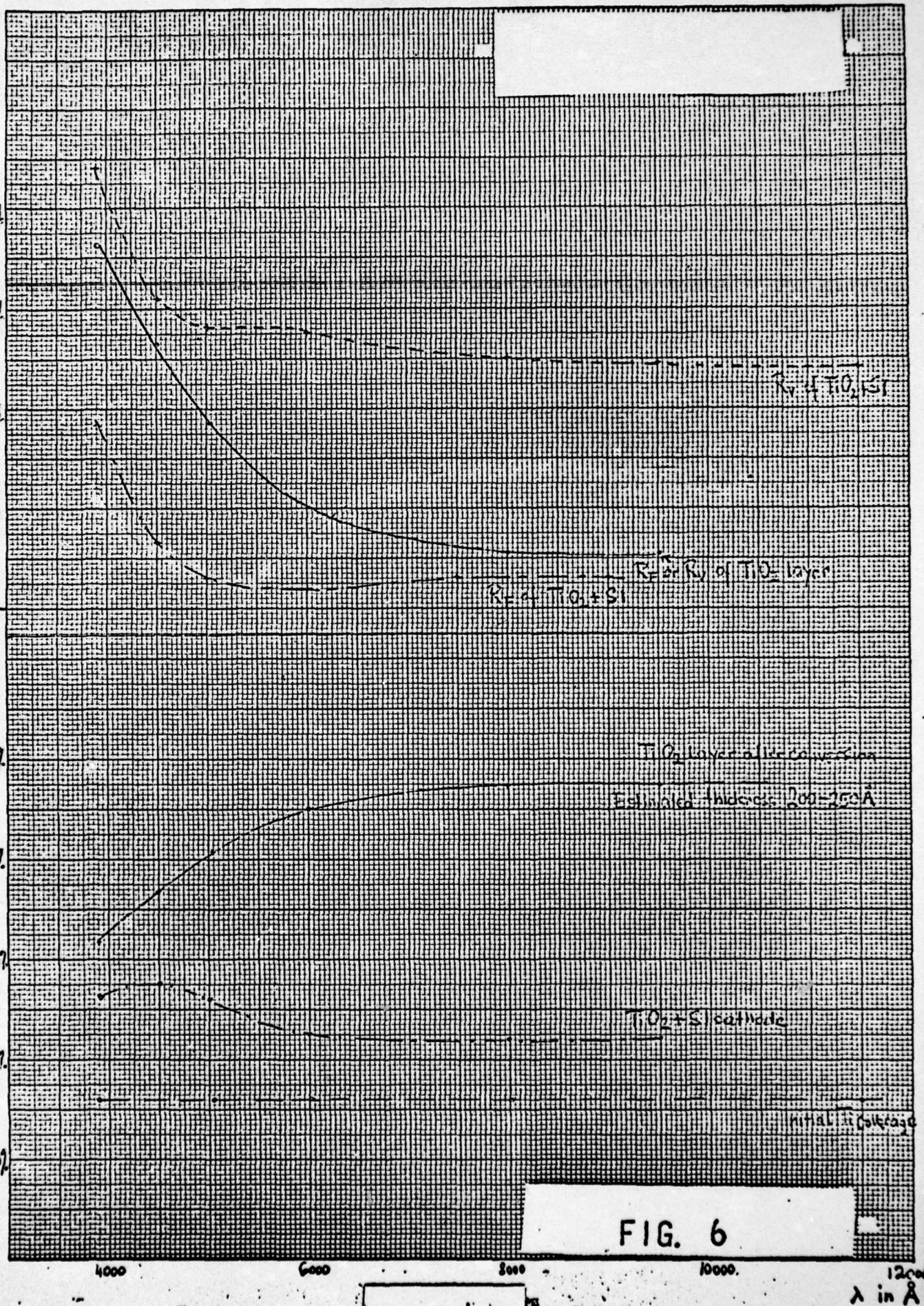


FIG. 6

x 8.30

TUBE NO. 0-308T

K-E 10 X 10 TO THE CENTIMETER 46 1513
MADE IN U. S. A.
KUPFFEL & ESSER CO.

FRONT ABSORPTION A_F VACUUM ABSORPTION A_V

RATIOS OF ABSORPTION AND PHOTORESPONSE

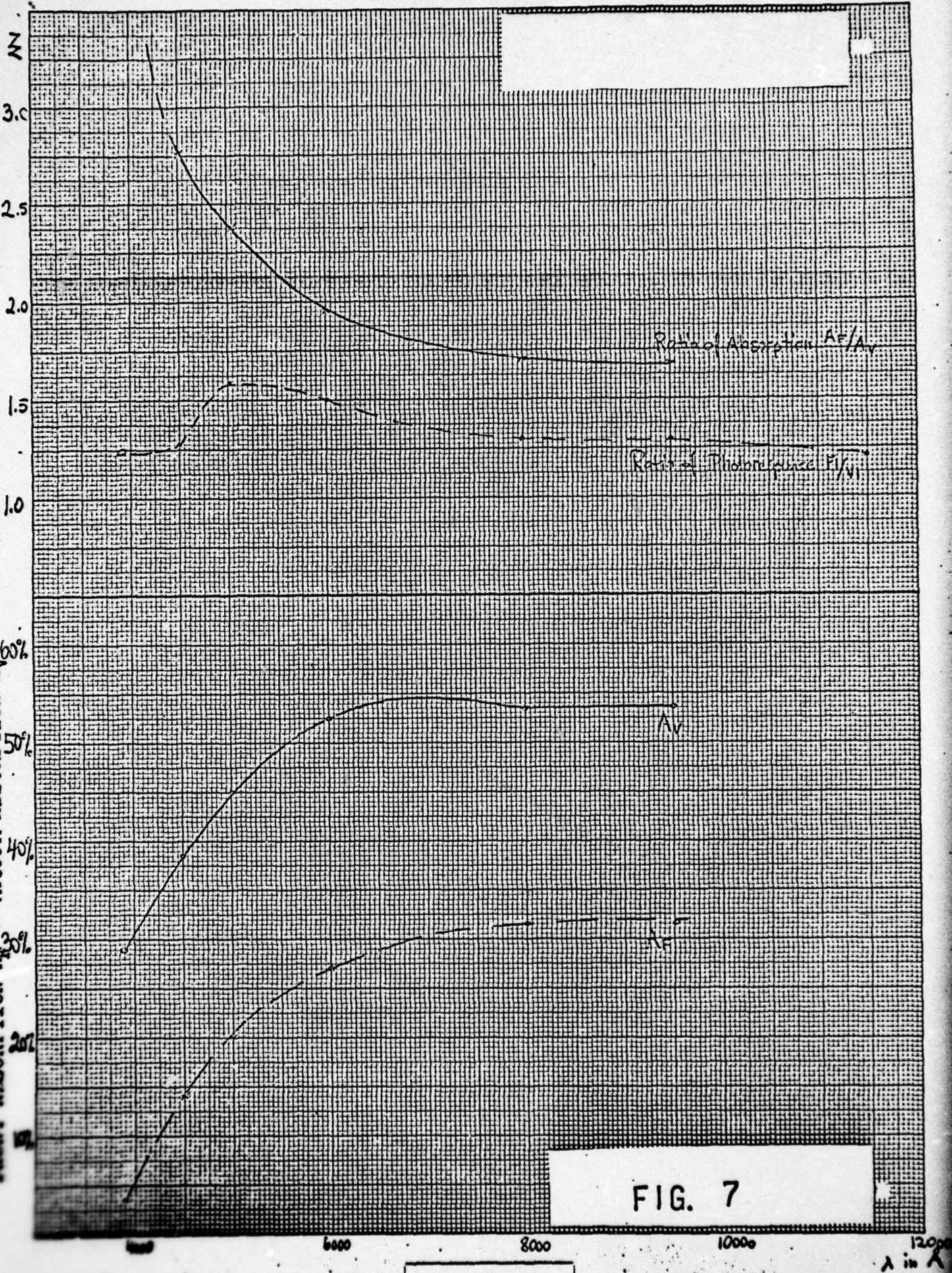


FIG. 7

-- FORMATION OF A HEAVY Cs-O LAYER ON THIN Ag SUBSTRATE

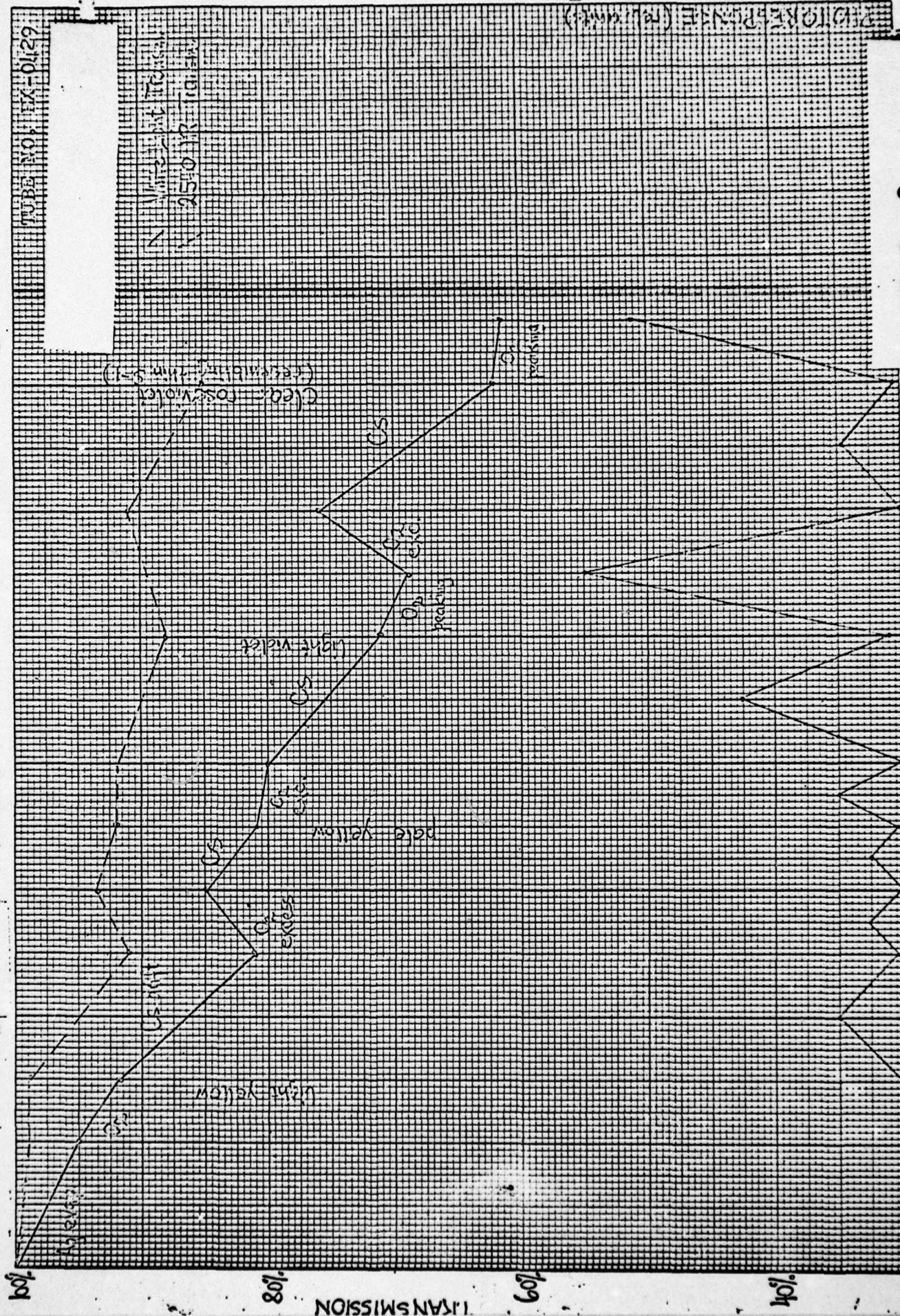


FIG. 8

EUGENE DIETZGEN CO.
MADE IN U. S. A.

FORMATION OF A HEAVY Cs-O LAYER ON THIN Ag SUBSTRATE

UTEX INC. EX-6130

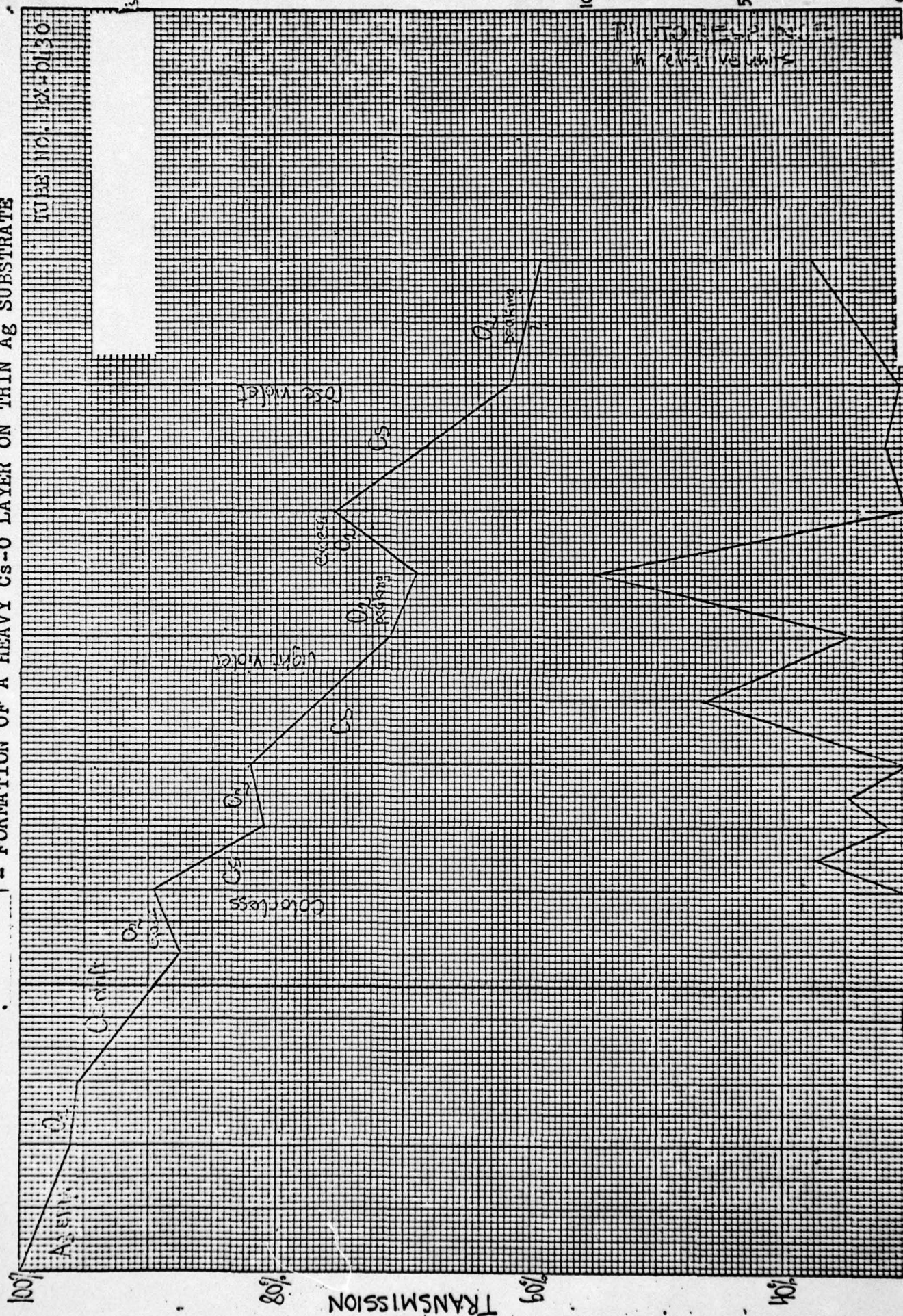


FIG. 9

EUGENE DIETZGEN CO.
MADE IN U. S. A.

NO. 340R-20 DIETZGEN GRAPH PAPER
30 X 20 PER INCH

SPECTRAL RESPONSE CURVE
FOR IR DIODE #5635
RUN NO. 1292
DATE: 3/24/69

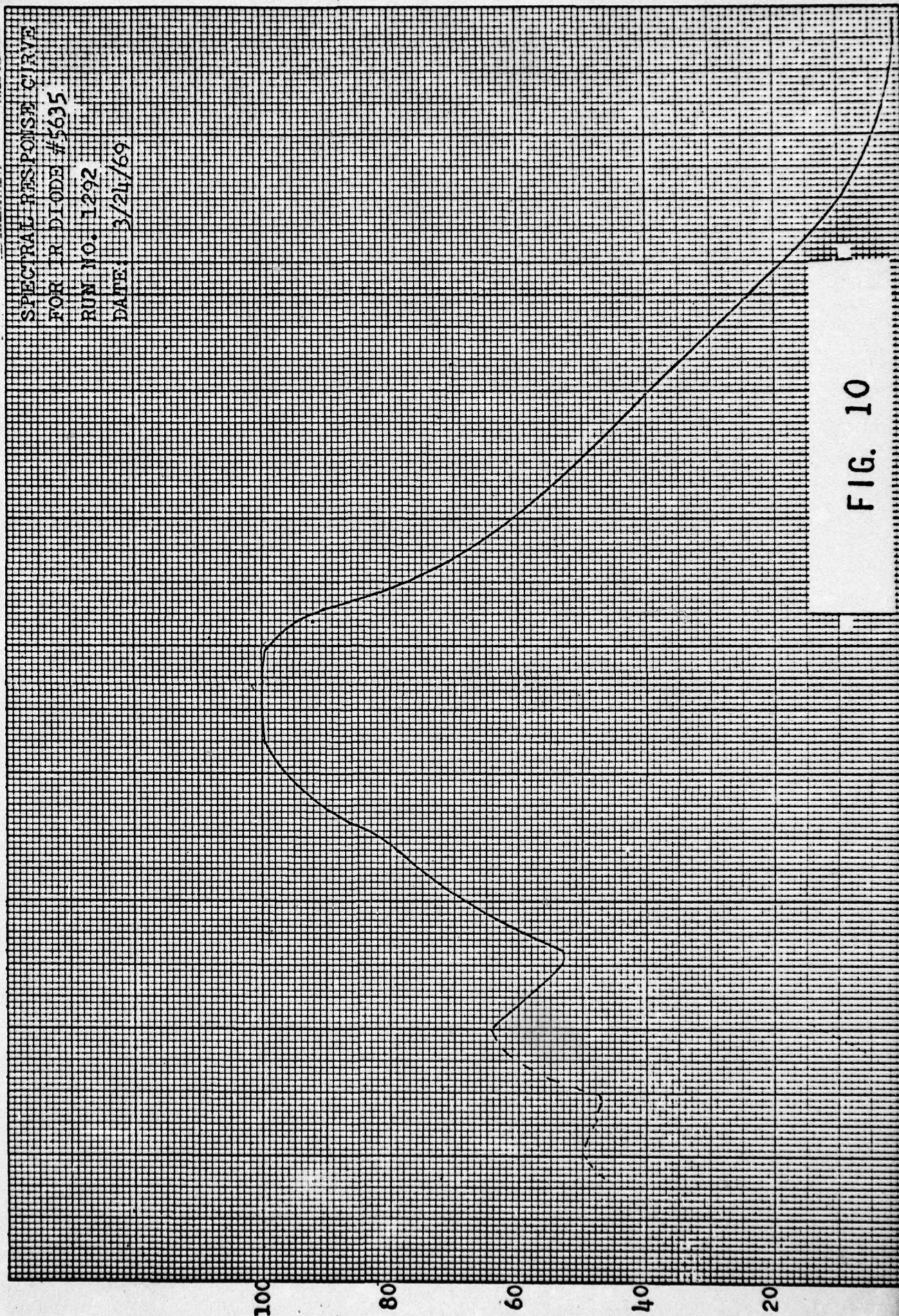


FIG. 10

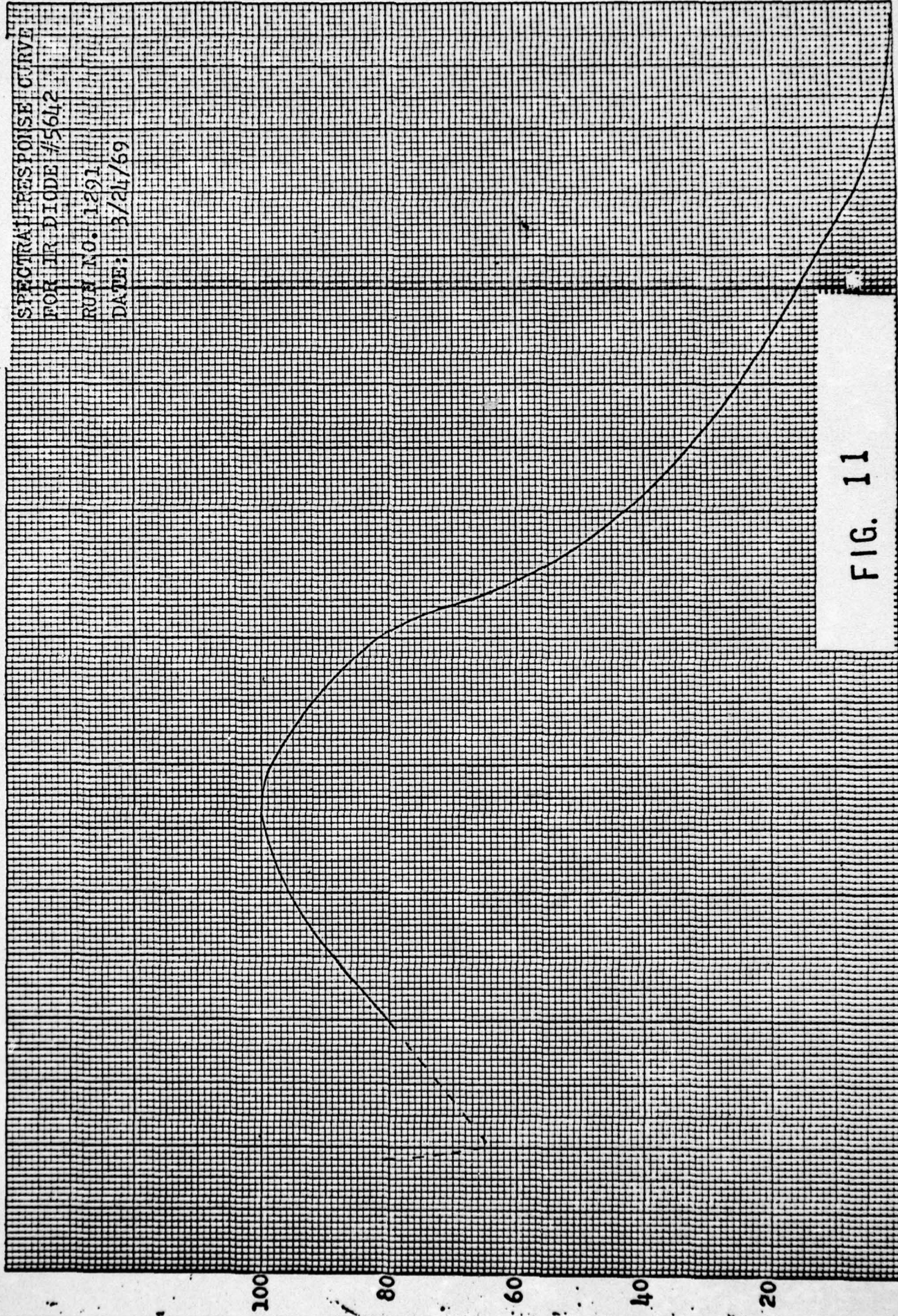
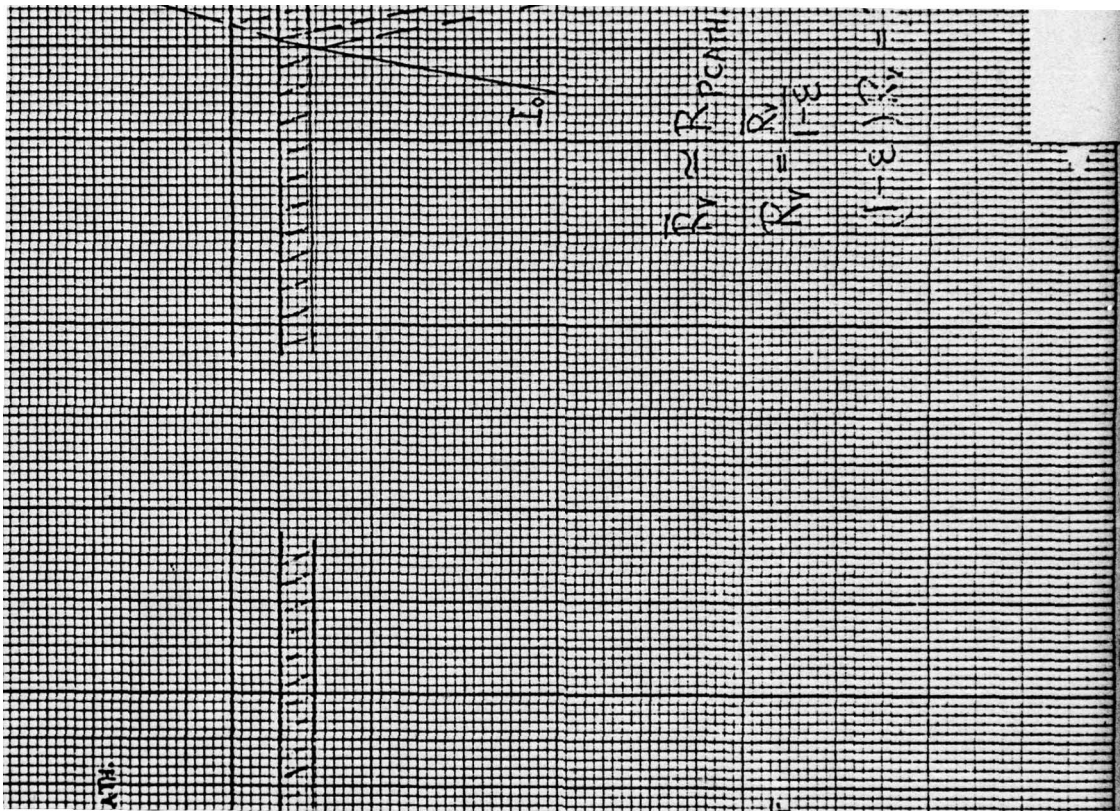


FIG. 11

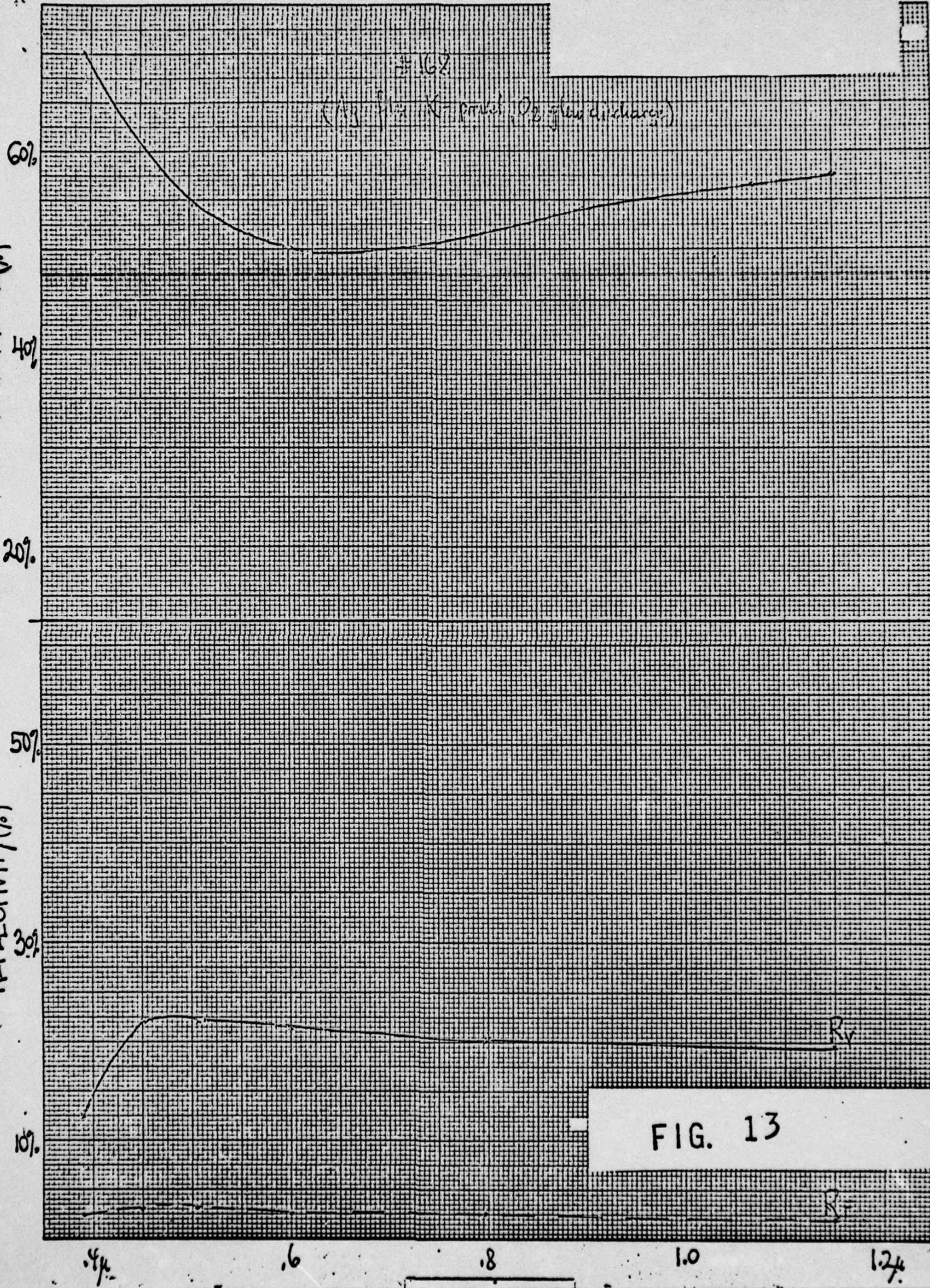


K-E 10 X 10 TO THE CENTIMETER 46 1513
18 X 25 CM. MADE IN U.S.A.

REUFFEL & ESSER CO.

REFLECTIVITY(%)

TRANSMISSION(%)



K-E 10 X 10 TO THE CENTIMETER 46 1513
MADE IN U.S.A.
KEUFFEL & ESSER CO.

TRANSMISSION (%)

REFLECTIVITY (%)

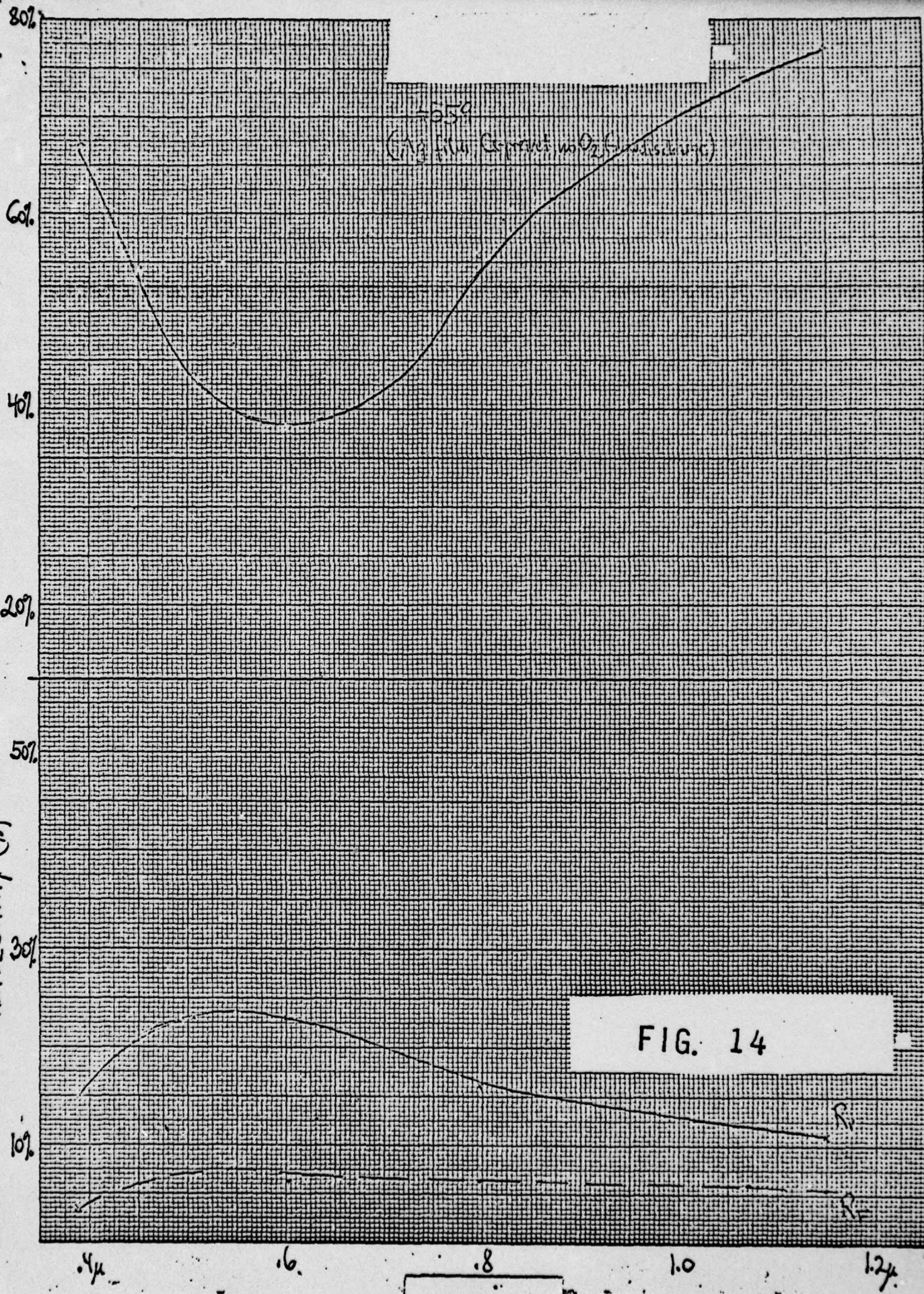


FIG. 14

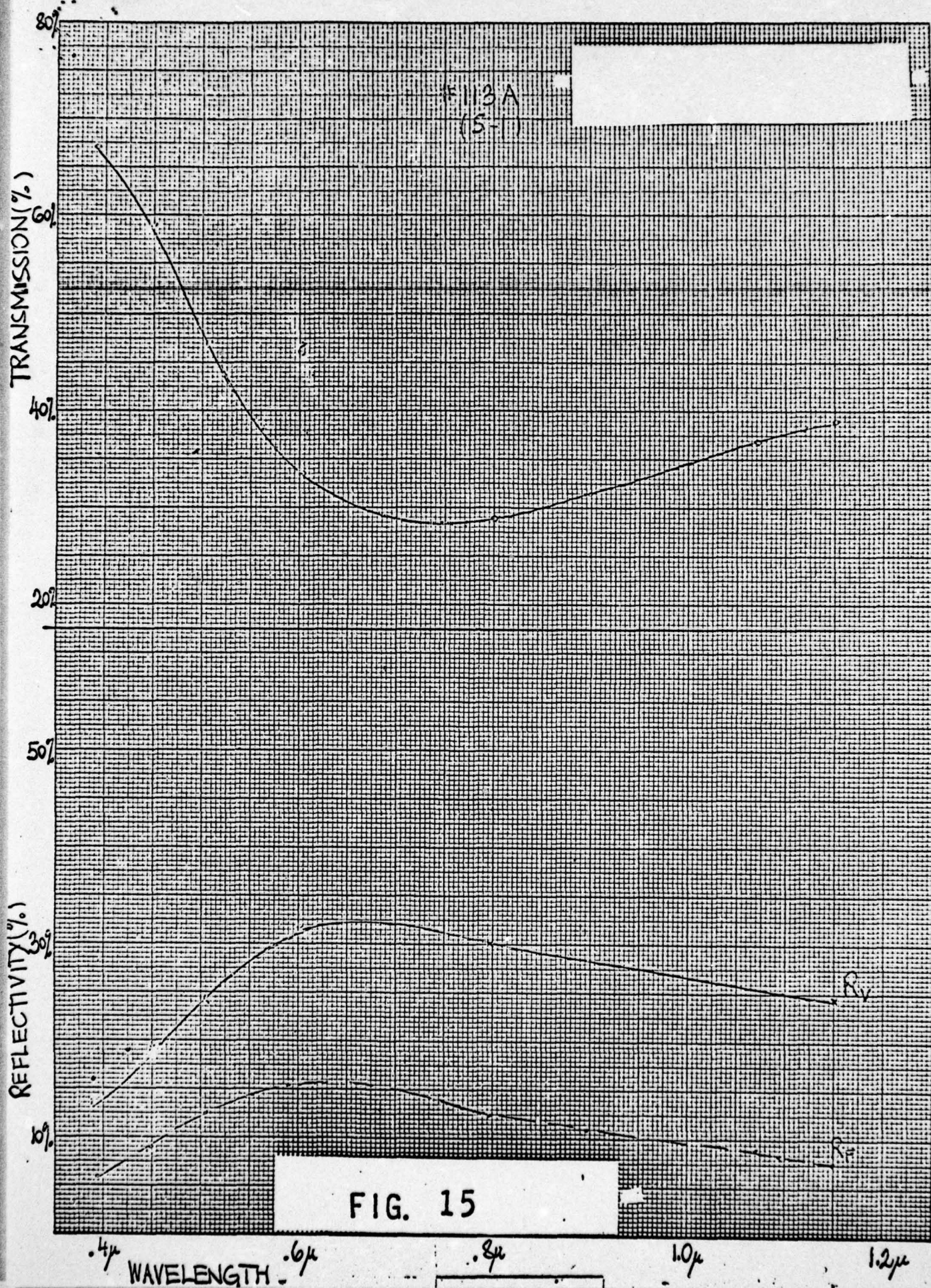


FIG. 15

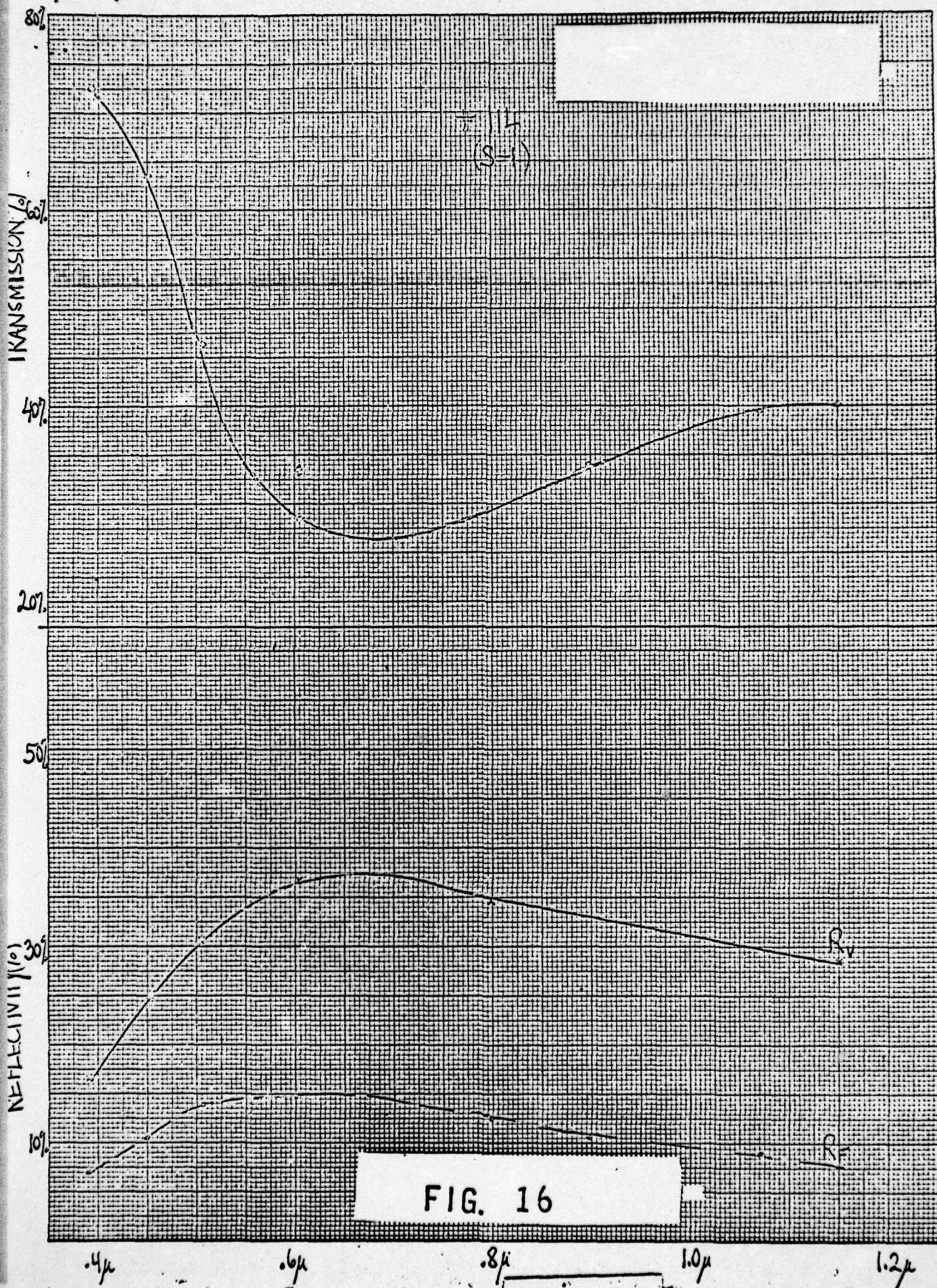


FIG. 16

K₁₀ 10 X 10 THE CENTIMETER 40 1513
MADE IN U.S.A.
KEUFFEL & ESSER CO.

TRANSMISSION(%)

REFLECTIVITY(%)

60%

40%

20%

0%

30%

10%

.4 μ

.6

.8

1.0

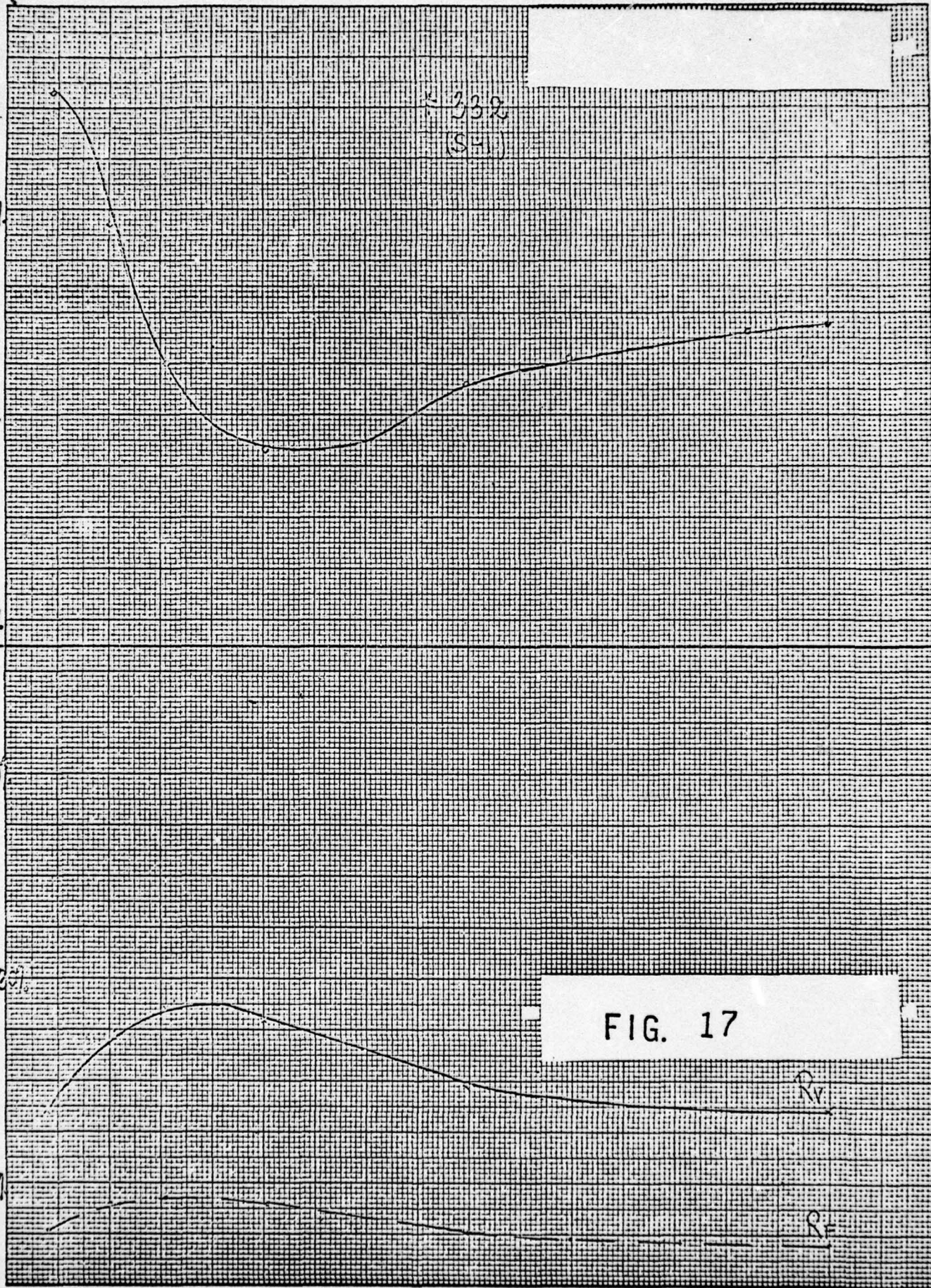
1.2 μ

332
(S.F.)

FIG. 17

R_v

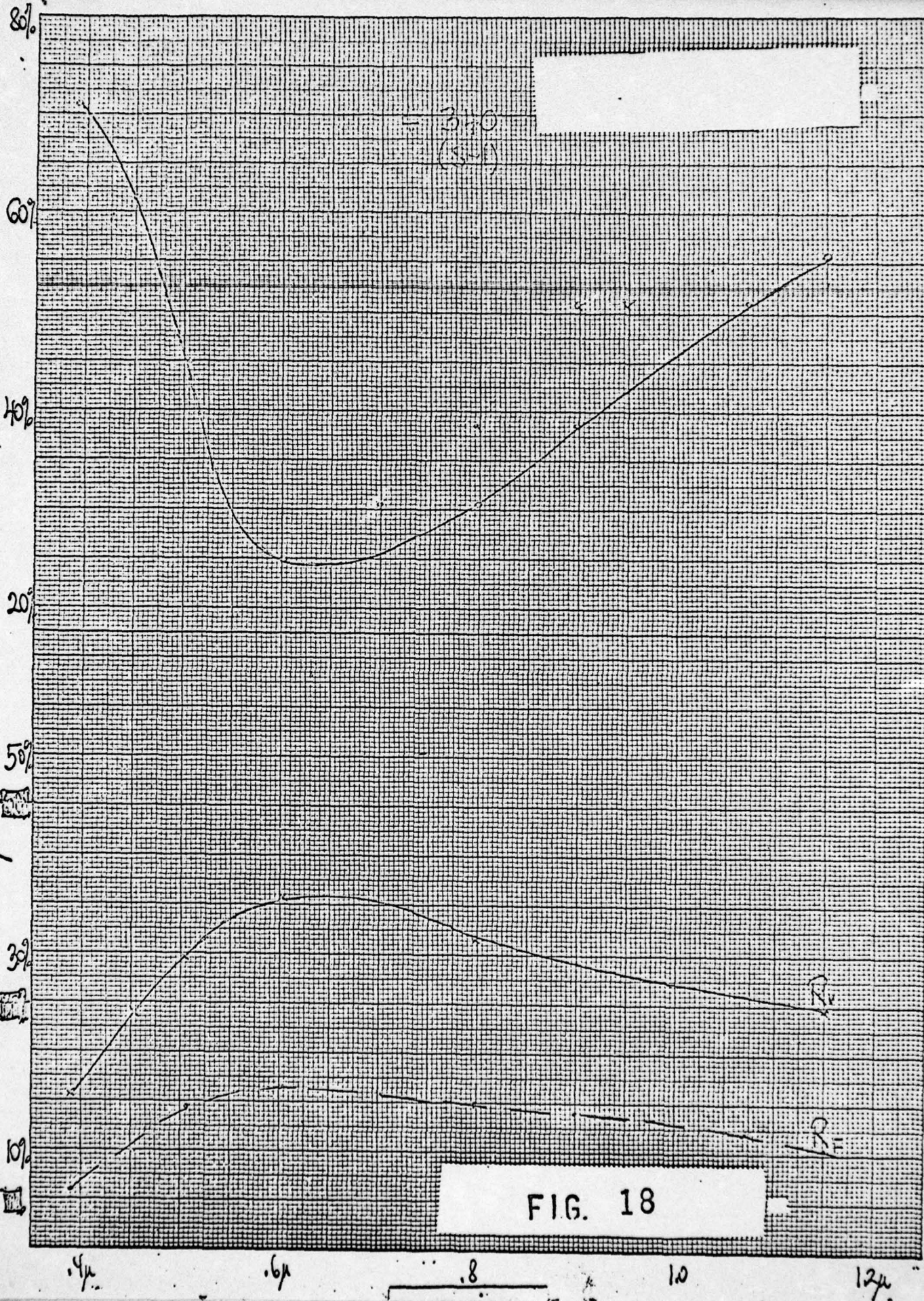
R_h



KE 10 X 10 TO THE CENTIMETER 46 1513
MADE IN U. S. A.
KEUFFEL & ESSER CO.

REFLECTIVITY

TRANSMISSION



K&E 10 X 10 TO THE CENTIMETER 46 1513
MADE IN U.S.A.

KEUFFEL & ESSER CO.

REFLECTIVITY(%)

TRANSMISSION(%)

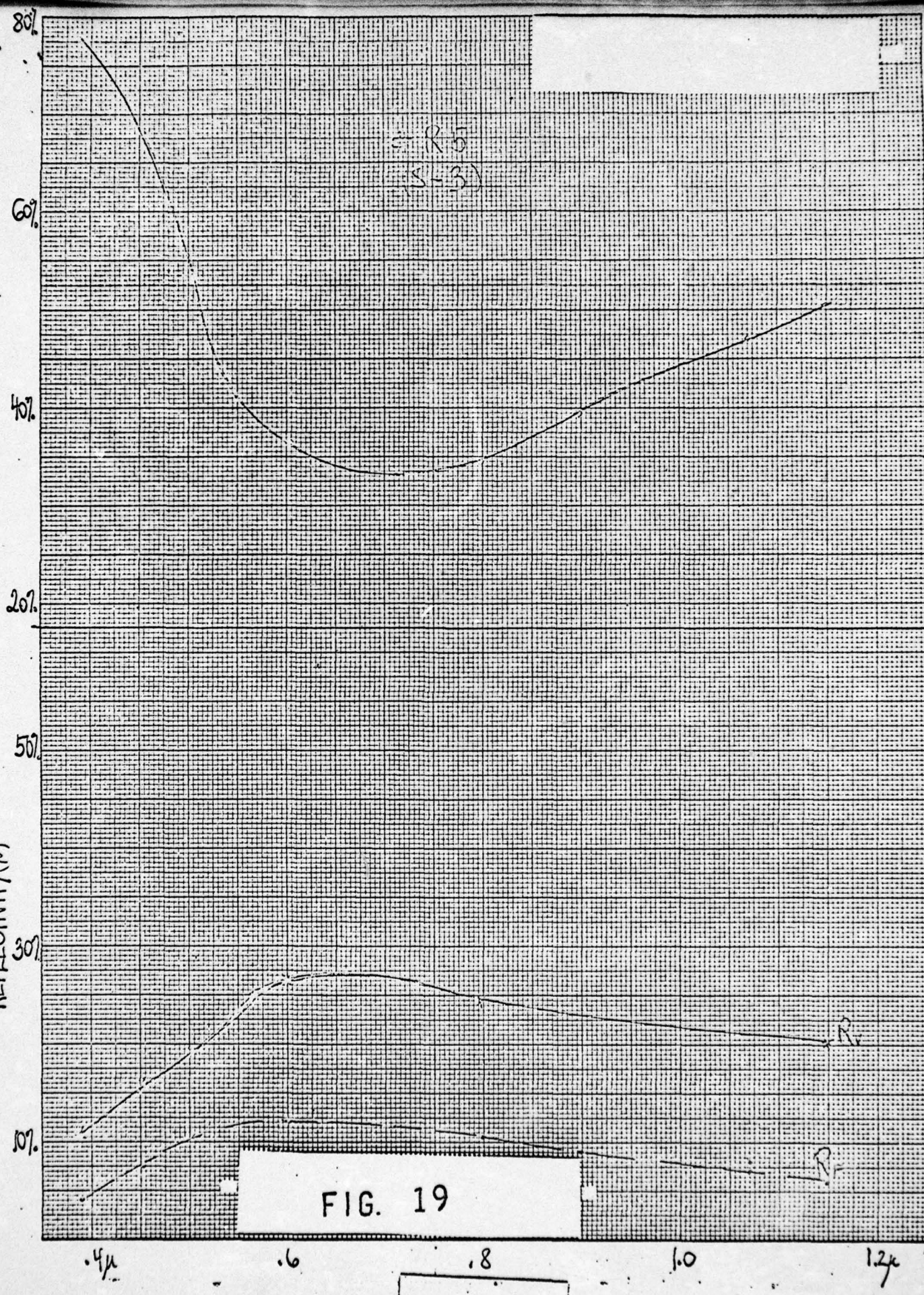


FIG. 19

K&E 10 X 10 TO THE CENTIMETER 46 1513
IN X 2.5 CM. KEUFFEL & ESSER CO.

TRANSMISSION IN PERCENT

$K=0$ $n=VAR.$

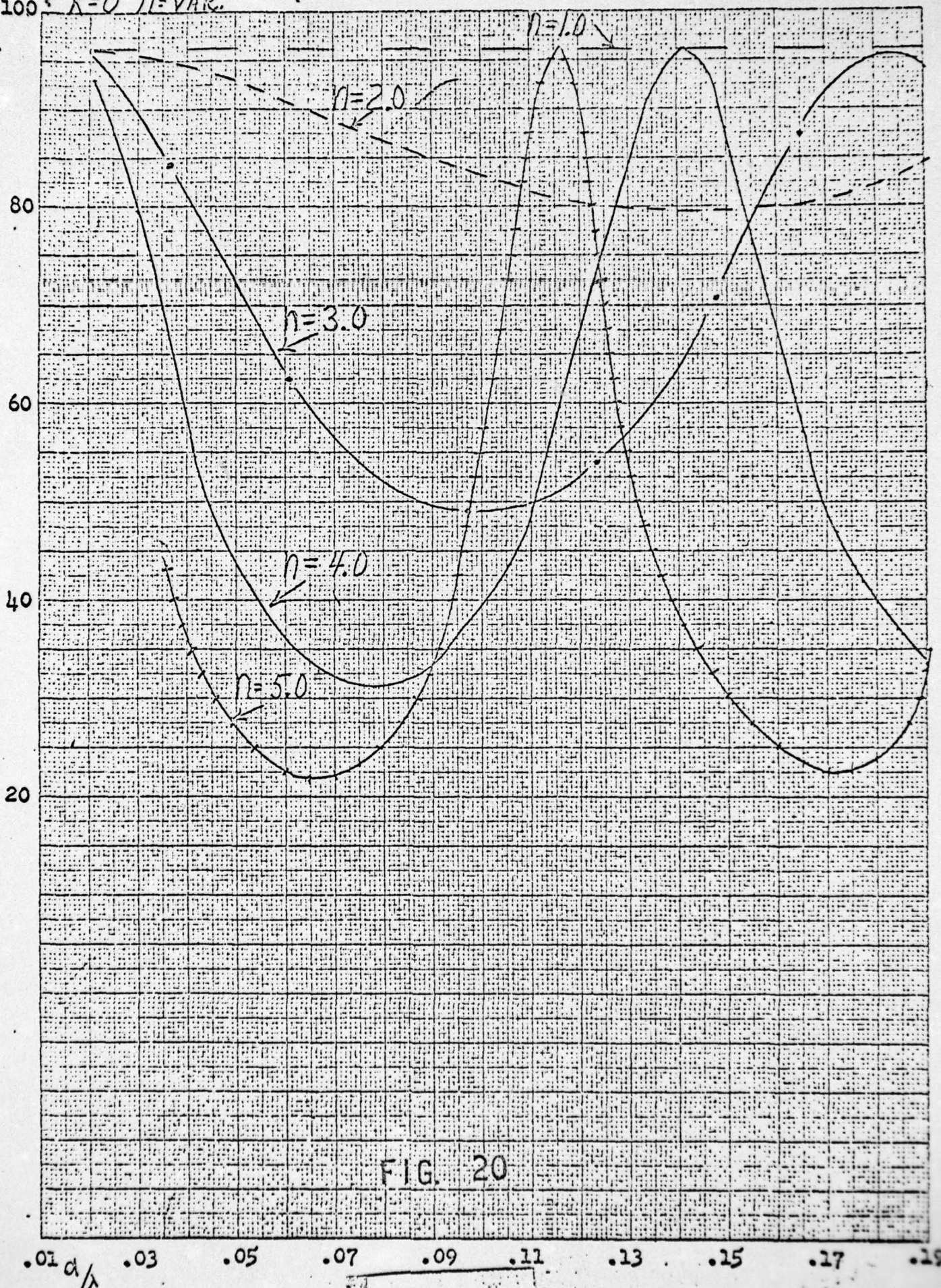


FIG. 20

AD-A034 076

DUMONT ELECTRON TUBES CLIFTON N J
STUDY AND IMPROVEMENT OF THE S-1 PHOTOEMISSIVE SURFACE.(U)
JUL 69 H TIMAN

F/G 17/5

DA-44-009-AMC-1811(E)

UNCLASSIFIED

ETC-116-69-A

NL

2 OF 2

AD
A034076

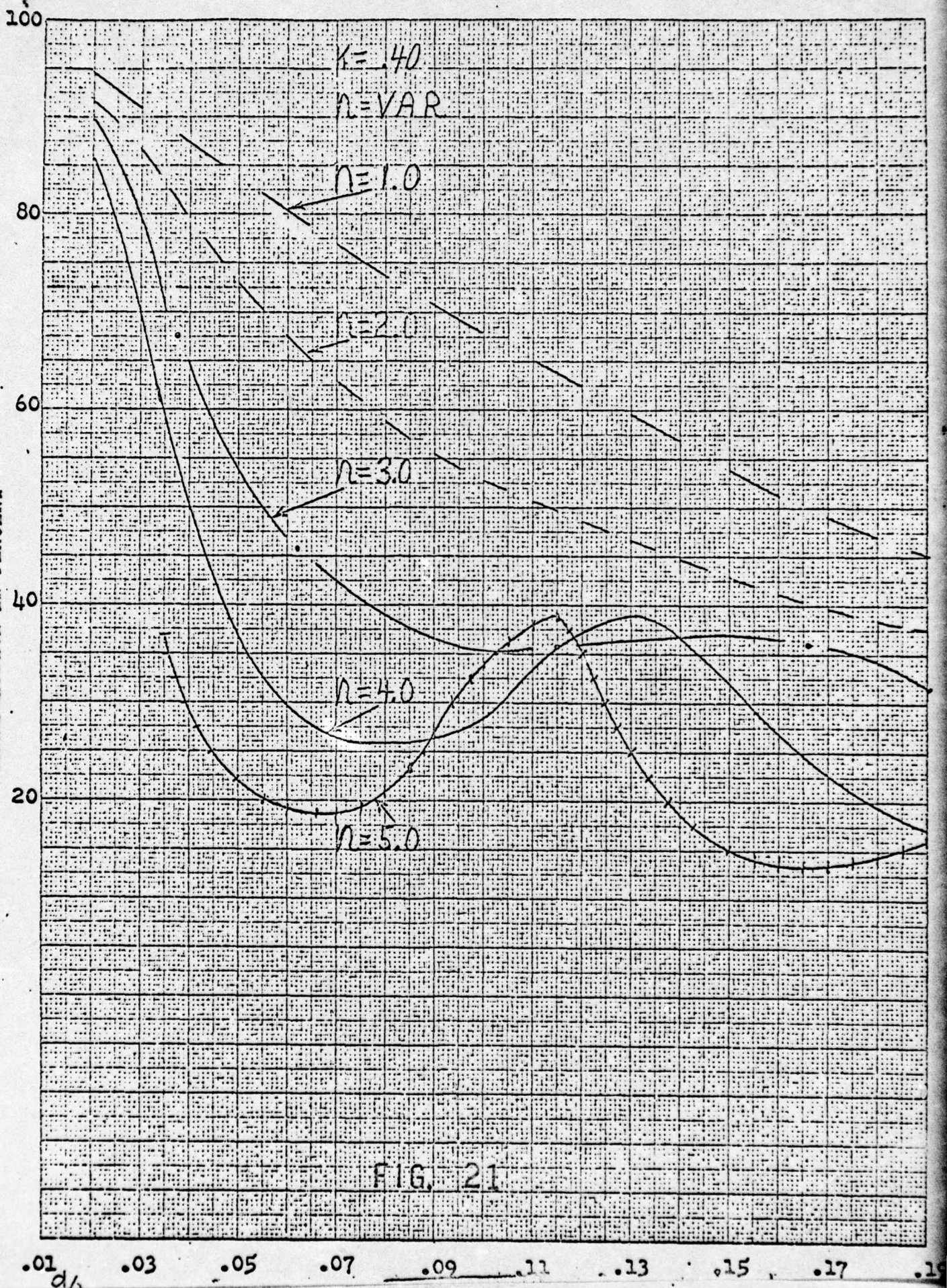




MICROCOPY RESOLUTION TEST CHART
NATIONAL BUREAU OF STANDARDS-1963-A

K&E 10 X 10 TO THE CENTIMETER 4G 1513
P. K. & G. CO.
KEUFFEL & ESSER CO.

TRANSMISSION IN PERCENT



K&E 10 X 10 TO THE CENTIMETER 4G 1513
MADE IN U.S.A.
KEUFFEL & ESSER CO.

TRANSMISSION IN PERCENT

100

80

60

40

20

.01

.03

.05

.07

.09

.11

.13

.15

.17

.19

d/λ

$K=.80$

$n=VAR.$

$n=1.0$

$n=2.0$

$n=4.0$

$n=3.0$

$n=5.0$

FIG. 22

REF 10 X 10 TO THE CENTIMETER 46 1513
10 X 25 CM.
KODAK SAFETY FILM CO.

TRANSMISSION IN PERCENT

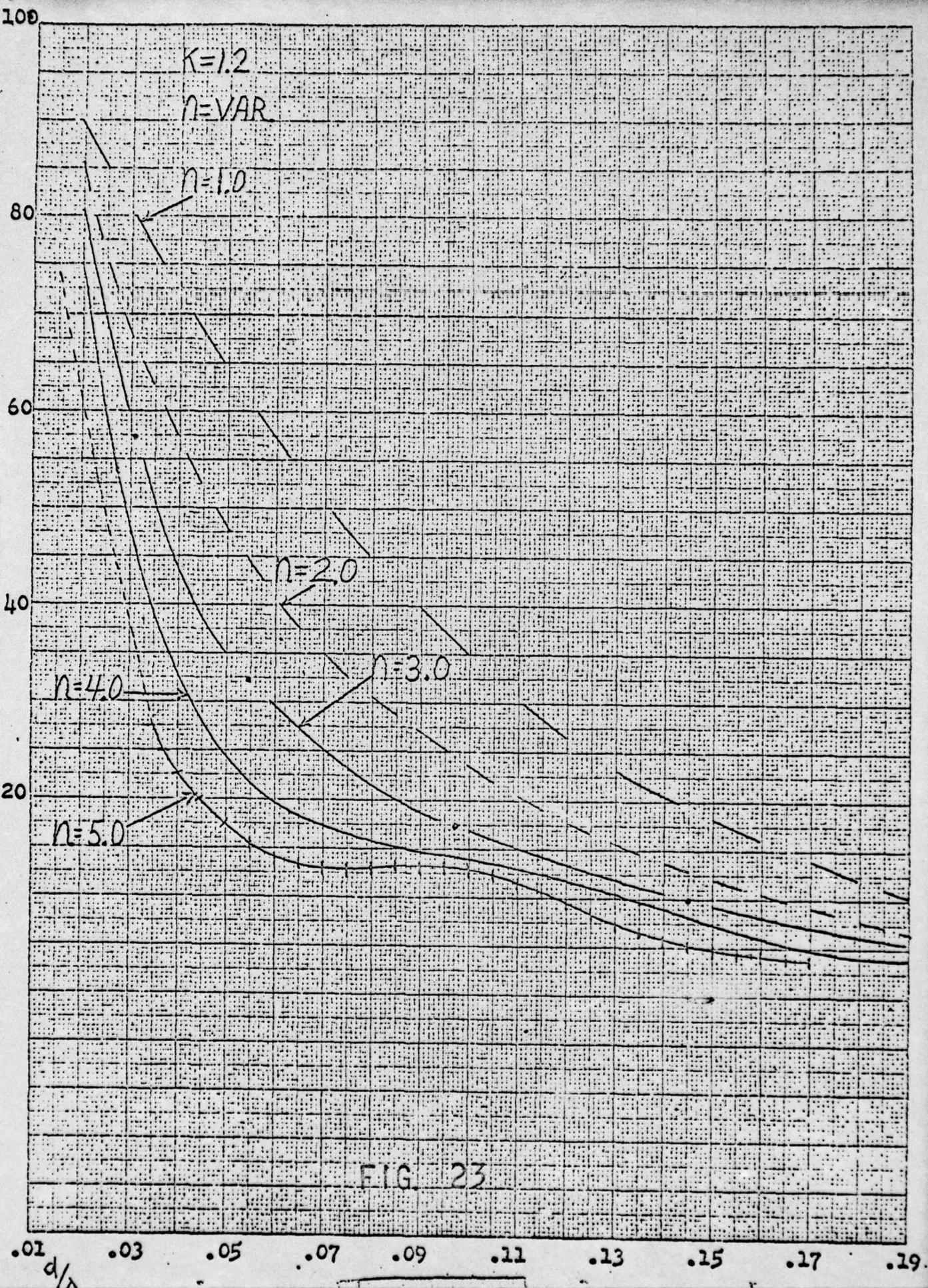


FIG. 23

TRANSMISSION IN PERCENT

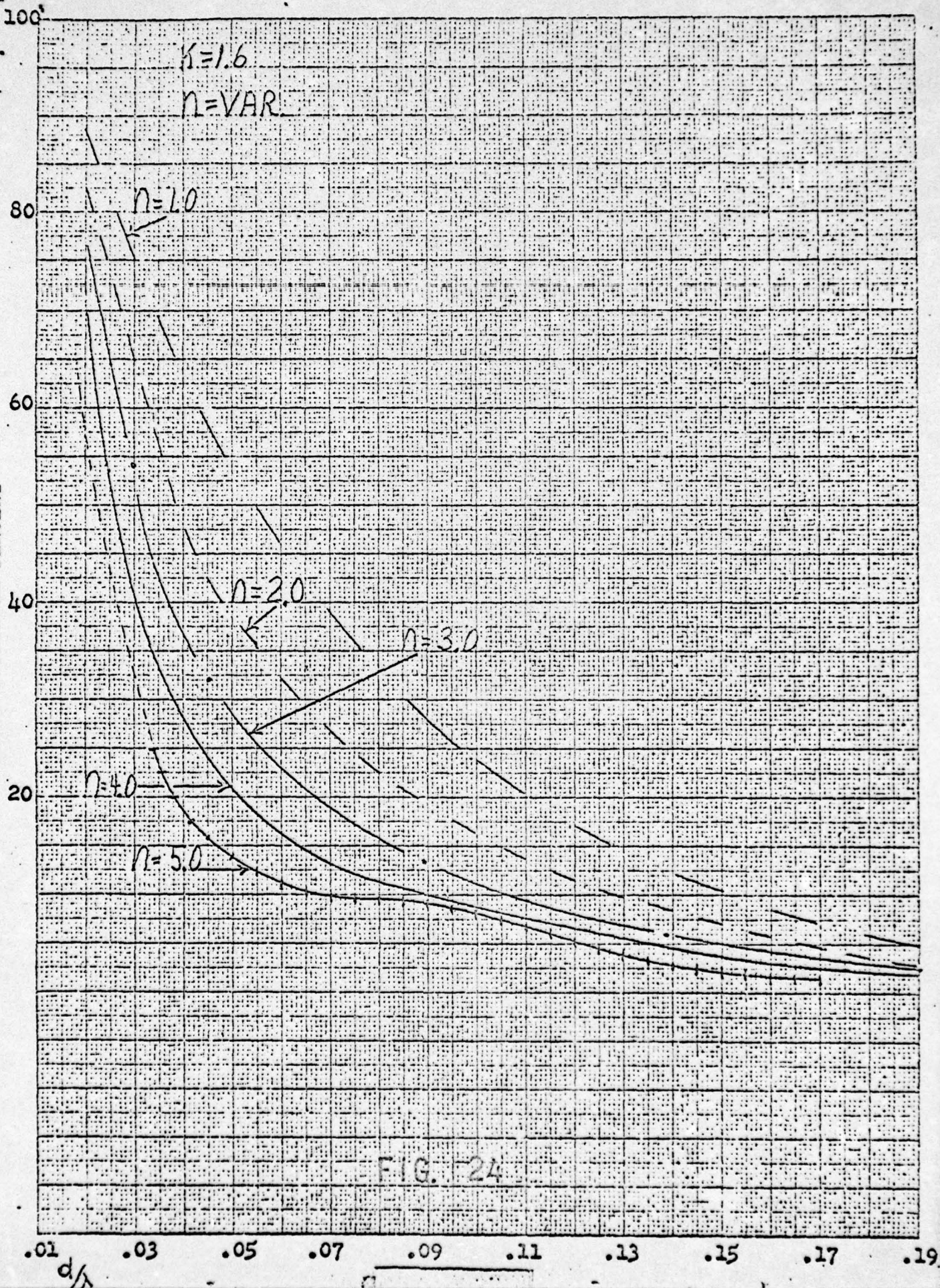
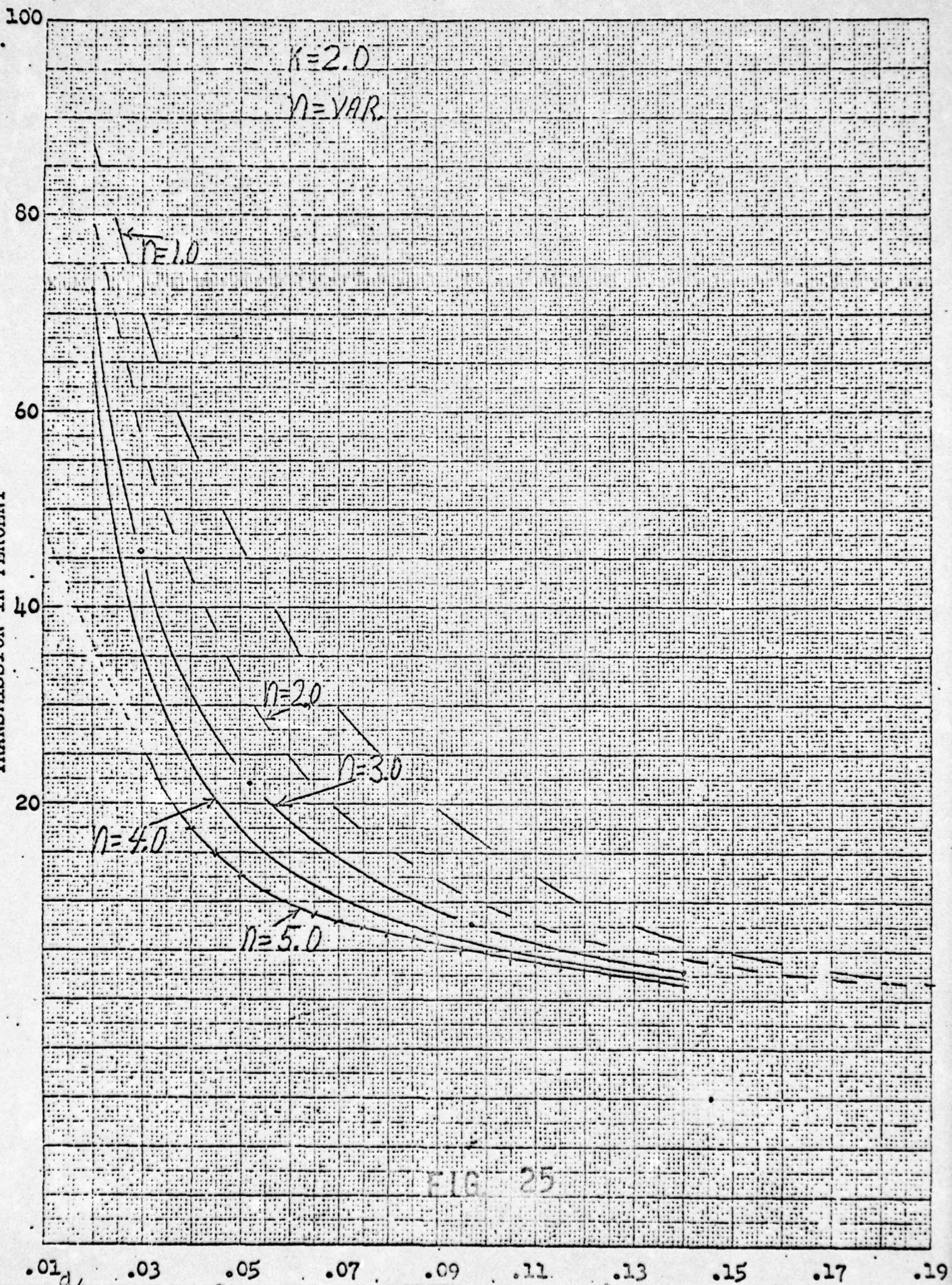


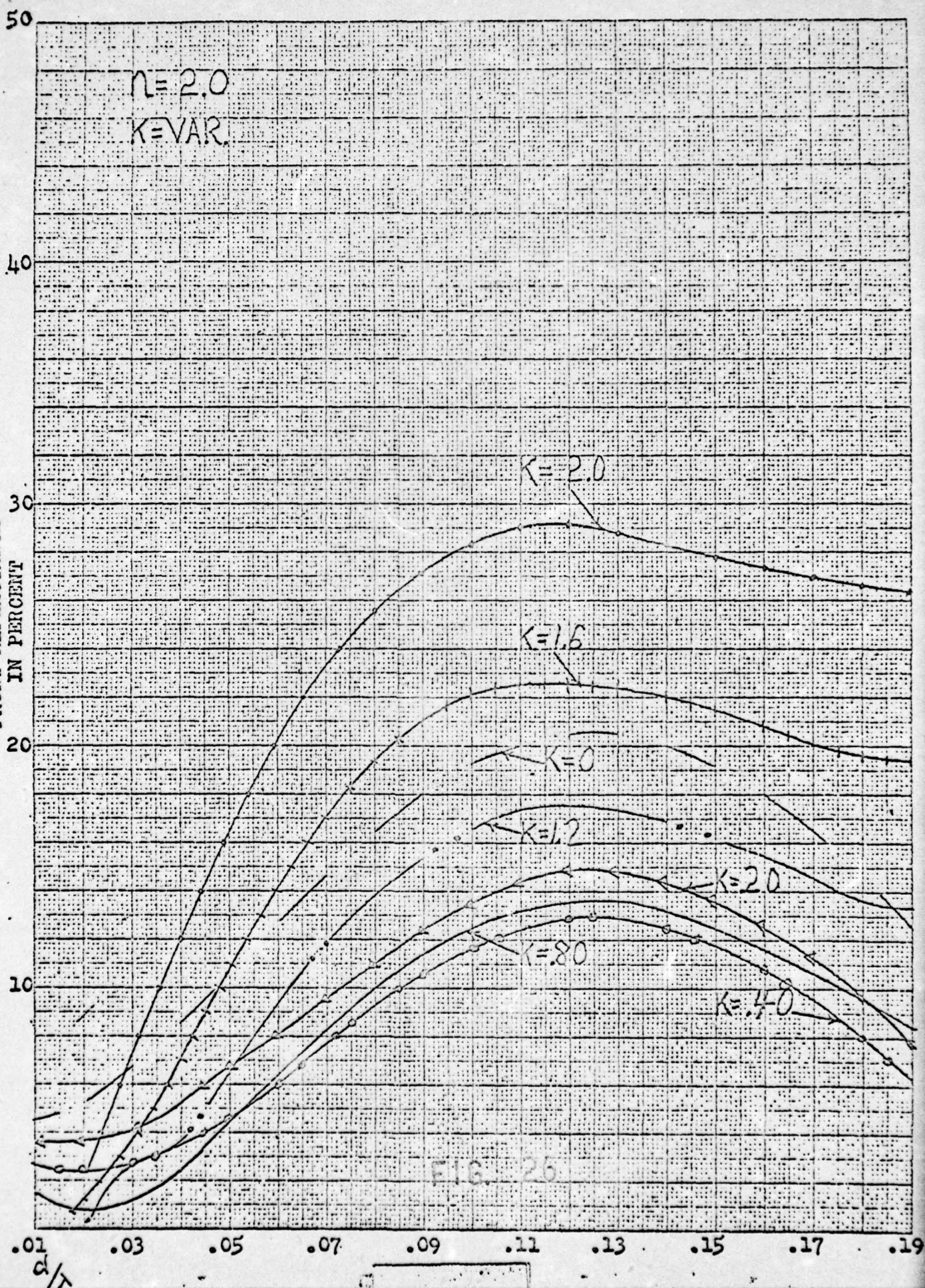
FIG. 24

TRANSMISSION IN PERCENT



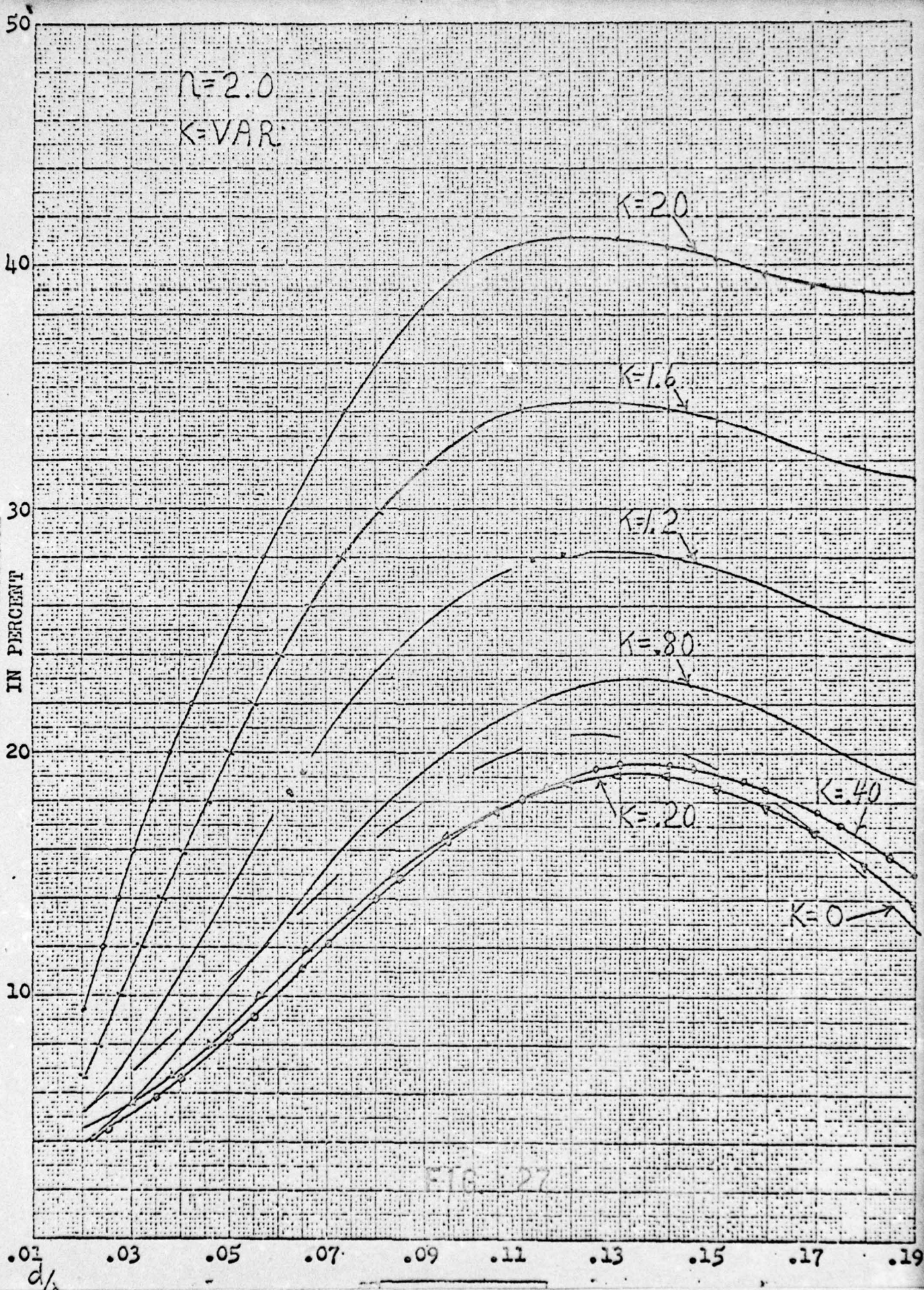
REF. 10 X 10 TO THE CENTIMETER 46 1513
 P. 10 X 25 CM.
 KODAK SAFETY FILM
 KODAK SAFETY FILM

FRONT REFLECTANCE
IN PERCENT



K&E 10 X 10 TO THE CENTIMETER 46 1513
U. S. GOVERNMENT PRINTING OFFICE
WASHINGTON, D. C. 20540
K&E 10 X 10 TO THE CENTIMETER 46 1513

VACUUM REFLECTANCE
IN PERCENT



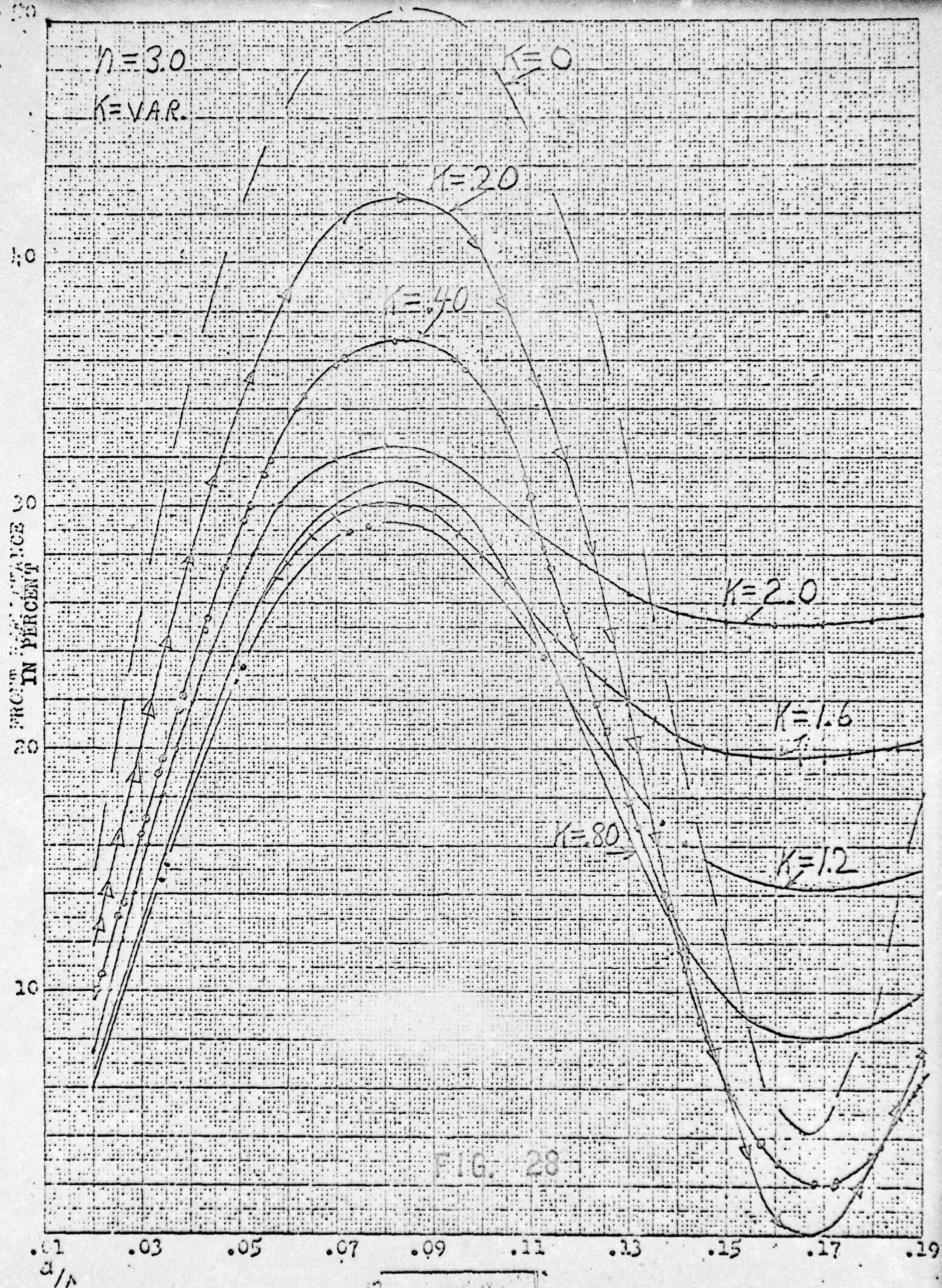


FIG. 28

VACUUM REFLECTANCE
IN PERCENT

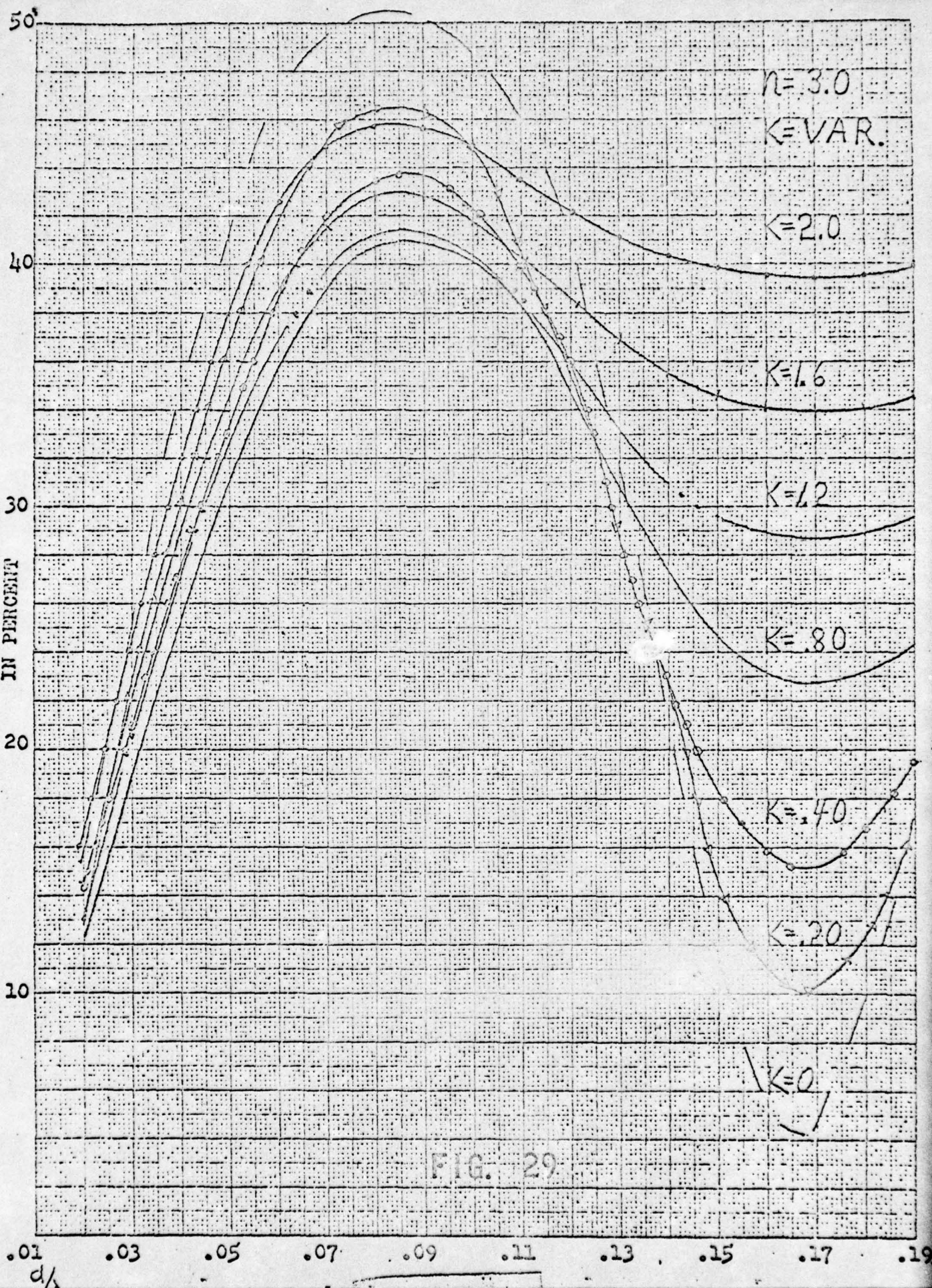


FIG. 29

12.5 10 X 10 TO THE CENTIMETER 46 1513
K. S. 10 X 10 TO THE CENTIMETER 46 1513
K. S. 10 X 10 TO THE CENTIMETER 46 1513

FRONT REFLECTANCE
IN PERCENT

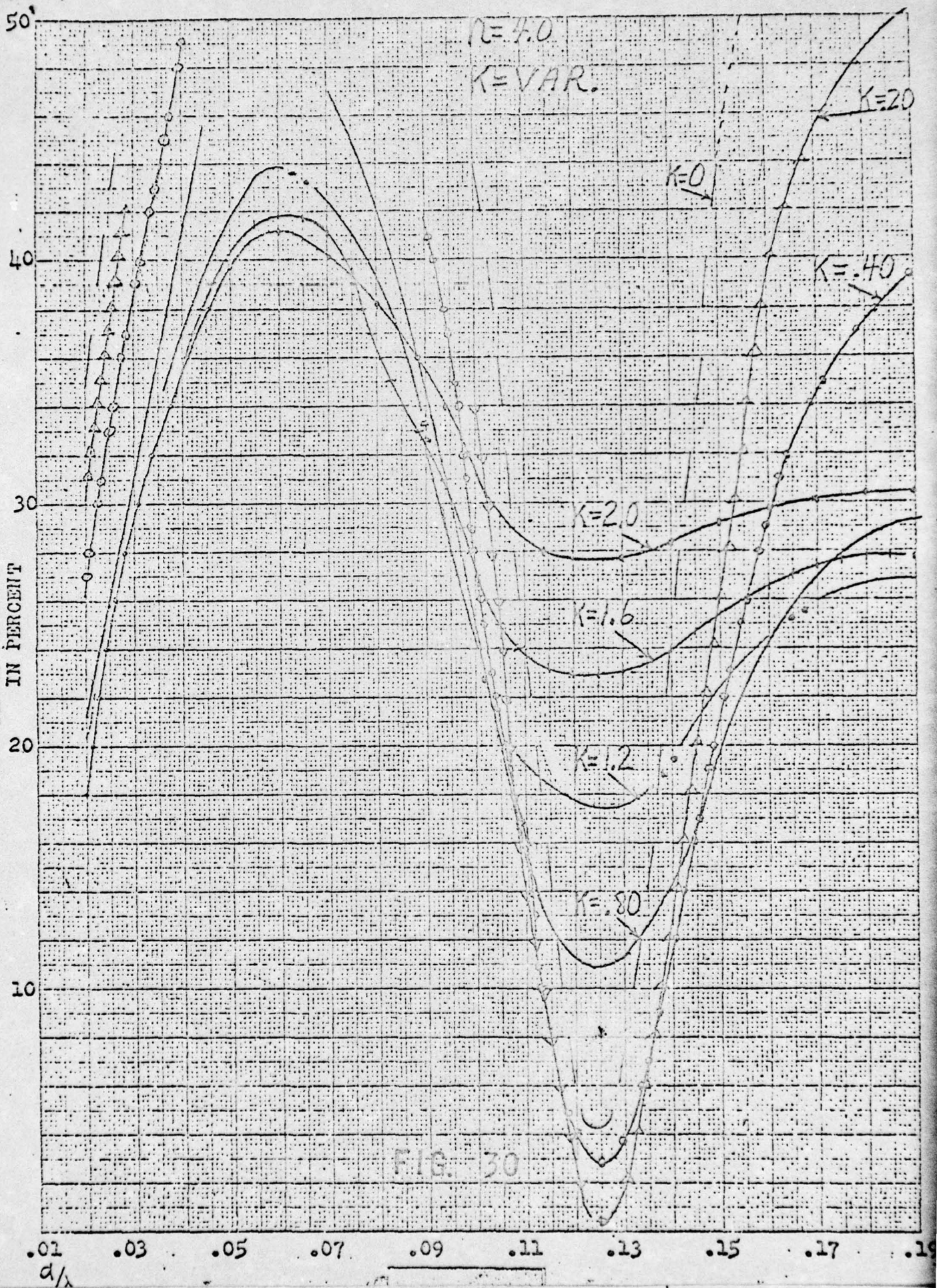


FIG. 30

VACUUM REFLECTANCE
IN PERCENT

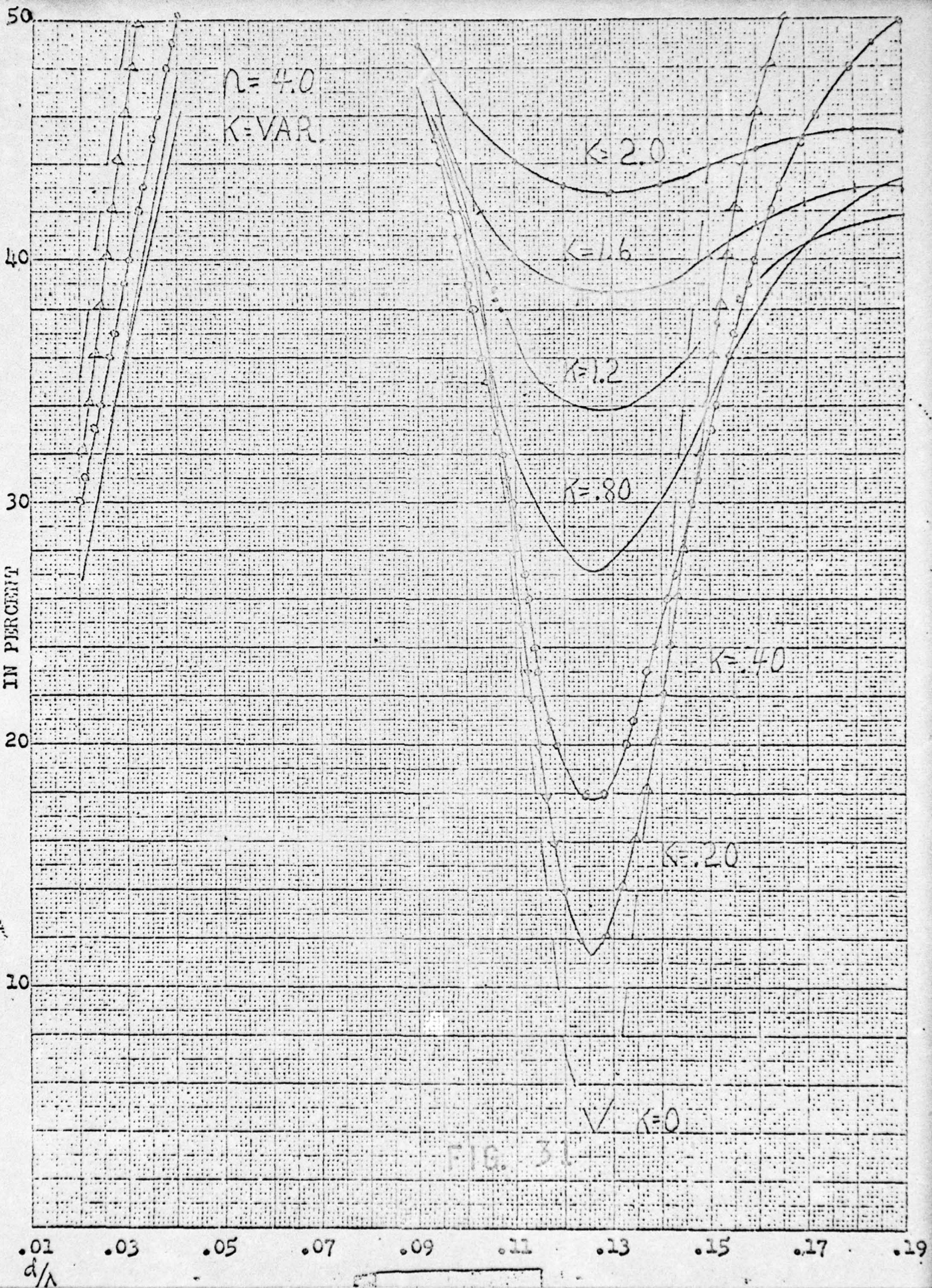


FIG. 31

FRONT REFLECTANCE
IN PERCENT

.01 .03 .05 .07 .09 .11 .13 .15 .17 .19
 d/λ

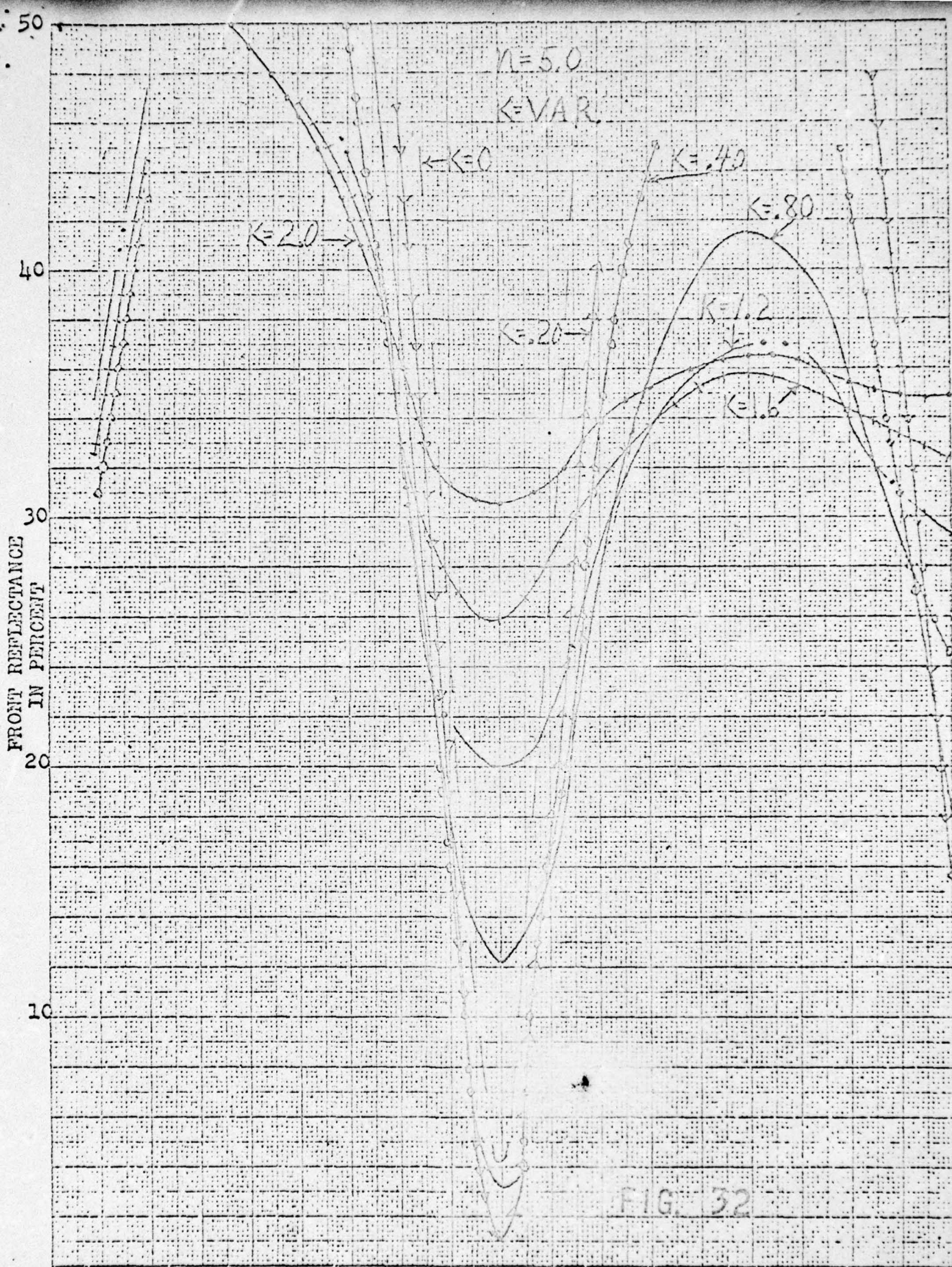


FIG. 32

WAVELENGTH TO THE CENTIMETER 46 1513
MAY 1954
FEDERAL BUREAU OF INVESTIGATION
FEDERAL BUREAU OF INVESTIGATION

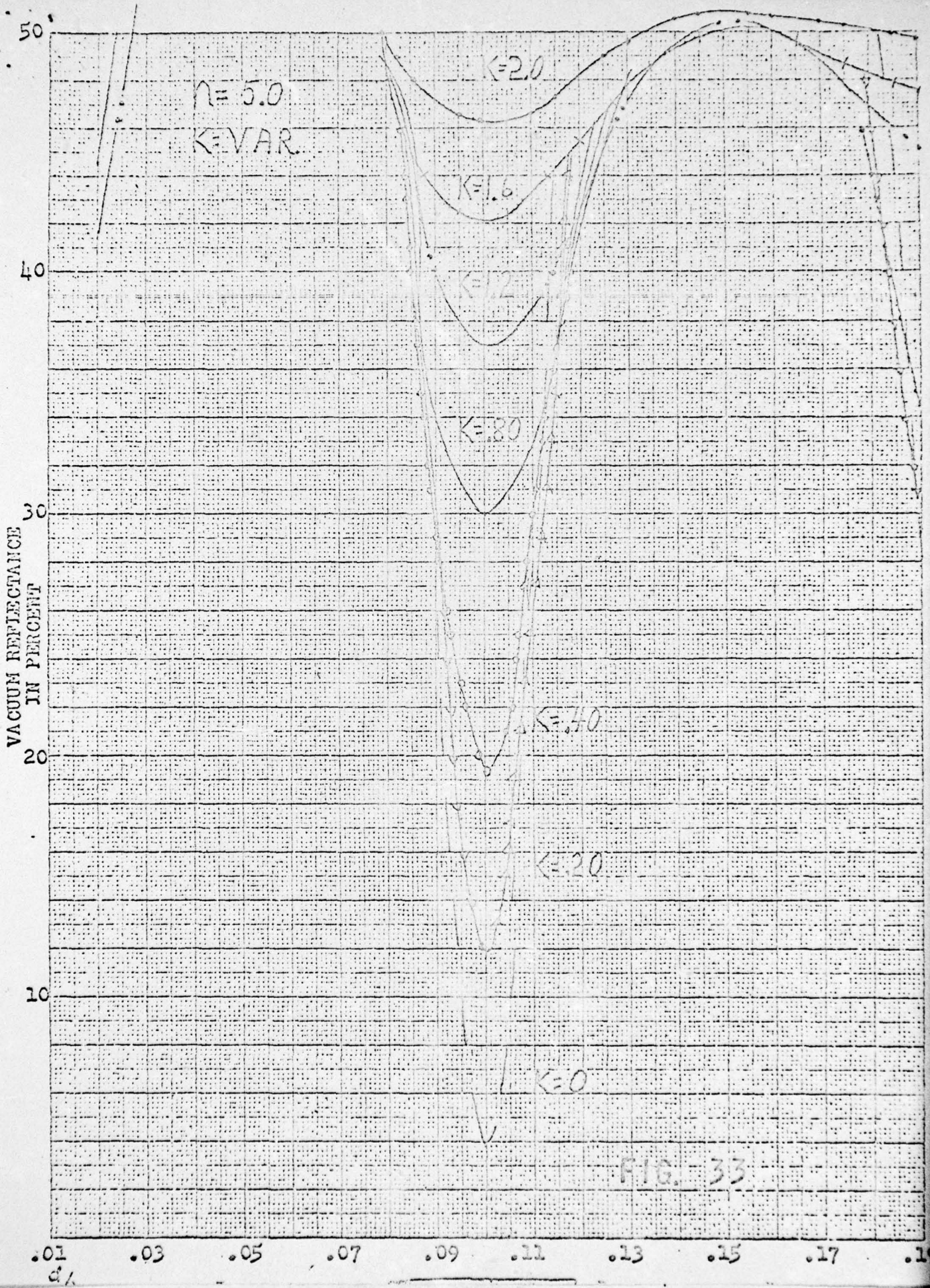
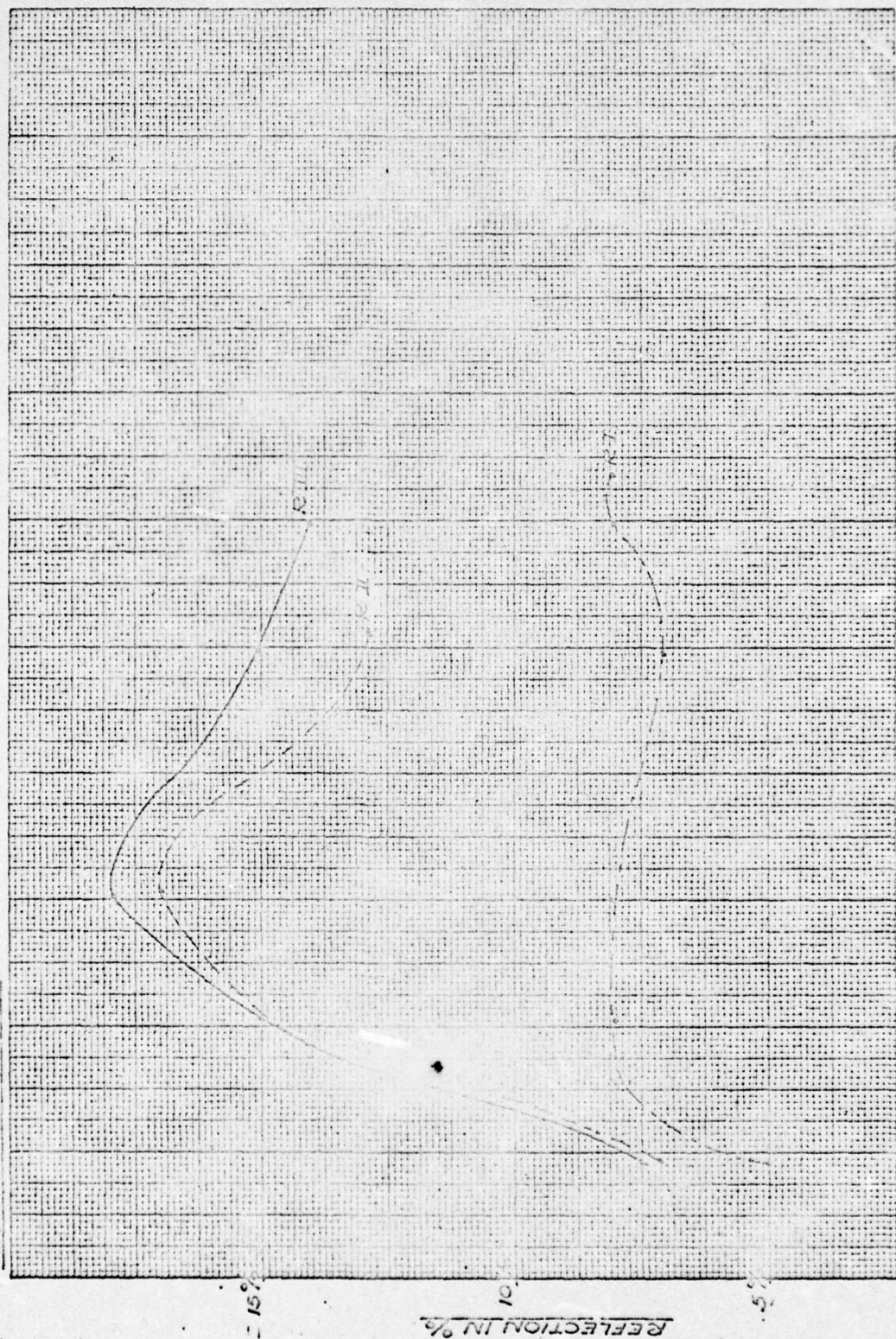


FIG. 33

#597 REFLECTION



WAVELENGTH

.9

.6

.3

FIG. 35

597 TRANSMISSION

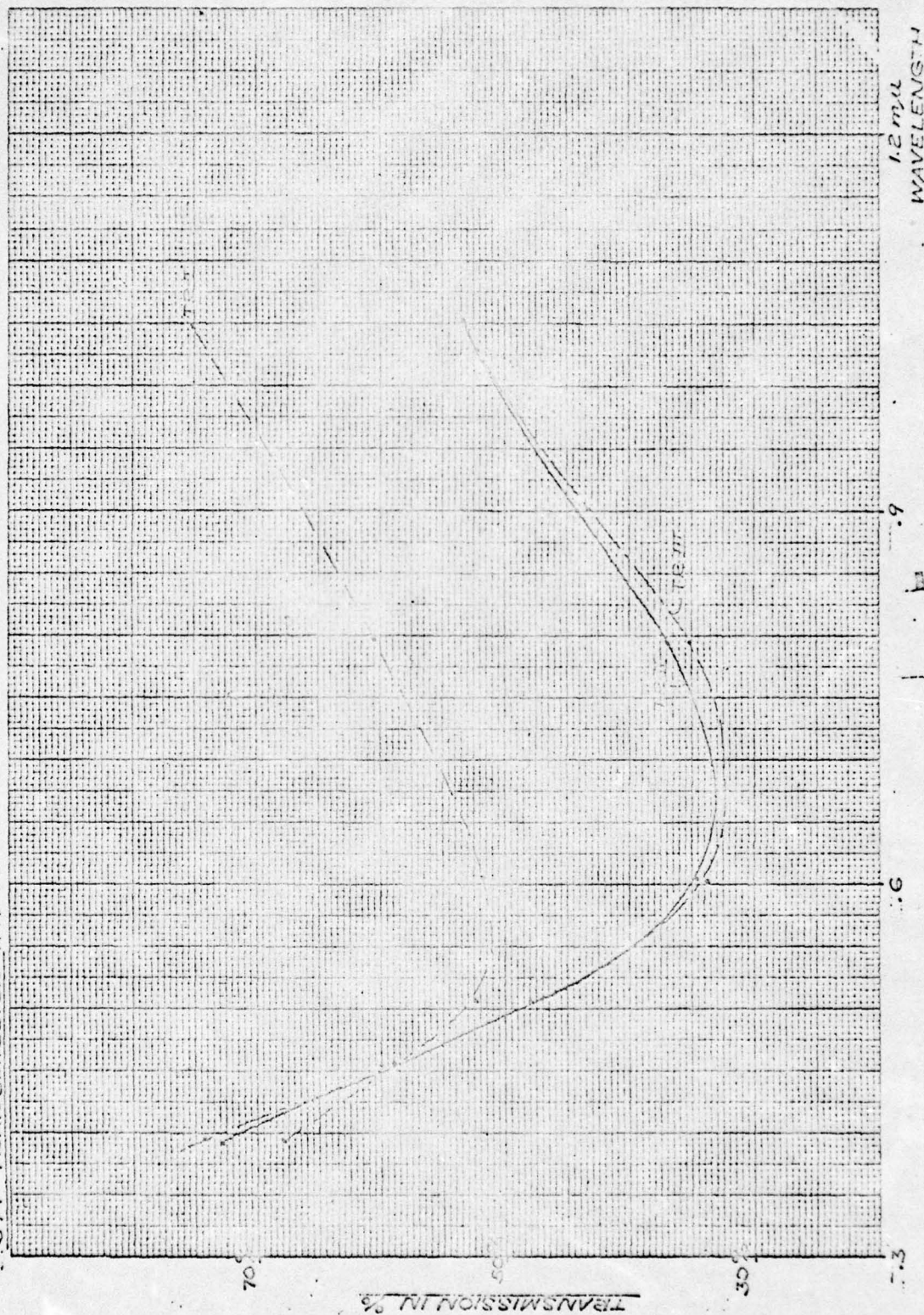


FIG. 36

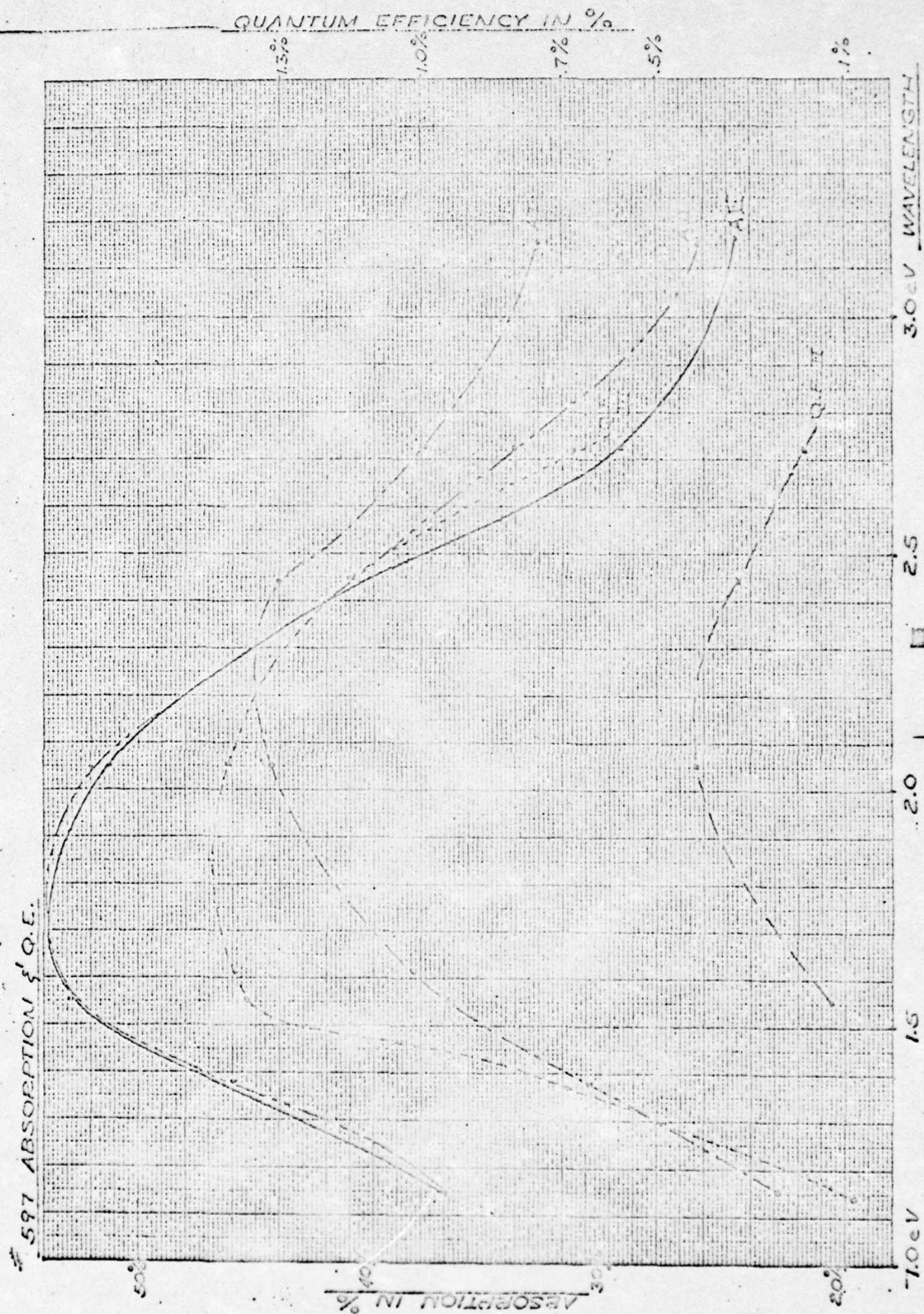
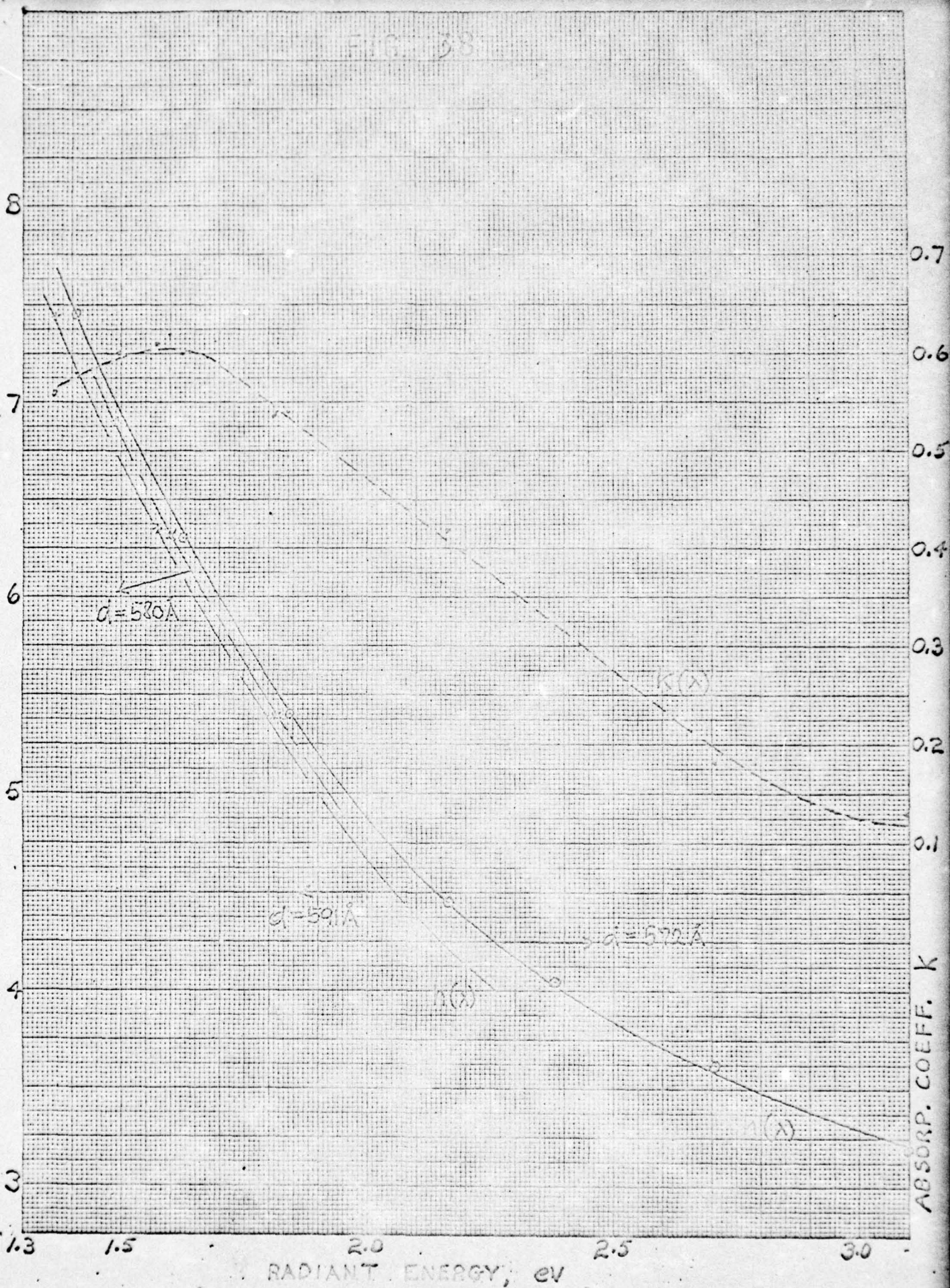


FIG. 37

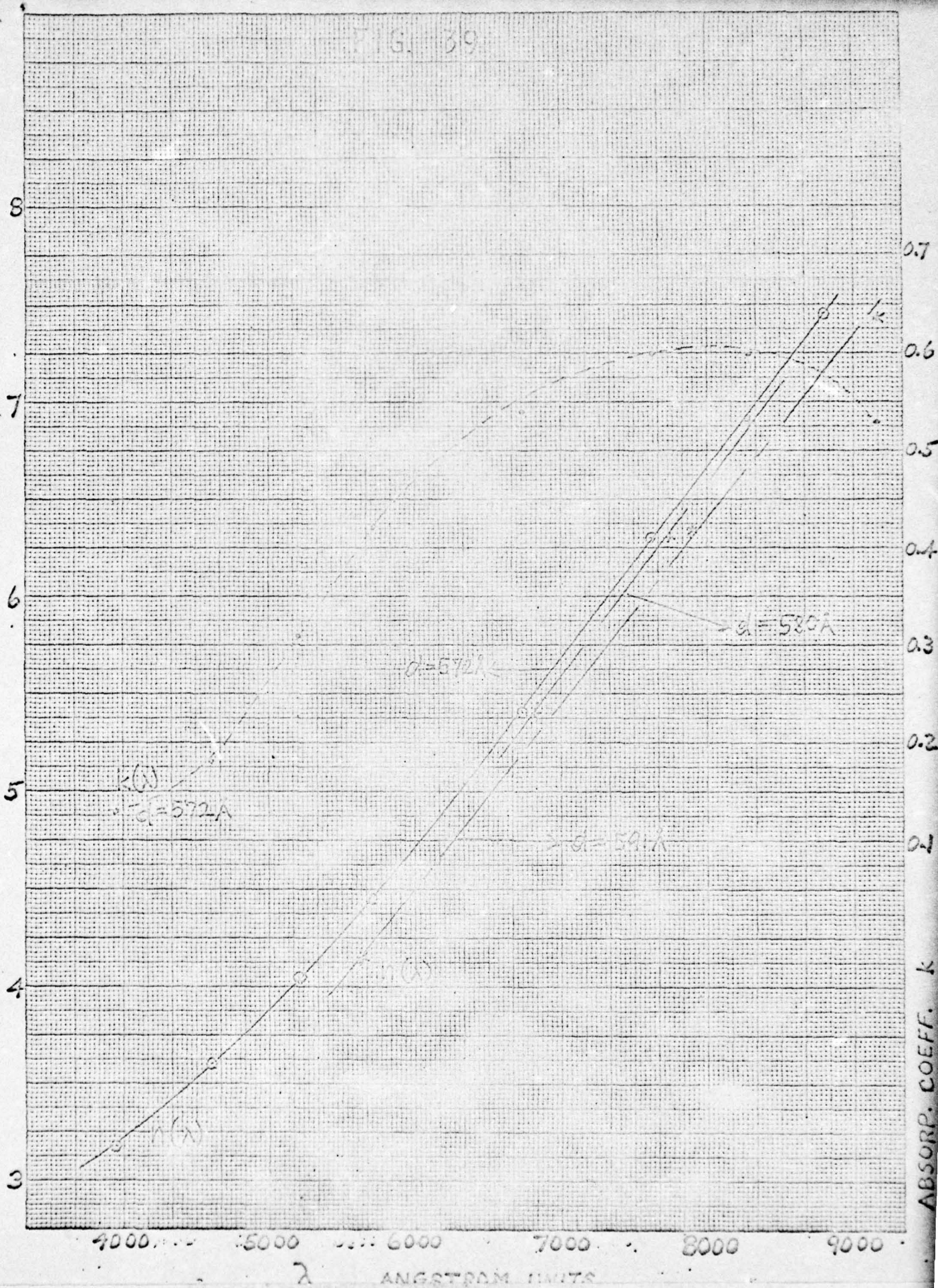
KE 10 X 10 TO THE CENTIMETER 4G 1513
MADE IN U.S.A.
KEUFFEL & ESSER CO.

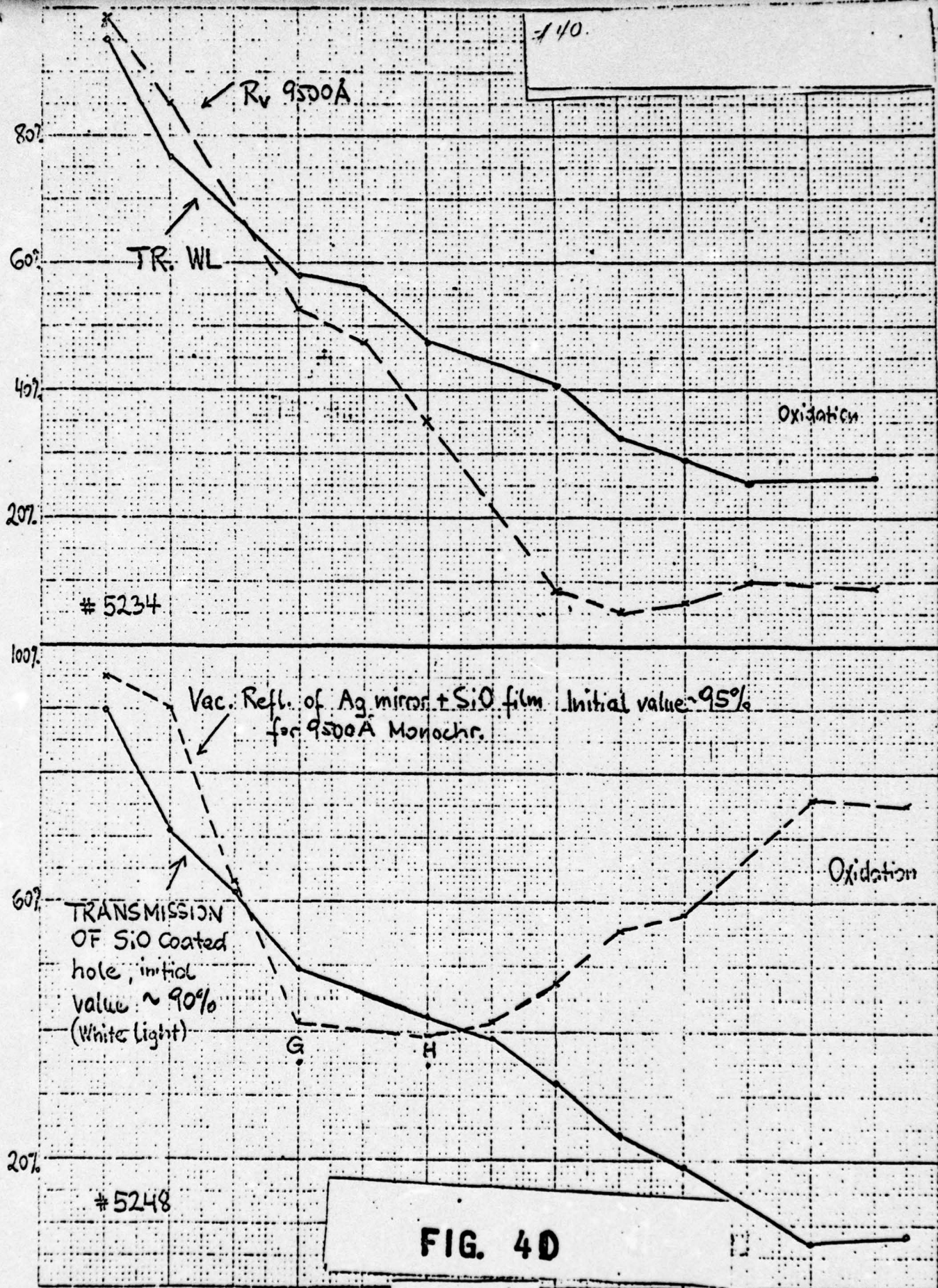
REFRACTIVE INDEX n



REF 10 X 10 TO THE CENTIMETER 46 1513
 10 X 25 CM.
 KLUFFEL & ESSER CO.

REFRACTIVE INDEX n





CHANGE OF TR. AND R_v UPON STEPWISE EVAPORATION OF AG

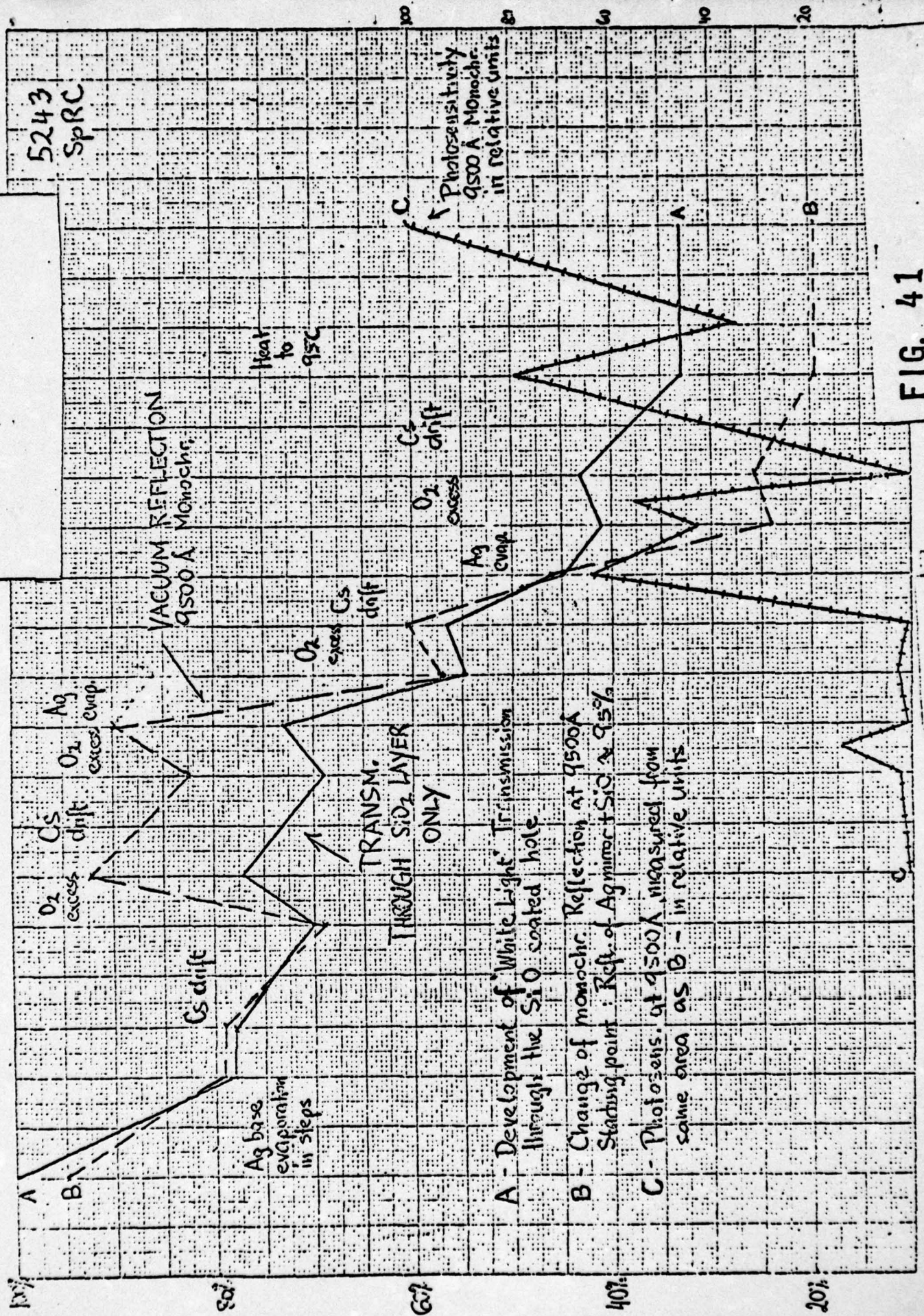


FIG. 41

K&E 104 10 TO THE CENTIMETER 40 10113
18 X 25 CM. MADE IN U.S.A.
NEUFFEL & ESSER CO.

% REFLECTION

FIG 42

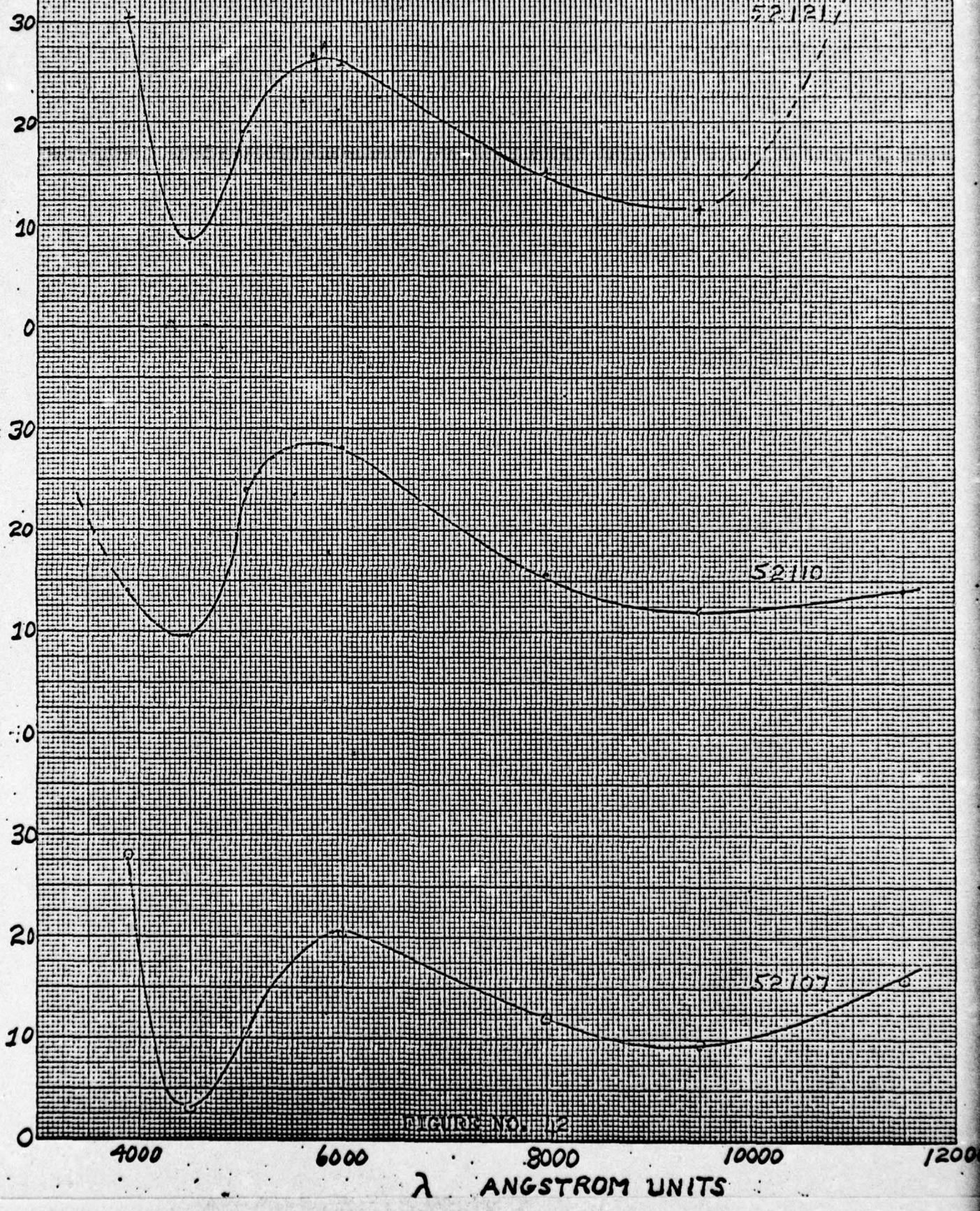


FIGURE NO. 12

EUGENE DIETZGEN CO.
MADE IN U. S. A.

NO. 34DR-20 DIETZGEN GRAPH PAPER
20 X 20 PER INCH

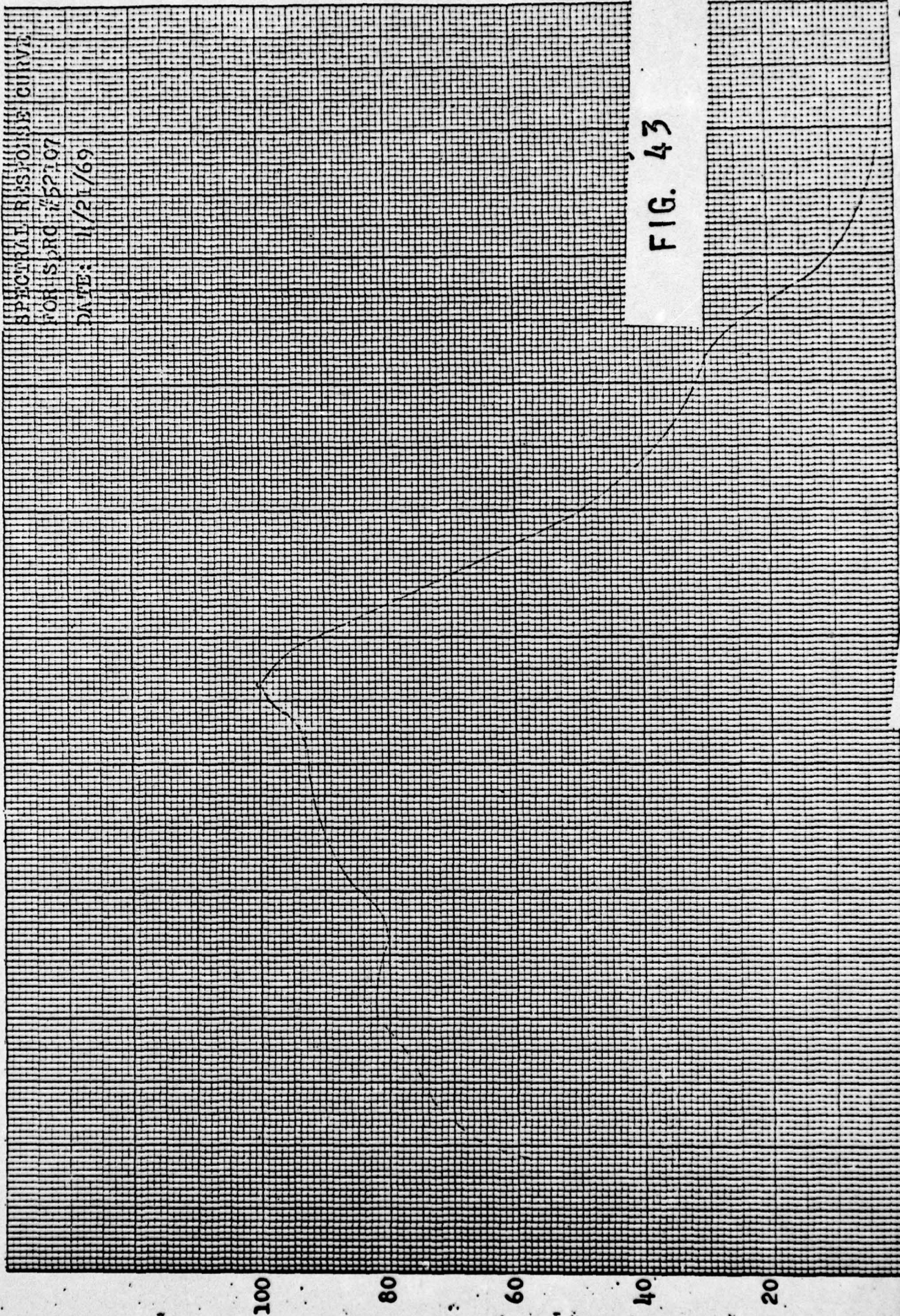
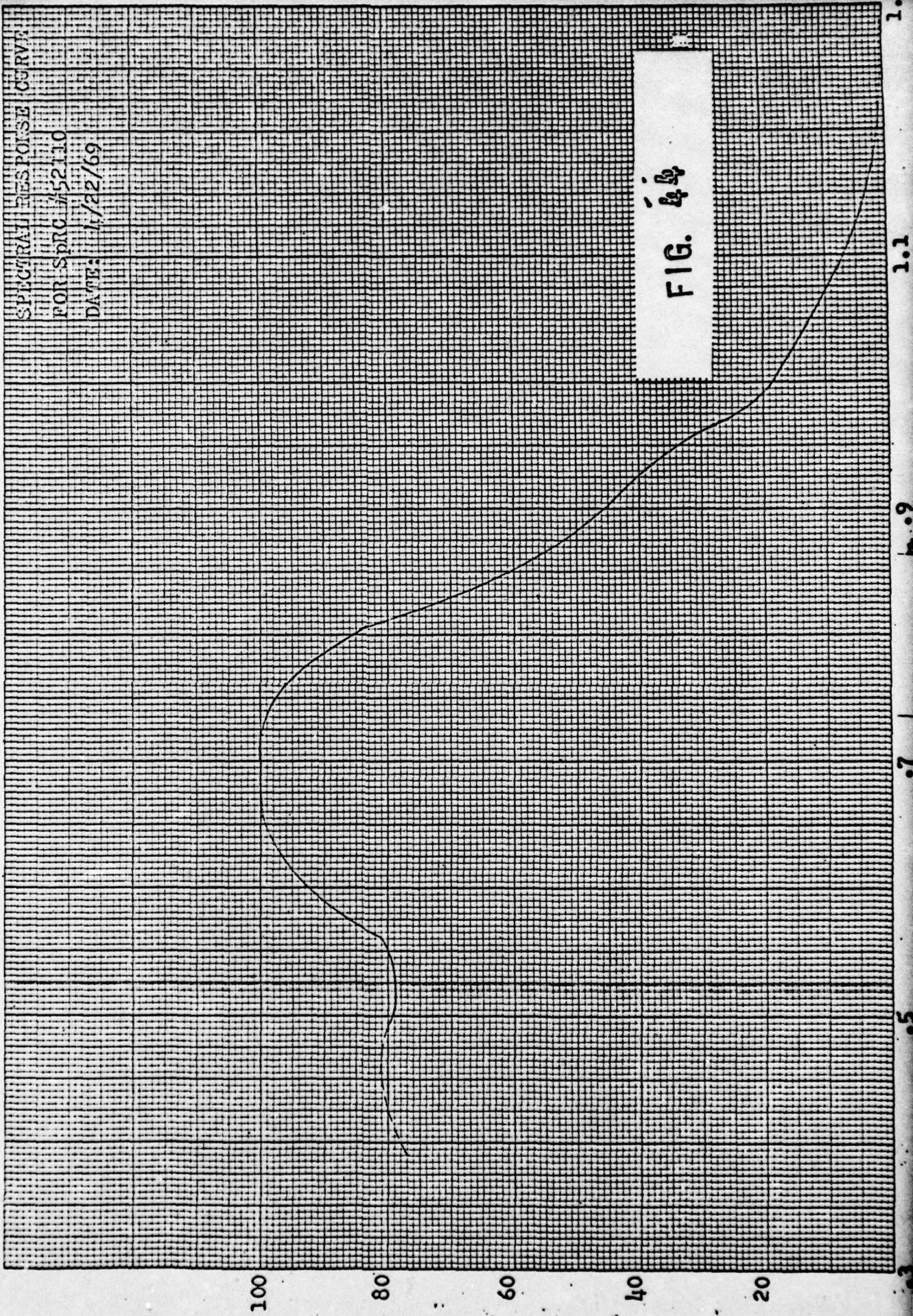


FIG. 43

EUGENE DIETZEN CO.
MADE IN U. S. A.

NO. 340R-20 DIETZEN GRAPH PAPER
20 X 20 PER INCH



A computer program has now been received through private communication and will be evaluated. In order to establish the optical data of the cathode proper, formulas for the above-mentioned correction have developed.

The computer program gives the following three quantities for the single film, which are essentially equivalent with those of Rpt. #36, Figure 9.

$$(I) \quad R_{Fc} = \frac{1}{Z} (a_1^2 + b_1^2) e^{2\alpha_1} + (a_2^2 + b_2^2) e^{-2\alpha_1} + A \cos(2\delta_1) + B \sin(2\delta_1)$$

$$(II) \quad R_{Vc} = \frac{1}{Z} (a_1^2 + b_1^2) e^{-2\alpha_1} + (a_2^2 + b_2^2) e^{2\alpha_1} + A \cos(2\delta_1) + B \sin(2\delta_1)$$

$$(III) \quad T_{Fc} = T_{Vc} = \frac{n_2}{n_0} \frac{1}{Z} [(1+a_1)^2 + b_1^2] [(1+a_2)^2 + b_2^2]$$

$$Z = e^{2\alpha_1} + (a_1^2 + b_1^2)(a_2^2 + b_2^2) e^{-2\alpha_1} + C \cos(2\delta_1) + D \sin(2\delta_1)$$

Here are

$$a_1 = \frac{n_0^2 - n_1^2 - k_1^2}{(n_0 + n_1)^2 + k_1^2} ; a_2 = \frac{n_1^2 - n_2^2 + k_1^2}{(n_1 + n_2)^2 + k_1^2}$$

$$b_1 = \frac{2n_0 k_1}{(n_0 + n_1)^2 + k_1^2} ; b_2 = \frac{-2n_2 k_1}{(n_1 + n_2)^2 + k_1^2}$$

$$A = 2(a_1 a_2 + b_1 b_2) ;$$

$$B = 2(a_1 b_2 - a_2 b_1)$$

$$C = 2(a_1 a_2 - b_1 b_2) ;$$

$$D = 2(a_1 b_2 - a_2 b_1)$$

$$\alpha_1 = 2\pi k_1 d_1 / \lambda$$

$$\delta_1 = 2\pi n_1 d_1 / \lambda$$

Refractive Indices:

$$n_0 = 1.5 \text{ (Glass)}; \quad N_1 = n_1 - ik_1 \text{ (absorbing medium, here the photocathode)}$$

$$n_2 = 1.0 \text{ (Vacuum)}$$

d_1 = physical thickness of the absorbing layer.

With these definitions R_{FG} , R_{VG} , T_{FG} become respectively the Front or Glass reflectivity, the Vacuum reflectivity, and the Transmission in % of an incident light wave λ of unit intensity in the medium n_0 (Glass).

Actually these intensities are not measurable as we can measure only quantities in air, incident as well as emerging. Therefore, a correction has to be made to account for the air-glass interface. For exemplification, see Figure 20 of this report.

r_G : Percentage of light reflected from the air-glass interface

$$r_G = \left[\frac{n_0 - n_1}{n_0 + n_1} \right]^2 \approx .04$$

The computer values R_{FC} , R_{VC} , T_{FC} , are the % of the amplitude entering the glass: $1 - r_G$. Our recorded and measured value of front reflection $R_F = \bar{R}_F / R_{FAG} = \bar{R}_F / 1 - \epsilon_\lambda$

where R_{FAG} is the reflection of an Ag mirror in the same constellation. (ϵ_λ is a factor due to the imperfections of the Ag mirror. This factor is wavelength dependent.) Similarly for R_V , T_F . (See, e.g., Rpt. #21, pgs 7-8 and Figure 24). This gives in first order approximation:

$$(IV) R_{FC} = (1 + 2r_G - \epsilon_\lambda) R_F - r_G$$

where R_F , R_V , T_F , are the measured values.

$$(V) R_{VC} = (1 - \epsilon_\lambda) R_V$$

$$(VI) T_{FC} = (1 - r_G) T_F$$

If we consider the second order reflection on the air-glass interface we have:

$$(1 - \epsilon_\lambda) R_F - r_G R_F (R_F - 2r_G) = (1 - 2r_G) R_{FC} + r_G$$

$$T_{FC} = (1 - r_G - R_{FC} r_G) T_F$$

$$R_{VC} = (1 - \epsilon_\lambda) R_V - r_G T_F^2 (1 - 2r_G - 2R_V r_G)$$

Because of the very small terms of mostly third order involved, we can replace R_{FC} , R_{VC} , and T_{FC} by R_F , R_V , and T_F in the second and third equation for simplicity's sake. So we finally get:

$$(VII) R_{FC} = (1 + 2\epsilon_G - \epsilon_A) R_F - \epsilon_G R_F (R_F - 2\epsilon_G) - \epsilon_G$$

$$(VIII) T_{FC} = (1 - \epsilon_G - \epsilon_G R_F) T_F$$

$$(IX) R_{VC} = (1 - \epsilon_A) R_V - \epsilon_G T_F^2 (1 - 2\epsilon_G - 2R_V \epsilon_G)$$

These equations will now supply the values which can be used in (I), (II), (III) for the computer program.

ADDENDUM II

~~CONFIDENTIAL~~
RE: DD-254 4/14/70

In the following we show some of the tentative results on the S-1 and related:

Tube No.	Wanted Triplet R_F, R_V, T	Best Triplet Fit	d/λ	k	n
1) R-5	(See Rpt. #15, Fig. 13)	Rubidium processed S-1			
$\lambda = 6000\text{\AA}$	(.12, .26, .365)	(.117, .261, .366)	.195	.198	4.925

This is a very good agreement. Now the same thickness $d = 1170\text{\AA}$ is tried at different λ s.

$\lambda = 9360\text{\AA}$	(.103, .24, .355)	(.10 ⁺ , .242, .35)	.125	.45	3.55
		(.105, .235, .355)	.125	.37	4.35

This is a typical case of two possible solutions.

$\lambda = 10170\text{\AA}$	(.095, .215, .44)		.115	.33	3.75
			.115	.27	4.65

$\lambda = 11140\text{\AA}$	(.085, .20, .49)	(.08 ⁺ , .205, .49)	.105	.31	4.425
-----------------------------	------------------	--------------------------------	------	-----	-------

As we see, the curve for n is not at all smooth. The shorter wavelengths even demand an $n > 5.0$. However, all possible triplet solutions lead to a similar thickness.

2) 340 (See Rpt. #15, Fig. 12)

$\lambda = 11500\text{\AA}$	(.135, .23, .555)	(.133, .23, .55)	.10	.20	4.55
-----------------------------	-------------------	------------------	-----	-----	------

Thickness $d = 1150\text{\AA}$

This thickness does not give a good fit at other wavelengths with $n > 5.0$.

$\lambda = 8210\text{\AA}$	(.155, .305, .31)	(.155, .28, .315)	.14	.34	4.10
$\lambda = 6570\text{\AA}$	(.165, .340, .265)	(.165, .30, .265)	.175	.38	3.45

Shorter wavelengths become very poor; probably solutions $n > 5.0$ are required.

~~CONFIDENTIAL~~

~~CONFIDENTIAL~~

RE: DD-254 4/14/70

Tube No.	Wanted Triplet R_F, R_V, T	Best Triplet Fit	d/λ	k	n
3) 332	(See Rpt. #15, Fig. 11)				
$\lambda = 10500\text{\AA}$	(.05, .165, .485)	(.049, .169, .405)	.125	.295	3.75
Thickness $d = 1300\text{\AA}$					
$\lambda = 6500\text{\AA}$	(.070, .225, .375)	(.080, .19, .37 ⁺)	.20	.28	3.5
$\lambda = 8125\text{\AA}$	(.055, .185, .43)	(.057, .18, .43)		.27	3.41
but also a better second fit for					
$\lambda = 6500\text{\AA}$	(.075, .225, .375)	(.075, .226, .373)	.20	.205	4.92

4) 113A (See Rpt. #15, Fig. 9)

This has been most extensively computed. The best data are selected below.

One triplet has been fitted to the 11500 \AA data.

$$\lambda = 11500\text{\AA} \quad (.085, .24, .39) \quad (.085, .237, .394) \quad .094 \quad .40 \quad 4.0$$

Resulting in $d = 1080\text{\AA}$

This thickness fits down to $\approx 9800\text{\AA}$

$$\lambda = 9820\text{\AA} \quad (.10, .27, .345) \quad (.105, .265, .340) \quad .49 \quad 4.15$$

However, the R_V values become too small for still shorter wavelengths.

$$\lambda = 9660\text{\AA} \quad (.105, .28, .33) \quad (.105, .255, .33) \quad .115 \quad .50 \quad 3.925$$

And the agreement gets worse until $\approx 5750\text{\AA}$. Here again we get

a good fit.

$$\lambda = 5750\text{\AA} \quad (.150, .295, .36) \quad (.147, .29, .36) \quad .20 \quad 4.75$$

$$\lambda = 5600\text{\AA} \quad (.145, .285, .38) \quad (.145, .285, .38^+) \quad .18 \quad 4.75$$

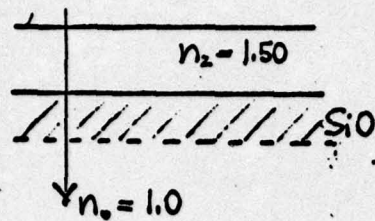
If we fit triplets to other wavelengths, similar thicknesses result, however with slightly different n values.

~~CONFIDENTIAL~~

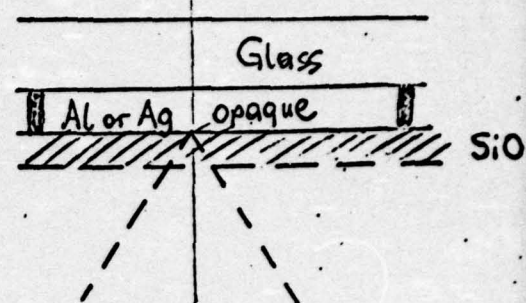
~~CONFIDENTIAL~~

RE DD-254 4/14/70

(U) In our case, the following two optical data are measured:



Transmission measured



Reflection measured

(U) We assume that the SiO is transparent in the red and near infrared and has a refractive index of $n_1 = 1.8$. The optical constants of the substrates Al, Ag at the wavelengths of interest are:

	<u>Al</u>	<u>Ag</u>	<u>R_{Al}</u>	<u>R_{Ag}</u>
4200Å	$n = .40$ $k = 4.00$	$n = 0.065$ $k = 2.18$	91.0%	95.6%
8000Å	$n = 1.99$ $k = 7.05$	$n = 0.11$ $k = 5.41$	86.5%	98.6%
9500Å	$n = 1.75$ $k = 8.50$	$n = 0.13$ $k = 6.48$	90.0%	98.8%

(U) The n, k values are from G. Hass, JOSA, Vol. 51, p. 719.

(U) The reflectances R are computed from the equation

$$R = \frac{(1-n_2)^2 + k_2^2}{(1+n_2)^2 + k_2^2}$$

~~CONFIDENTIAL~~

(U) Unfortunately, R_{A1} has a minimum around 8500Å

$$R_{8500\text{Å}} = \frac{(1.08)^2 + (7.15)^2}{(3.08)^2 + (7.15)^2} = 86.3\%$$

(U) For the reflectance of the composite Al and SiO₂, a more complicated formula applies

$$R = \frac{g_1^2 + (g_2^2 + h_2^2) + A \cos(2\phi_1) + B \sin(2\phi_1)}{1 + g_1^2(g_2^2 + h_2^2) + A \cos(2\phi_1) + B \sin(2\phi_1)} \quad (1)$$

(U) Here is $\phi_1 = 2\pi n_1 \frac{d_1}{\lambda}$

$$g_1 = \frac{n_0 - n_1}{n_0 + n_1}$$

$$g_2 = \frac{n_1^2 - n_2^2 - k_2^2}{(n_1 + n_2)^2 + k_2^2}$$

$$h_2 = \frac{2 n_1 k_2}{(n_1 + n_2)^2 + k_2^2}$$

$$A = 2 g_1 g_2$$

$$B = 2 g_1 h_2$$

(U) For a transparent film on a transparent substrate, this reduces to

$$R = \frac{g_1^2 + g_2^2 + 2g_1g_2 \cos(2\phi_1)}{1 + g_1^2g_2^2 + 2g_1g_2 \cos(2\phi_1)} = 1 - \text{Transmission} \quad (2)$$

(U) If we first consider the system Glass-SiO, we have

$$g_1 = \frac{1 - (1.8)^2}{(2.8)^2} = -.286$$

$$g_2 = \frac{(1.8)^2 - (1.5)^2}{(3.3)^2} = .091$$

$$R = \frac{.082 + .008 - .052 \times \cos(2\phi_1)}{1 - .052 \cos(2\phi_1)}$$

(U) The maxima of R are given by $\cos(2\phi_1) = -1$ $R_{\max.} = .153$

(U) The minima of R are given by $\cos(2\phi_1) = +1$ $R_{\min.} = .04$

For $\cos(2\phi_1) = 0$ $R = .089$

(U) Assuming transparency of the SiO deposit, the measured transmission would swing from 96% to 84.7% (first minimum) and back again. Expressed as percent of initial reading, we expect the transmission for the 8000Å and 9500Å line to vary from 100% to 88%.

(U) The thickness for the extreme transmission readings can now be easily computed from

$$2\phi_1 = \frac{4\pi}{\lambda} n_1 d_1 = \pi \quad R_{\max.}$$

$$2\phi_1 = \frac{4\pi}{\lambda} n_1 d_1 = 0, 2\pi \quad R_{\min.}$$

(U) We get thus: for $\lambda = 8000\text{Å}$ $d_1(R_{\max.}) = 1110\text{Å}$
 $d_1(R_{\min.}) = 2220\text{Å}$ (resp. 0Å)
 for $\lambda = 9500\text{Å}$ $d_1(R_{\max.}) = 1320\text{Å}$

UNCLASSIFIED

~~CONFIDENTIAL~~
RE DD-254 4/14/70

(U) The values actually measured for those two lines on stepwise evaporation of SiO conform reasonably to those calculated limits of change. We have never deposited heavier layers than those corresponding to the second maximum ($2\gamma_1 = 2\pi$).

(U) For the case of the reflection on Al (or Ag) we have to use the more complicated formula (1).

(U) For Al: $= 8000\text{\AA}$ $g_1 = -.285$ $R = \frac{.85 + .45 \cos(2\gamma_1) - .23 \sin(2\gamma_1)}{1.06 + .45 \cos(2\gamma_1) - .23 \sin(2\gamma_1)}$

$n_0 = 1.0$ $g_2 = -.785$

$n_1 = 1.8$ $h_2 = .397$

$n_2 = 2.0$ $A = .447$

$k_2 = 7.0$ $B = -.226$

The maxima and minima of R are given by the maxima and minima of the function.

(U) $F(y) = ay - b \cdot \sqrt{1-y^2}$ where $y = \cos(2\gamma_1)$

(U) The calculation shows $y_{\text{extrema}} = \pm \frac{(a/b)^2}{1 + (a/b)^2}$

(U) With these values for $2\gamma_1$ we get $R_{\text{min.}} = 62.5\%$. The initial reflection without film is 86.5% as shown before. Again expressed as percent of initial reading, the swing would be from 100% to 72.2% for the first and following minima.

(U) In the specific case of our example: $\sin 2\gamma_1 = .62$
 $\cos 2\gamma_1 = -.79$

UNCLASSIFIED

~~CONFIDENTIAL~~

UNCLASSIFIED

~~CONFIDENTIAL~~
RE DD-254 4/14/70

(U) It follows that $2\gamma_1 = 2.48$ or $d_1 = \frac{2.48}{4\pi n_1} 8000\text{\AA} = 880\text{\AA}$ for the first minimum

(U) For 9500\AA, a similar calculation yields $d_1(\text{min.}) = 1137\text{\AA}$

(U) The reflection minima on the Al substrate occur approximately at 80% of the thickness which results in transmission minima in the glass.

(U) Again the expected variations of reflectance have been observed in actual measurements. For example:

Tube No. 5266 - Reflection 8000\AA : 100% down to 69.5%, then up again to 94%; estimated $d_1 \sim 1550\text{\AA}$.

Tube No. 5268 - Reflection 8000\AA : 100% to 75.5% then up again to 96%; estimated $d_1 \sim 1650\text{\AA}$.

(U) The expected slow change of R around the minima and maxima has also been observed.

(U) A similar computation for the Ag mirror leads to a much smaller variation of reflectance. For example, at 9500\AA, the reflectance changes only from 98.8% to 96.5% for a similar thickness. This explains the difficulties which we encountered in observation of IR reflection changes on the SiO+Ag.

(U) In the blue region, the SiO film exhibits considerable absorption (probably also a much higher refractive index), and the above given equations can no longer be used.

UNCLASSIFIED

~~CONFIDENTIAL~~